

**Biochemical Adaptations in *Pseudomonas fluorescens* Exposed to Nitric Oxide, an
Endogenous Antibacterial Agent**

by

Christopher Scott Auger

**Thesis submitted in partial fulfillment
of the requirements for the degree of
Doctor of Philosophy (PhD) in Biomolecular Sciences**

**School of Graduate Studies
Laurentian University
Sudbury, Ontario**

© Christopher S. Auger, 2014

THESIS DEFENCE COMMITTEE/COMITÉ DE SOUTENANCE DE THÈSE

Laurentian University/Université Laurentienne School of Graduate Studies/École des études supérieures

Title of Thesis Titre de la thèse	BIOCHEMICAL ADAPTATIONS IN <i>PSEUDOMONAS FLUORESCENS</i> EXPOSED TO NITRIC OXIDE, AN ENDOGENOUS ANTIBACTERIAL AGENT		
Name of Candidate Nom du candidat	Auger, Christopher Scott		
Degree Diplôme	Doctor of Philosophy		
Department/Program Département/Programme	Biomolecular Sciences	Date of Defence Date de la soutenance	May 12, 2014

APPROVED/APPROUVÉ

Thesis Examiners/Examineurs de thèse:

Dr. Vasu Appanna
(Supervisor/Directeur de thèse)

Dr. Stefan Siemann
(Committee member/Membre du comité)

Dr. Céline Boudreau-Larivière
(Committee member/Membre du comité)

Dr. William T. Self
(External Examiner/Examineur externe)

Dr. Sandra Dorman
(Internal Examiner/Examinatrice interne)

Approved for the School of Graduate Studies
Approuvé pour l'École des études supérieures
Dr. David Lesbarrères
M. David Lesbarrères
Director, School of Graduate Studies
Directeur, École des études supérieures

ACCESSIBILITY CLAUSE AND PERMISSION TO USE

I, **Christopher Scott Auger**, hereby grant to Laurentian University and/or its agents the non-exclusive license to archive and make accessible my thesis, dissertation, or project report in whole or in part in all forms of media, now or for the duration of my copyright ownership. I retain all other ownership rights to the copyright of the thesis, dissertation or project report. I also reserve the right to use in future works (such as articles or books) all or part of this thesis, dissertation, or project report. I further agree that permission for copying of this thesis in any manner, in whole or in part, for scholarly purposes may be granted by the professor or professors who supervised my thesis work or, in their absence, by the Head of the Department in which my thesis work was done. It is understood that any copying or publication or use of this thesis or parts thereof for financial gain shall not be allowed without my written permission. It is also understood that this copy is being made available in this form by the authority of the copyright owner solely for the purpose of private study and research and may not be copied or reproduced except as permitted by the copyright laws without written authority from the copyright owner.

Thesis Abstract:

Nitric oxide (NO), a free radical released by macrophages (a subset of white blood cells) as a response to infection, is noxious to organisms due to its ability to disable crucial biomolecules such as lipids, proteins and DNA. Although normally effective at eradicating invading bacteria, several pathogens have developed mechanisms to detoxify NO and its toxic by-products, reactive nitrogen species (RNS). While some of these detoxification processes have been characterized, very little is known about the metabolic changes that enable microbes to survive this deleterious environment.

Investigations into the effects of RNS on microbial physiology have shown that these harmful radicals inactivate the citric acid cycle and oxidative phosphorylation, the series of reactions responsible for making energy aerobically. The central aim of this thesis was to determine how the organism counteracts the detrimental effects of RNS, while bypassing the ineffective central metabolic pathways. The findings presented herein show that *P. fluorescens* engineers an elaborate metabolic network to generate ATP whilst withstanding the injurious effects of nitrosative stress. Crucial to this adaptation is the ability to produce energy via substrate level phosphorylation, a necessity that arises out of the cells' inability to produce a substantial amount of ATP using the electron transport chain (ETC).

The up-regulation of the enzymes citrate lyase (CL), phosphoenolpyruvate carboxylase (PEPC) and pyruvate, phosphate dikinase (PPDK) helps the organism accomplish this feat. Blue native polyacrylamide gel electrophoresis (BN-PAGE), high performance liquid chromatography (HPLC) as well as co-immunoprecipitation (CO-IP) studies were applied to demonstrate that these proteins form a metabolon, a transient complex of enzymes that ensures citrate is converted into its desired end products, pyruvate and ATP. In order to gauge the individual contributions

of phosphoenolpyruvate-dependent kinases, a novel in-gel activity assay was developed to probe these enzymes under disparate conditions.

These results suggest that the organism switches from an ATP-dependent metabolism to one based on the utilization of pyrophosphate (PP_i). The rationale for this appears to be energy efficiency, as pyrophosphate-dependent glycolysis can theoretically produce five ATP rather than the two yielded by Embden-Meyerhof glycolysis. Additionally, the up-regulation in activity of the enzymes adenylate kinase, nucleoside diphosphate kinase and acetate kinase seem to ensure that ATP generated by PPDK is properly shuttled and stored when aerobic metabolism is defective. The lower activity of inorganic pyrophosphatase likely ensures an adequate supply of pyrophosphate for the activity of PPDK.

Taken together, this research reveals the critical role metabolism plays in the survival of microbes under the onslaught of NO and RNS. As several of these enzymes are absent in mammalian systems, they present themselves as novel targets for the development of new antibacterial agents. A comprehensive awareness of bacterial defense systems in response to NO may lay the groundwork to developing more effective treatments to impede microbial infections.

Keywords: Metabolism, Bacteria, Nitric oxide, Reactive Nitrogen Species, Metabolon, Phosphotransfer, Electrophoresis

Acknowledgements:

First and foremost, I would like to extend my deepest gratitude to my supervisor and mentor, Dr. Vasu Appanna. A constant reservoir of knowledge and inspiration, he allowed me to surmount obstacles and achieve goals I would not have conceived possible without his guidance. His research prowess awakened a sense of scientific curiosity in me that never would have seen the light of day had I not come into his presence. Truly, any success I find in my career can be traced back to his teachings, and for that I will always be indebted to him and his leadership.

I thank Dr. Joseph Lemire for training and giving me direction when I began my graduate studies. It could not have been easy to guide someone as stubborn and inept as I once was, but he performed admirably in providing me the insight I required to conduct research and transition into my role as laboratory manager. Most of all, I'm grateful to call him a friend, and hope he finds happiness and prosperity in all walks of life.

I also extend my gratitude to members of my supervisory committee, which includes Dr. Céline Boudreau-Larivière and Dr. Stefan Siemann. Their guidance and support over the course of my doctoral studies was greatly appreciated. Going forward, the Laurentian community is fortunate to have such resourceful faculty members in place, helping Greater Sudbury remain one of the strongest research hubs in the North. I'm also grateful to Dr. William Self and Dr. Sandra Dorman for acting as external and internal examiners, respectively. Their feedback was instrumental to the completion of this thesis.

I would like to thank Appanna lab researchers, past and present, for keeping me humble during the good times, and helping me fight through the bad ones. They are some of the brightest students I've had the privilege of working with, and without a doubt, will become great doctors,

dentists, pharmacists and researchers. To my friends, too numerous to name: When everything in my life seemed like an uphill battle, thanks for throwing down a rope to help me climb to the top. I could never tell you all how helpful it was that you were there to listen, but I'll forever cherish the memories we made during the journey.

To my mother, Cecile, and my little sister, Sarah: You are two of the strongest women I've ever met. Thank you for sitting through my presentations and reading my papers, and being so very proud even when you could not understand the significance of what you were looking at. Everything I am and hope to become would never have been possible without your love and support. Thank you both for being my rock.

Table of Contents:

Page #

Thesis Abstract	iii
Acknowledgements	v
Table of Contents	vii
List of Tables	viii
List of Figures	ix
List of Original Publications	xi
List of Abbreviations	xiv
Chapter 1: Introduction	1
1.1 - The state of antibiotic research and development	1
1.2 - The disparate roles of the gaseous messenger, nitric oxide (NO)	4
1.2.1 - eNOS, NO and vasodilation	6
1.2.2 - nNOS and neurotransmission	7
1.2.3 - iNOS, a cornerstone of the innate immune system	7
1.3 - Bacterial defense systems against NO	10
Chapter 2: Hypothesis and objectives	11
Chapter 3: The metabolic reprogramming evoked by nitrosative stress	13
Chapter 4: A facile electrophoretic technique to monitor phosphoenolpyruvate-dependent kinases.....	43
Chapter 5: A citrate-degrading metabolon and phosphotransfer network to counter nitrosative stress.....	65
Chapter 6: Contribution to other research.....	92
Chapter 7: Conclusions and future directions	94
References	100
Appendix I	111
Appendix II.....	113
Appendix III.....	114

List of Tables

Page #

Table 1.1 – The biological targets of select reactive nitrogen species.....**9**

Table 9.1 – Microarray analysis of *P. fluorescens* exposed to 10 mM SNP.....**114**

List of Figures

Page

Figure 1.1 – Timeline of antibiotic implementation	1
Figure 1.2 – Targets of commercially-available antibiotics	3
Figure 1.3 – Nitric oxide synthase	5
Figure 1.4 – eNOS and vasolidation	6
Figure 1.5 – Reactive nitrogen species	8
Figure 3.1 - Nitrosative stress in <i>P. fluorescens</i>	27
Figure 3.2 - RNS detoxifying mechanisms in <i>P. fluorescens</i>	29
Figure 3.3 - Influence of NO on the TCA cycle	32
Figure 3.4 - Activity and expression analysis of CL from <i>P. fluorescens</i>	34
Figure 3.5 - Oxaloacetate and PEP metabolism	37
Figure 3.6 - Pyruvate and acetate utilizing enzymes	38
Figure 3.7 - Citrate metabolism in <i>Pseudomonas fluorescens</i> under nitrosative stress.....	42
Figure 4.1 - A schematic depiction of the electrophoretic method to detect PEP-dependent kinases	55
Figure 4.2 - Identification of pyruvate kinase by BN-PAGE	57
Figure 4.3 - Monitoring of pyruvate, phosphate dikinase (PPDK) by BN-PAGE	59
Figure 4.5 - The biochemical application of this electrophoretic method	61
Figure 4.4 - BN-PAGE analysis of kinases generating ATP from PEP	63
Figure 5.1 - Nucleotide and ETC analysis in <i>P. fluorescens</i> exposed to nitrosative stress	79
Figure 5.2 - Citrate catabolism and metabolon formation	82
Figure 5.3 - Metabolon phosphorylation and dissociation	84
Figure 5.4 - Nucleotide production and phosphotransfer networks	86
Figure 5.5 - Bioenergetics in <i>Pseudomonas fluorescens</i> exposed to nitrosative stress	91
Figure 7.1 – Holistic approach to adaptation in living systems	99

Figure 9.1 – PPDK in-gel activity assays	111
Figure 9.2 – Complex IV in-gel activity assays	112
Figure 9.3 – In-gel activity assays from <i>P. fluorescens</i> grown on glucose	113

List of Original Publications

Submitted

1. Appanna, V.P., Thomas, S.C., **Auger, C.**, Omri, A. (2014) Fumarate metabolism and ATP production in *Pseudomonas fluorescens* exposed to nitrosative stress in a fumarate growth medium. *Antonie van Leeuwenhoek* (Submitted).
2. **Auger, C.** and Appanna, V.D. (2014) A citrate-degrading metabolon and phosphotransfer network to counter nitric oxide, an endogenous antibacterial agent. *Free Radic. Bio.* (Submitted).
3. Castonguay, Z., **Auger, C.**, Thomas, S.C., Chahma, M., Appanna, V.D. (2014) Nuclear lactate dehydrogenase-modulated NAD⁺ levels mediate epigenetic modifications in human hepatocytes. *J. Mol. Cell Biol.* (Submitted).

Published

4. Alhasawi, A., **Auger, C.**, Appanna, V.P., Chahma, M., Appanna, V.D. (2014) Zinc toxicity and ATP production in *Pseudomonas fluorescens*. *J. Appl. Microbiol.* (Accepted).
5. Thomas, S.C., Alhasawi, A., Appanna, V.P., **Auger, C.**, Appanna, V.D. (2014) Energy metabolism and Alzheimer's disease: The prospect of a metabolite-based therapy. *J. Nutr. Health Aging* (Accepted).
6. Lemire, J., **Auger, C.**, Mailloux, R., Appanna, V.D. (2013) Mitochondrial lactate metabolism is involved in anti-oxidative defense in human astrocytoma cells. *J. Neurosci. Res.* **10**:23338.
7. Han, S., **Auger, C.**, Thomas, S.C., Beites, C., Appanna, V.D. (2013) Mitochondrial biogenesis and energy production in differentiating murine stem cells: A functional metabolic study. *Cell Reprogram.* **16**:84-90.
8. Bignucolo, A., Appanna, V.P., Thomas, S.C., **Auger, C.**, Han, S., Omri, A., Appanna, V.D. (2013) Hydrogen peroxide stress provokes a metabolic reprogramming in *Pseudomonas fluorescens*: enhanced production of pyruvate. *J. Biotechnol.* **167**:309-15.
9. Han, S., Lemire, J., Appanna, V.P., **Auger, C.**, Castonguay, Z., Appanna, V.D. (2013) How aluminum, an intracellular ROS generator promotes hepatic and neurological diseases: the metabolic tale. *Cell Biol. Toxicol.* **29**:75-84.
10. **Auger, C.**, Han, S., Appanna, V.P., Thomas, S.C., Ulibarri, G., Appanna, V.D. (2013) Metabolic reengineering invoked by microbial systems to decontaminate aluminum: implications for bioremediation technologies. *Biotechnol Adv.* **31**:266-73.

11. Han, S., **Auger, C.**, Castonguay, Z., Appanna, V.P., Thomas, S.C., Appanna, V.D. (2013) The unravelling of metabolic dysfunctions linked to metal-associated diseases by blue native polyacrylamide gel electrophoresis. *Anal. Bioanal. Chem.* **405**:1821-31.
12. Han, S., **Auger, C.**, Appanna, V.P., Lemire, J., Castonguay, Z., Akbarov, E., Appanna, V.D. (2012) A blue native polyacrylamide gel electrophoretic technology to probe the functional proteomics mediating nitrogen homeostasis in *Pseudomonas fluorescens*. *J. Microbiol. Methods.* **90**:206-10.
13. Reinoso, C.A., **Auger, C.**, Appanna, V.D., Vásquez, C.C. (2012) Tellurite-exposed *Escherichia coli* exhibits increased intracellular α -ketoglutarate. *Biochem. Biophys. Res. Commun.* **421**:721-6.
14. **Auger, C.**, Lemire, J., Cecchini, D., Bignucolo, A., Appanna, V.D. (2011) The metabolic reprogramming evoked by nitrosative stress triggers the anaerobic utilization of citrate in *Pseudomonas fluorescens*. *PLoS ONE* **6**:e28469.
15. **Auger, C.**, Appanna, V., Castonguay, Z., Han, S., Appanna, V.D. (2011) A facile electrophoretic technique to monitor phosphoenolpyruvate-dependent kinases. *Electrophoresis.* **33**:1095-101.
16. **Auger, C.**, Lemire, J., Appanna, V., Appanna, V.D. (2011) Gallium in bacteria: Metabolic and medical implications. Encyclopedia of Metalloproteins. *Springer Science.*
17. Lemire, J., Mailloux, R., Darwich, R., **Auger, C.**, Appanna, V.D. (2011) The disruption of l-carnitine metabolism by aluminum toxicity and oxidative stress promotes dyslipidemia in human astrocytic and hepatic cells. *Toxicol Lett.* **203**:219-26.
18. Bignucolo, A., Lemire, J., **Auger, C.**, Castonguay, Z., Appanna, V.P., Appanna, V.D. (2011) The molecular connection between aluminum toxicity, anemia, inflammation and obesity: Therapeutic cues. *InTech – Open Access Publisher.*
19. Lemire, J., **Auger, C.**, Bignucolo, A., Appanna, V., Appanna, V.D. (2010) Metabolic strategies deployed by *Pseudomonas fluorescens* to combat metal pollutants: Biotechnological prospects. Current Research, Technology and Education Topics in Applied Microbiology and Microbial Biotechnology. *Microbiology Book Series – Number 2.*
20. Lemire, J., Mailloux, R., **Auger, C.**, Whalen, D., Appanna, V.D. (2010) *Pseudomonas fluorescens* orchestrates a fine metabolic-balancing act to counter aluminum toxicity. *Environ. Microbiol.* **12**:1384-90.
21. Lemire, J., Milandu, Y., **Auger, C.**, Bignucolo, A., Appanna, V.P., Appanna, V.D. (2010) Histidine is a source of the anti-oxidant α -ketoglutarate in *Pseudomonas fluorescens* challenged by oxidative stress. *FEMS Microbiol. Lett.* **309**:170-7.

22. Mailloux, R., Singh, R., Brewer, G., **Auger, C.**, Lemire, J., Appanna, V.D. (2009) Alpha-ketoglutarate dehydrogenase and glutamate dehydrogenase work in tandem to modulate the antioxidant alpha-ketoglutarate during oxidative stress in *Pseudomonas fluorescens*. *J. Bacteriol.* **191**:3804-10.

Abbreviations

μM	Micromolar
μL	Microlitre
μg	Microgram
ACN	Aconitase
ACS	Acetyl-CoA synthase
ADP	Adenosine diphosphate
AK	Adenylate kinase
Al	Aluminum (III)
APS	Ammonium persulfate
ATP	Adenosine triphosphate
AU	Absorbance units
BN	Blue native
BN-PAGE	Blue native polyacrylamide gel electrophoresis
BSA	Bovine serum albumin
C	Celsius
CFE	Cell free extract
CK	Creatine kinase
CL	Citrate lyase
cm	Centimeters
CoA	Coenzyme A
CO-IP	Co-immunoprecipitation
CSB	Cell storage buffer
Cu	Copper
DCIP	Dichloroindophenol
ddH ₂ O	Deionized and distilled water
DEANO	Diethylamine NONOate
DNPH	Dinitrophenyl hydrazine
EDRF	Endothelium-derived relaxation factor
EDTA	Ethylenediaminetetraacetic acid
ETC	Electron transport chain
FAD	Flavin adenine dinucleotide (oxidized)
FADH ₂	Flavin adenine dinucleotide (reduced)
Fe	Iron
FUM	Fumarase
GAPDH	Glyceraldehyde 3-phosphate dehydrogenase
GDH	Glutamate dehydrogenase
Glu	Glutamate
GR	Glutathione reductase
GSH	Glutathione (reduced)
GSNO	S-nitrosylated glutathione
GSNOR	S-nitrosylated glutathione reductase
GSSG	Glutathione (oxidized)
h	hours

HCl.....	Hydrochloric acid
H ₂ O ₂	Hydrogen peroxide
HPLC.....	High performance liquid chromatography
ICL.....	Isocitrate lyase
INT.....	Iodonitrotetrazolium
KDa.....	Kilodaltons
KG.....	α -Ketoglutarate
KGDH.....	α -Ketoglutarate dehydrogenase
LDH.....	Lactate dehydrogenase
M.....	Molar
ME.....	Malic enzyme
MDH.....	Malate dehydrogenase
min.....	Minutes
mL.....	Millilitre
mM.....	Milimolar
mm.....	Millimeters
N.....	Normal (normality)
nm.....	Nanometers
NaCl.....	Sodium chloride
NAD.....	Nicotinamide adenine dinucleotide (oxidized)
NADH.....	Nicotinamide adenine dinucleotide (reduced)
NADP.....	Nicotinamide adenine dinucleotide phosphate (oxidized)
NADPH.....	Nicotinamide adenine dinucleotide phosphate (reduced)
NAD-ICDH.....	NAD-dependent isocitrate dehydrogenase
NADP-ICDH.....	NADP-dependent isocitrate dehydrogenase
NDPK.....	Nucleotide diphosphate kinase
NIR.....	Nitrite reductase
NO.....	Nitric oxide
NOS.....	Nitric oxide synthase
NR.....	Nitrate reductase
O ₂	Molecular oxygen
ONOO.....	Peroxynitrite
P _i	Inorganic phosphate
PP _i	Pyrophosphate
PC.....	Pyruvate carboxylase
PDH.....	Pyruvate dehydrogenase
PEP.....	Phosphoenolpyruvate
PEPC.....	Phosphoenolpyruvate carboxylase
PEPCK.....	Phosphoenolpyruvate carboxykinase
PEPS.....	Phosphoenolpyruvate synthase
PMS.....	Phenazine methosulfate
PPase.....	Inorganic pyrophosphatase
PPDK.....	Pyruvate, phosphate dikinase
PTB.....	Protein transfer buffer
RNS.....	Reactive nitrogen species
ROS.....	Reactive oxygen species

sec.....	Seconds
SDH.....	Succinate dehydrogenase
SDS-PAGE.....	Sodium dodecyl sulfate polyacrylamide gel electrophoresis
SNP.....	Sodium nitroprusside
SOD.....	Superoxide dismutase
TBARS.....	Thiobarbituric acid reactive species
TBS.....	Tris-buffered saline
TCA.....	Tricarboxylic acid
TTBS.....	Tween-20 tris-buffered saline
TEMED.....	N,N,N,N –Tetramethylethylenediamine
v/v.....	Volume/volume
w/v.....	Weight/volume
WB.....	Western blot

Chapter 1: Introduction

1.1 – The state of antibiotic research and development

The discovery, characterization and implementation of antibiotics in Western medicine are arguably some of our greatest scientific achievements. Indeed, Alexander Fleming’s finding that penicillin isolated from the mold *Penicillium notatum* could effectively eliminate some of our greatest scourges set in course a medical revolution (1). Between 1935 and 1962, the accelerated nature of antibiotic research helped uncover all of the major drug classes we know today (2). This era of discovery was followed by a period of approximately 40 years, referred to as the innovation gap, where no new antimicrobials were introduced to the market. While oxazolidinones, acid lipopeptides and pleuromutilins were first patented during this innovation gap, their application to combat microbial pathogens did not transpire until the new millennium (3) (Figure 1.1).

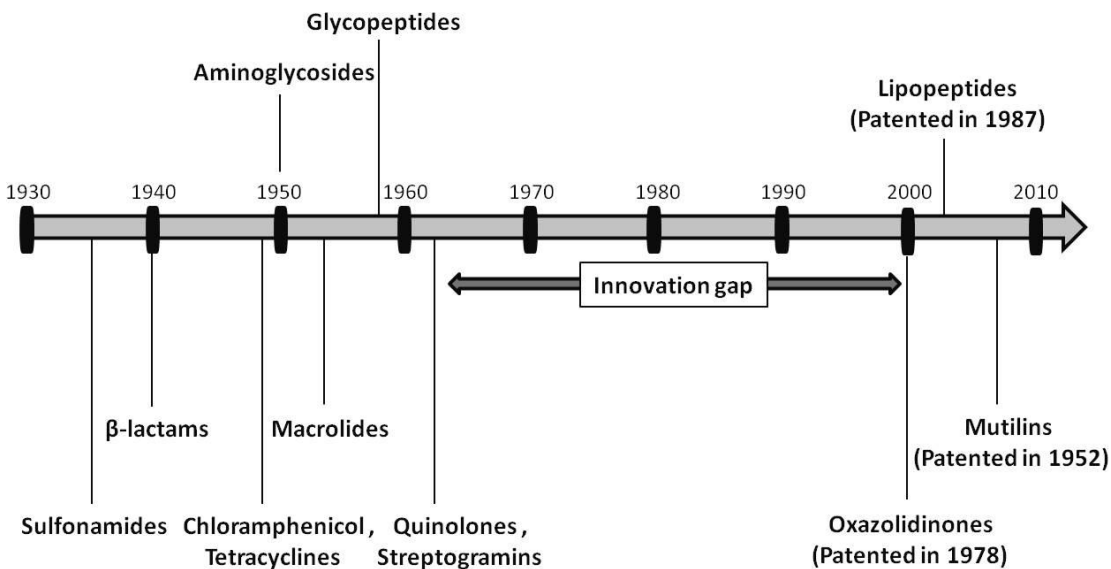


Figure 1.1 – Timeline of antibiotic implementation. Most antimicrobial classes were brought to market by the mid 20th century. The subsequent innovation gap is characterized by a lack of novel antibiotics. Adapted from (2, 3).

The lack of antibiotic research during the innovation gap could be attributed to a collective arrogance, the perception that our drug repertoire would forever be sufficient to treat the array of microbial infections in the community. The prevailing view was that we had won the war on infectious diseases, and as such, antibiotic research departments were dismantled and funding to this field was limited. Although antibiotic-resistant microbes had been reported as early as the 1950s, our understanding of the mechanisms underlying this resistance and how it proliferates would not suffice to predict the emergence of multi- and pandrug-resistant pathogens that threaten us today (4). Chief among these are the ESKAPE pathogens (*Enterococcus faecium*, *Staphylococcus aureus*, *Klebsiella pneumoniae*, *Acinetobacter baumannii*, *Pseudomonas aeruginosa*, and *enterobacteriaceae*), so named for their ability to escape the effects of even our most potent antibiotics (5).

Selective pressure, imposed by the application and often superfluous use of antibiotics, has brought about the evolution of a number of mechanisms to resist our drug repertoire. These include such stratagems as drug efflux, enzymatic cleavage/inactivation of the antibiotic, as well as genetic or post-translational modification of the drug target to resist the effects of the antibiotic administered (6). Once elaborated, genes encoding for drug resistance can be passed on to other organisms, normally in the form of large mobile genetic cassettes and by the process of horizontal gene transfer. While a comprehensive review of the mechanisms by which microbes resist antibiotic treatment would be outside the scope of this work, it is important to note that we have yet to create a drug to which resistance has not eventually developed (7). This underscores the fatal flaw behind the use of antibiotics. Our current armory of antimicrobials targets crucial biomolecules, such as the cell wall and components involved in transcription and protein synthesis (**Figure 1.2**). The indiscriminate killing of microorganisms generates enough

selective pressure to assure that antibiotic resistance will always be present in the environment. As such, the continuous development of antimicrobial treatments should be a priority moving forward.

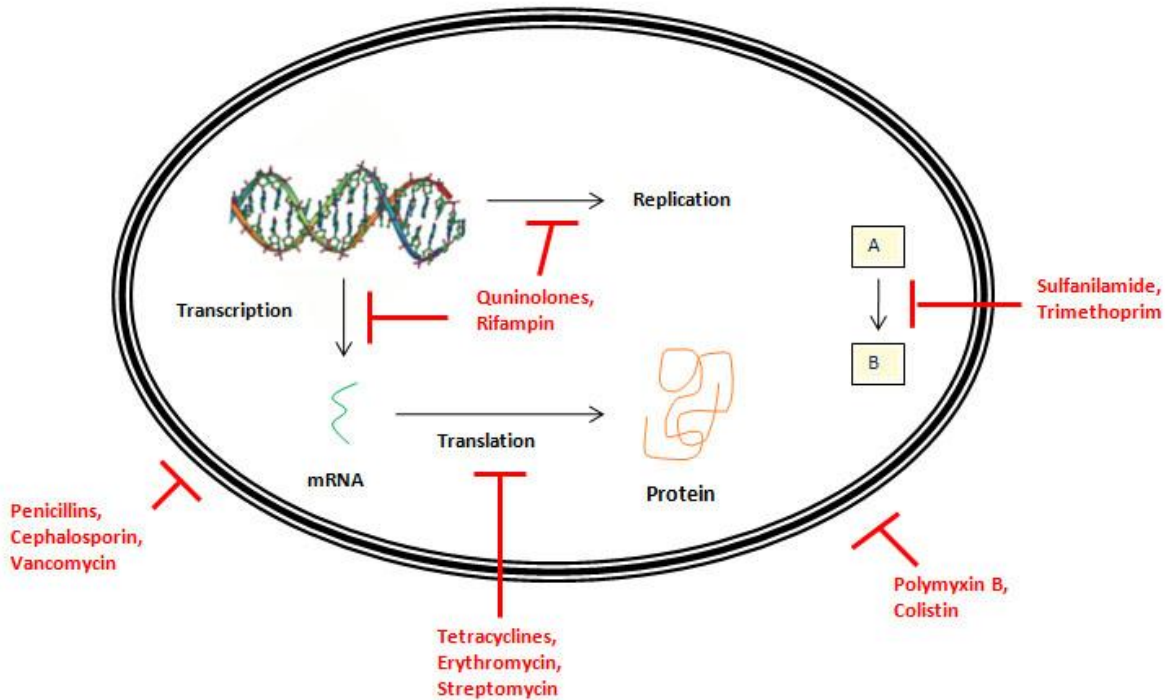


Figure 1.2 – Targets of commercially-available antibiotics. Antimicrobial treatments target necessary cellular functions like cell wall synthesis, transcription and translation. Adapted from (7).

Unfortunately, the current climate is not conducive to antibiotic development. The problem is multifactorial, ranging from unfavorable economics to a lack of experienced researchers, and has been reviewed extensively (2,8-10). Briefly, the short-term nature of antibiotic treatment, combined with the tendency to reserve novel drugs for serious bacterial infections has driven pharmaceutical companies away from research in this field. While multiple economic stimuli have been proposed to bolster antibiotic research, the number of drugs in the development pipeline begets a degree of pessimism. There is currently a dire shortage of

effective drugs targeting pathogenic gram-negative microorganisms, such as *P. aeruginosa*, *Acinetobacter baumannii*, *Klebsiella* spp. and *Enterobacter* spp (5). Additionally, most antibacterial agents in the development pipeline are simply variations of older scaffolds for which resistance may already be rampant (11). However, as grim as this predicament seems, there are reasons to be optimistic for the future of antimicrobial discovery.

The resurgence in antibiotic research, a product of our current plight, has identified a number of alternative approaches to combat drug-resistant pathogens. For instance, quorum quenching, the act of interfering with bacterial lines of communication, shows promise as a means of subduing virulence without killing the microbe and thus, should impose less pressure to develop resistance (12,13). The inhibition of bacterial defense systems that are utilized to counteract the immune response represents another innovative means of slowing pathogenesis, while allowing our innate defenses to clear the infection (14).

In summary, the era of antibiotics is quickly coming to a close. The overexploitation of this technology, in addition to a lagging research and development industry, has physicians dreading the further emergence of multi- and pandrug-resistant superbugs on which contemporary treatments will prove inadequate. As such, there is a dire need for new and improved antimicrobial therapies, thus underscoring the importance of research on bacterial physiology and metabolism.

1.2 – The disparate roles of the gaseous messenger, nitric oxide (NO)

When it was first uncovered that NO was generated *in vivo*, the concept that this free radical could be involved in signalling functions was foreign to the scientific community. Unlike neurotransmitters and hormones, NO is a gas and as such, cannot be stored in vesicles or directed

to specific compartments via receptors (15). Indeed, the lipophilic nature of this molecule, combined with its high reactivity, demands that the biosynthetic enzymes responsible for its formation be exquisitely and dynamically regulated, lest there be dire physiological consequences. Nitric oxide synthases (NOS) are a family of enzymes involved in the production of NO from arginine, as depicted (16) (**Figure 1.3**).

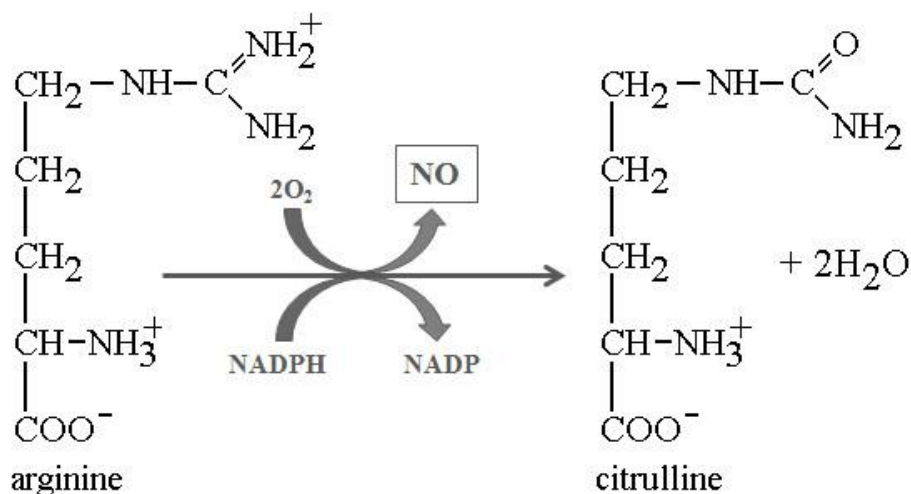


Figure 1.3 – Nitric oxide synthase. This family of enzymes is responsible for the generation of the signalling moiety nitric oxide (NO) in biological systems. Adapted from (16).

While the reduction of inorganic nitrate also forms NO, the bulk of this compound is produced by three NOS isoforms, namely endothelial NOS (eNOS), neuronal NOS (nNOS) and inducible NOS (iNOS). Tight regulatory control over NO production is achieved using the Ca²⁺-sensing intermediate calmodulin. The latter, along with the cofactors flavin adenine dinucleotide (FAD), flavin mononucleotide (FMN) and tetrahydrobiopterin, allows for the proper functioning of NOS in response to a rise in intracellular Ca²⁺ levels (17).

1.2.1 – eNOS, NO and vasodilation

NO, also known as the endothelium-derived relaxation factor (EDRF), plays a key role in signalling the smooth muscles surrounding blood vessels to relax, thus leading to increased blood flow. Found primarily in endothelial cells, eNOS contributes to such crucial functions as vasodilation, leukocyte adhesion and angiogenesis (18). Briefly, an extracellular signal leading to the increase in the secondary messenger inositol triphosphate causes the opening of Ca^{2+} channels in the endoplasmic reticulum (ER). The spike in Ca^{2+} concentrations activates eNOS and the formation of NO. The most prominent means by which NO exerts its signaling effects is via its binding to a heme group on soluble guanylyl cyclase which subsequently leads to its activation. The increase in cyclic guanosine monophosphate (cGMP) activates protein kinase G (PKG). The latter is responsible for the phosphorylation of myosin light chain phosphatase, thus activating this enzyme and dephosphorylating myosin light chains, which manifests itself as smooth muscle relaxation (19) (**Figure 1.4**).

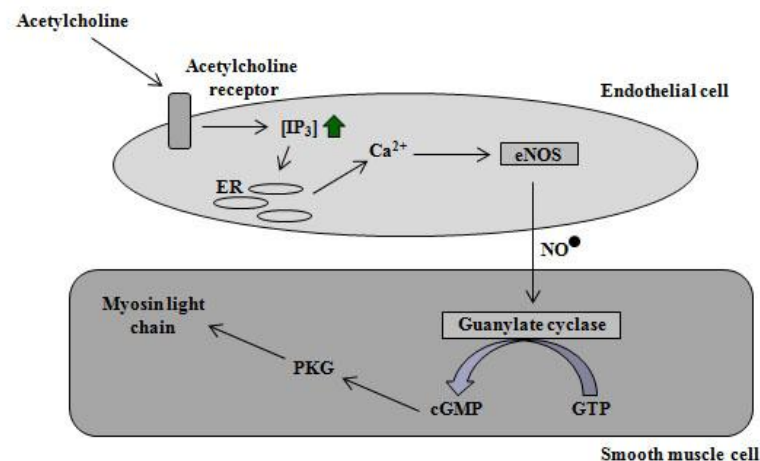


Figure 1.4 – eNOS and vasodilation. Autocrine signaling via NO allows endothelial cells to stimulate the relaxation of smooth muscle cells. IP₃: inositol triphosphate; GTP: guanosine triphosphate

1.2.2 – nNOS and neurotransmission

Immunohistochemistry assays on nNOS have uncovered this enzyme in a number of tissues, including the brain, spinal cord, sympathetic ganglia, adrenal glands and kidneys (20). This isoform has been implicated in such physiological functions as learning, memory and the generation of neurons. NO formed in brain tissues appears to act on N-methyl-D-aspartate receptors (NMDAR), whose stimulation is responsible for long-term potentiation, one of the major cellular mechanisms underlying learning and memory (21). The activation of NMDAR leads to the opening of a non-specific cation channel allowing the passage of Ca^{2+} which promotes nNOS activity. NO, a retrograde neurotransmitter, exerts its effects through soluble guanylyl cyclase as well as by S-nitrosylation of cysteine residues on a number of proteins, including glutamate receptors, alpha-tubulin, sodium pumps and metabolic enzymes such as glyceraldehydes-3-phosphate dehydrogenase (22). While the exact biological mechanisms have yet to be elucidated, abnormal NO signaling in neuronal tissues likely contributes to a variety of neurological disorders, such as multiple sclerosis, Alzheimer's and Parkinson's diseases. Other physiological functions of nNOS, such as the regulation of cardiac function and sexual arousal, further confound our understanding of this isoform (18).

1.2.3 – iNOS, a cornerstone of the innate immune system

While eNOS and nNOS are constitutively expressed, the gene for iNOS is only transcribed in response to specific agents. The latter include bacterial lipopolysaccharide, as well as cytokines such as interferon gamma and tumor necrosis factor, among others. While this enzyme can be found in any tissue, given the proper stimuli, its primary site of action is in

macrophages, a subset of white blood cells (18). This is also the only NOS isoform that operates independent of Ca^{2+} . As such, turnover is assured via strong inhibitory signals, such as those stemming from transforming growth factor beta, which represses iNOS expression (23). In macrophages, the primary function of iNOS is to kill invading pathogens via the formation of noxious concentrations of NO. The latter, in conjunction with superoxide ($\text{O}_2^{\bullet-}$) produced by NADPH oxidase, creates a highly oxidative environment (24,25). While NO in itself is relatively innocuous, the radical-radical coupling of this moiety with superoxide produces peroxynitrite (ONOO^-), a powerful oxidant. The entire subset of NO-derived intermediates is collectively known as reactive nitrogen species (RNS) (**Figure 1.5**).

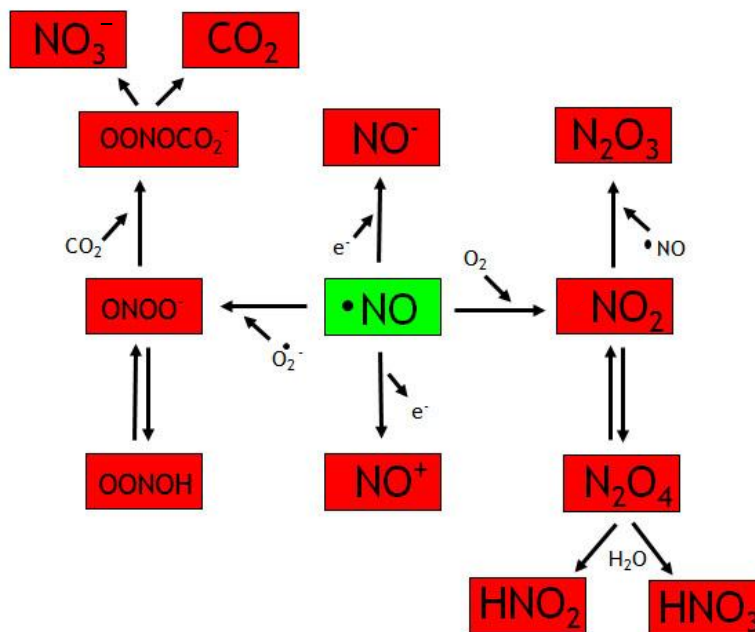


Figure 1.5 – Reactive nitrogen species. The high reactivity of NO may lead to the formation of a number of toxic intermediates, each with their own biological targets. Adapted from (25, 26).

While there is a degree of overlap between the biological targets of the various reactive nitrogen intermediates, some have a more specific modus operandi (**Table 1.1**). For instance, the nitrosylation of tyrosine residues is a hallmark of peroxynitrite formation, and a marker for several pathological conditions (26).

Table 1.1 – The biological targets of select reactive nitrogen species

<u>Reactive nitrogen species</u>	<u>Targets/Effects</u>
NO [•]	Heme groups; guanylyl cyclase; iron-sulfur proteins; zinc- and copper-containing proteins (26)
NO ⁻	Sulfhydryls and redox metals (26)
NO ⁺	-S, -N, -O, -C centers in organic molecules (26)
N ₂ O ₃	Nitrosation of amines; S-nitrosothiol formation; zinc finger degradation; inhibition of alkyl transferases (26)
ONOO ⁻	Tyrosine nitrosylation; sulfhydryls; iron-sulfur proteins; zinc-thiolates (25, 26)

The increase in RNS *in vivo* leads to the death of the invading microbe via the inhibition of key enzymes such as complex I and II of the electron transport chain, as well as the iron-sulfur cluster-containing aconitase and ribonucleotide reductase (18). Not only do microorganisms feel the burden of NO, but the strong induction of iNOS and the local inflammation brought about by ONOO⁻ has been linked to such disorders as arthritis and inflammatory bowel diseases (26)

1.3 – Bacterial defense systems against NO

Given the injurious effects of RNS, it isn't surprising that bacteria have elaborated mechanisms to detoxify these moieties. In most microorganisms, NO is predominantly managed via flavohemoglobin and flavorubredoxin. The former is a dioxygenase that catalyzes the conversion of NO to NO_3^- , using NADPH as a cofactor, while the latter is a reductase that creates N_2O in anaerobic conditions. Both proteins serve to mitigate the effects of NO on cellular functions, and are up-regulated in response to exogenous NO donors such as sodium nitroprusside (SNP) and diethylamine NONOate (25,27). In addition, the tripeptide and common antioxidant glutathione (GSH) can be S-nitrosylated by nitrogen oxides such as NO^+ and N_2O_3 . The product, S-nitrosoglutathione (GSNO), is transformed to glutathione disulfide (GSSG) and hydroxylamine (NH_2NO) via the activity of S-nitrosoglutathione reductase (GSNOR). The regeneration of GSH can then proceed using the enzyme glutathione reductase, allowing this peptide to resume its role as an antioxidant (28). These stress response proteins, and others like catalase and superoxide dismutase, fall under the regulatory control of such transcription factors as NsrR and NorR (29). Although other enzymes catalyzing the reduction of nitrite and nitrate have been identified, the entire repertoire exploited by microbes to help fend off nitrosative stress has not been uncovered (30,31).

Chapter 2: Thesis hypothesis and objectives

Macrophages are the first line of defense against menacing microorganisms and therefore play a crucial role in the immune response. Once recognized by these vigilant sentinels, foreign bodies are bombarded by the toxic radical nitric oxide (NO) in an endeavor to neutralize the threat to our body. Although some NO detoxifying mechanisms have been reported, relatively little attention has been paid to the effects of RNS on metabolic networks and the means by which microbes surmount deficiencies in the tricarboxylic acid (TCA) cycle and ETC. The dearth of research in this area is surprising when one considers the number of moieties in these pathways that display sensitivity to free radicals. Examples include the iron-sulfur clusters of aconitase and fumarase, metal centres and heme groups in complexes of the ETC, as well as lipoic acid in pyruvate and α -ketoglutarate dehydrogenases (PDH and KGDH, respectively).

Hypothesis

Most research on NO and RNS has converged on the mechanisms by which bacteria detoxify these compounds with the hope of finding key components for the development of new antimicrobial agents. Since the ETC is detrimentally affected by free radicals, it is hypothesized that the organism is coerced to reengineer metabolic networks to generate ATP by substrate-level phosphorylation (SLP). Using an array of biochemical techniques, it should be possible to unearth the targets of NO *in vivo*. Once these are ascertained, the means by which the bacterium circumvents the deleterious effects of RNS, including how it produces ATP, can be elucidated. With this knowledge in hand, it may be feasible to design novel therapeutic agents to counteract

microbial pathogens, so long as the biomolecules used to fend off RNS and synthesize ATP in bacteria have no human analogues.

Objectives

The objective of this work is to delineate the biological targets of nitrosative stress on the soil microbe *Pseudomonas fluorescens* using exogenous NO donors, such as sodium nitroprusside (SNP) and diethylamine NONOate (DEANO). Using a functional proteomic approach, via techniques such as blue native polyacrylamide gel electrophoresis (BN-PAGE), high performance liquid chromatography (HPLC) and immunoblotting, it should be possible to unearth the exact biological targets of NO and RNS. The metabolic versatility of this microbe, a feature of pseudomonads in general, renders it an ideal model organism for this work. In addition, the means by which this microbe counteracts the effects of SNP and DEANO will be investigated. This will be accomplished via an analysis of antioxidant defense systems, as well as enzymes mediating the catabolism of carbon sources and production of the energy currency ATP (e.g., oxidative and substrate-level phosphorylation). The cellular dysfunction initiated by RNS and systems mediating adaption to these moieties can provide cues to treat NO-resistant microbial invaders.

Chapter 3: The metabolic reprogramming evoked by nitrosative stress

It is a common misconception that central metabolic networks are static, where in fact, they are quite malleable. Typically, the consumption of glucose produces 2 ATP and 2 molecules of pyruvate which are then metabolized via the TCA cycle. The latter generates the reducing agent NADH, which can be used to synthesize ATP for cellular processes. However, ATP production is not the only function of these metabolic nodules, and variant TCA cycles and glycolytic pathways can arise, particularly under the insult of environmental stressors. These may include such threats as metal toxicity stemming from industrial pollution, radiation from nuclear waste as well as reactive oxygen species (ROS) and RNS (25).

The metabolic versatility displayed by pseudomonads allows these microbes to flourish in the presence of various sources of carbon and nitrogen. For instance, *P. fluorescens* isolated from wastewater has been shown to grow on compounds such as hexadecane and glycerol (32). Knowledge of the metabolic nodules underlying the adaptability of pseudomonads has strong applications in the fields of biotechnology and bioremediation. Indeed, *P. fluorescens* exposed to oxidative stress with glucose as the sole source of carbon stockpiles large concentrations of pyruvate. This is rendered possible via an up-regulation of the enzymes pyruvate kinase (PK) and phosphoenolpyruvate synthase (PEPS), while the ROS-mediated inhibition of PDH limits the entry of this ketoacid into the TCA cycle (33). Additionally, the pooling of pyruvate may help counteract the insult of H₂O₂, as the non-enzymatic decarboxylation of ketoacids allows them to act as antioxidants and scavenge ROS *in situ* (34,35).

When exposed to aluminum (Al) or gallium (Ga), two common industrial pollutants, *P. fluorescens* elects to metabolize citrate using a variant TCA cycle. In the latter, NAD-dependent

isocitrate dehydrogenase (ICDH-NAD) and KGDH show decreased activity and isocitrate is instead channeled towards ICDH-NADP and isocitrate lyase (ICL). This allows the organism to meet its ATP demands by SLP using the increased activity of succinyl-CoA synthetase to generate this moiety (36,37). In addition, this metabolic reprogramming provides the microbe with oxalate, a chelator of Al, which is used to bioprecipitate and decontaminate this metal. The ability of *P. fluorescens* to tolerate elevated concentrations of Al renders it an ideal candidate for the construction of bioreactors to treat metal-containing effluents (38).

In this chapter, the metabolic flexibility of *P. fluorescens* in regards to its adaptation to NO and RNS is analyzed. As carbon catabolite repression systems in pseudomonads show preference for organic acids such as citrate, this is used as the sole source of carbon for the growth of the organism (39). SNP, a cost-effective NO donor, is utilized to introduce a nitrosative environment. The effects of NO on the organism, including key biological targets and mechanisms to detoxify RNS, are shown. The diversion of citrate away from an ineffective TCA cycle in order to generate ATP anaerobically is discussed further herein.

**The metabolic reprogramming evoked by nitrosative stress triggers the anaerobic
utilization of citrate in *Pseudomonas fluorescens***

(Original Research)

Auger, C., Lemire, J., Cecchini, D., Bignucolo, A., and Appanna, V.D.

[Published in *PLoS One*]

Auger, C., Lemire, J., Cecchini, D., Bignucolo, A., Appanna, V.D. (2011) The metabolic reprogramming evoked by nitrosative stress triggers the anaerobic utilization of citrate in *Pseudomonas fluorescens*. *PLoS ONE* **6**:e28469.

Abstract

Nitrosative stress is an ongoing challenge that most organisms have to contend with. When nitric oxide (NO) that may be generated either exogenously or endogenously encounters reactive oxygen species (ROS), it produces a set of toxic moieties referred to as reactive nitrogen species (RNS). As these RNS can severely damage essential biomolecules, numerous organisms have evolved elaborate detoxification strategies to nullify RNS. However, the contribution of cellular metabolism in fending off nitrosative stress is poorly understood. Using a variety of functional proteomic and metabolomic analyses, we have identified how the soil microbe *Pseudomonas fluorescens* reprogrammed its metabolic networks to survive in an environment enriched by sodium nitroprusside (SNP), a generator of nitrosative stress. To combat the RNS-induced ineffective aconitase (ACN) and tricarboxylic acid (TCA) cycle, the microbe invoked the participation of citrate lyase (CL), phosphoenolpyruvate carboxylase (PEPC) and pyruvate phosphate dikinase (PPDK) to convert citrate, the sole source of carbon into pyruvate and ATP. These enzymes were not evident in the control conditions. This metabolic shift was coupled to the concomitant increase in the activities of such classical RNS detoxifiers as nitrate reductase (NR), nitrite reductase (NIR) and S-nitrosoglutathione reductase (GSNOR). Hence, metabolism may hold the clues to the survival of organisms subjected to nitrosative stress and may provide therapeutic cues against RNS-resistant microbes.

Introduction

Nitric oxide (NO) is a gaseous free radical bestowed with several crucial roles in living organisms. It has emerged as an important endogenous signaling molecule in organisms as diverse as mammals and plants. It is usually derived from arginine with the aid of the enzyme nitric oxide synthase (NOS) and is known to be a modulator of blood pressure in mammals. NO also regulates information in nervous systems and is a messenger for mitochondrial functions (40). In plants, the signaling roles of NO extend to germination, senescence, and cell wall construction (41). NO is also synthesized in the phagocytes in response to microbial infection where in combination with ROS, it generates highly toxic derivatives that are utilized to combat the bacterial invasion (42,43).

Nitrosative stress arises when the production of RNS outmatches an organism's ability to neutralize and dispose of them. These moieties are capable of damaging nucleic acids, lipids and amino acids. They disrupt proteins containing Fe-S clusters, transition metals, hemes, thiols and tyrosyl groups (25). These RNS-triggered modifications inhibit essential cellular metabolism, lead to irreversible damage and eventually to the demise of the organism. Hence, it is not surprising that intricate strategies are elaborated by living systems to eliminate the dangers posed by RNS. Numerous heme proteins are known to be induced by nitrosative stress and have been shown to play a pivotal role in countering RNS. For instance, flavohemoglobin and cytochrome C reductase enable *E. coli* to be resistant to excessive NO (25,44). GSNOR, catalase and NADPH-utilizing enzymes have all been reported to quell the toxic influence of RNS (43,45). Although the RNS-detoxifying role of these enzyme systems has been well documented, the participation of metabolism in combating the dangers posed by NO has yet to be fully uncovered.

In this study, we have evaluated the metabolic responses of *P. fluorescens* to nitrosative stress. Owing to its nutritional versatility, and its ability to adapt to diverse environmental situations, this bacterium affords an excellent model system to study global metabolic processes. It appears that *P. fluorescens* reprograms its metabolism in an effort to utilize citrate in an anaerobic fashion. Faced with an ineffective ACN, the organism up-regulates CL, a stratagem designed to bypass the TCA cycle and oxidative phosphorylation. The subsequent generation of the high-energy metabolite phosphoenolpyruvate (PEP) allows for ATP synthesis via substrate-level phosphorylation. The pivotal role of metabolism in the adaptation to nitrosative stress and its significance in countering RNS-resistant bacteria are discussed.

Materials and Methods

Bacterial culture and isolation of cellular fractions

The bacterial strain *P. fluorescens*, ATCC 13525, was maintained (on 2% agar) and grown in a phosphate mineral medium containing Na₂HPO₄ (6 g), KH₂PO₄ (3 g), MgSO₄·7H₂O (0.2 g), NH₄Cl (0.8 g), and citric acid (4 g) per litre of distilled and deionized H₂O. Trace elements were added. Nitrosative stress was induced via the addition of 1, 5, 10, 15 or 20 mM of sodium nitroprusside (SNP), respectively (25). Control cultures had no added SNP and/or contained 10 mM sodium ferrocyanide (SFC). The latter has a similar composition to SNP except for the absence of the nitroso functional group and hence is unable to act as a source of NO. For select experiments, nitrosative stress was initiated by the addition of 1 mM diethylamine NONOate (DEANO), in an effort to ascertain if indeed NO was the stressor and not any other component of SNP. The only similarity between SNP and DEANO is their ability to generate NO. The pH was adjusted to 6.8 with dilute NaOH. The media was then dispensed in aliquots of 200 mL into 500 mL Erlenmeyer flasks with foam plugs and autoclaved for 20 min at 121°C. Inoculations were made with 1 mL of stationary phase cells grown in a control culture and aerated on a gyratory water bath shaker (Model 76; New Brunswick Scientific). To ensure an ongoing nitrosative response, a second dose of DEANO was introduced after 16 hours of growth. Cells and spent fluids were isolated at various growth phases.

P. fluorescens cells were pelleted by centrifugation at 10,000 x g for 10 min at 4°C. After a washing with 0.85% NaCl, cells were resuspended in cell storage buffer consisting of 50 mM Tris-HCl, 5 mM MgCl₂ and 1 mM phenylmethylsulphonyl fluoride (pH 7.3). Cells were disrupted ultrasonically and then centrifuged at 3,000 x g for 30 min at 4°C to remove intact

bacteria. The supernatant was collected and centrifuged at 180,000 x g for 3 h, resulting in a soluble cell free extract (CFE) and a membrane CFE. The soluble fraction was further centrifuged at 180,000 x g for 1 to obtain a membrane-free system. The Bradford assay was performed in triplicate in order to quantify the protein contents and bovine serum albumin was used as the standard (46). Purity of the fractions was ascertained as described in (47). These CFE fractions were kept at 4°C for up to 5 days or frozen at -20°C for storage up to a maximum of 4 weeks. The pH of the spent fluid was also recorded.

Metabolomic studies in cell-free extracts: selective inhibition of PEPC

Spent fluid and soluble CFE from control and SNP-stressed cells were used to determine various metabolite levels via high performance liquid chromatography (HPLC). Two mg/mL of protein equivalent of soluble CFE was heated gently for 10 minutes to precipitate proteins and lipids and analyzed by HPLC as described in (48). To verify the disparate citrate metabolism, 2 mg/mL protein equivalent of soluble CFE was incubated for 2 hrs at 26°C in a reaction buffer (25 mM Tris, 5 mM MgCl₂; pH 7.0) containing 2 mM citrate and 0.5 mM nicotinamide adenine dinucleotide phosphate (NADP). To confirm the importance of PEPC in the metabolic adaptation to SNP, 2 mg/mL protein equivalent of soluble CFE was incubated for 30 min in reaction buffer containing 2 mM citrate, 1.0 mM P_i and 0.5 mM AMP with or without a 1:500 dilution of antibody against PEPC. Chemical shifts were referenced to standard compounds and internal standards under the same conditions and the peaks were quantified using the Empower Software (Waters Corporation). The HPLC was standardized using a five-point calibration protocol prior to each injection. The relative quantities of nitrite and nitrate in the various cellular components were monitored by Griess reaction (49).

Blue Native PAGE and in-gel enzyme activity staining

Blue Native (BN) polyacrylamide gel electrophoresis (PAGE) and in-gel activity staining were performed as described previously (48,50). Soluble proteins from *P. fluorescens* were prepared in a native buffer (50 mM Bis-Tris, 500 mM ϵ -aminocaproic acid, pH 7.0, 4°C) at a final concentration of 4 mg of protein per ml. Membrane proteins were prepared in a similar manner except 1% (v/v) β -dodecyl-D-maltoside was added to the preparation to facilitate the solubilization of the membrane-bound proteins. To ensure optimal protein separation, 4–16% linear gradient gels were cast with the Bio-Rad MiniProtein™ 2 system using 1 mm spacers. Sixty micrograms of protein from soluble or membrane CFE was loaded into the wells. Gels were electrophoresed as described in (51). Following electrophoresis, gel slabs were equilibrated for 15 min in a reaction buffer (25 mM Tris-HCl, 5 mM MgCl₂, at pH 7.4). Enzyme activities were detected in the gel by the reduction and precipitation of iodinitrotetrazolium (INT) as formazan.

ACN activity was visualized using a reaction mixture consisting of a reaction buffer, 5 mM citrate, 0.5 mM NADP, 5 units/mL isocitrate dehydrogenase (Sigma), 0.2 mg/mL phenazine methosulfate (PMS) and 0.4 mg/mL of INT. Tricarballic acid (1 mM) was utilized to maintain the stability of ACN (52). NADP-dependent isocitrate dehydrogenase (ICDH-NADP) activity was visualized using a reaction mixture containing 5 mM isocitrate, 0.5 mM NADP, 0.2 mg/mL PMS and 0.4 mg/mL INT. The same reaction mixture was utilized for ICDH-NAD except 0.5 mM nicotinamide adenine dinucleotide (NAD) was utilized in lieu of NADP. The activity band for isocitrate lyase (ICL) was made apparent using reaction buffer, 5 mM isocitrate, 0.5 mM NAD, 10 units of lactate dehydrogenase (LDH), 0.2 mg/mL of PMS and 0.4 mg/mL of INT. Complex 1 was detected by the addition of 5 mM NADH, and 0.4 mg/mL INT. Succinate

dehydrogenase (SDH) was monitored by the addition of 60 mM succinate, 5 mM KCN, 0.2 mg/mL of PMS and 0.4 mg/mL of INT (53). Complex IV was assayed by the addition of 10 mg/mL of diaminobenzidine, 10 mg/mL cytochrome C, and 562.5 mg/mL of sucrose. 5 mM KCN was added to the reaction mixture to confirm the identity of Complex IV (54). Malate dehydrogenase (MDH) was assayed by the addition of 5 mM malate, 0.5 mM NAD, 0.2 mg/mL of PMS and 0.4 mg/mL of INT. The activity of acetate kinase was assessed with a reaction mixture of 5 mM acetyl phosphate, 1 mM ADP, 5 mM glucose, 10 units of glucose-6-phosphate dehydrogenase (G6PDH), 10 units hexokinase, 1 mM NADP, 0.2 mg/mL of PMS and 0.4 mg/mL of INT.

Pyruvate dehydrogenase (PDH) was detected utilizing a reaction mixture consisting of 5 mM pyruvate, 0.1 mM CoA, 0.5 mM NAD, 0.2 mg/mL of PMS and 0.4 mg/mL of INT. LDH was assayed using a reaction mixture containing 5 mM lactate, 0.5 mM NAD, 0.2 mg/mL of PMS and 0.4 mg/mL of INT. For NAD(P)-producing enzymes PMS was replaced by 2,4-dichloroindophenol (DCIP) as the electron coupler (51). The activities of CL, phosphoenolpyruvate carboxykinase (PEPCK) and pyruvate carboxylase (PC) were ascertained by utilizing enzyme-coupled assays as described in (51). PEPC was assayed in a similar manner as PEPCK except no ADP was present in the mixture. Pyruvate kinase (PK) was probed as described in (55). PPDK was monitored using a reaction mixture consisting of 5 mM PEP, 0.5 mM AMP, 0.5 mM sodium pyrophosphate, 0.5 mM NADH, 10 units of LDH, 0.0167 mg/mL of DCIP and 0.4 mg/mL of INT. S-nitrosoglutathione (GSNO) was freshly prepared by adding 1 mL of a 100 mM solution of reduced glutathione (GSH) to 1 mL of a 100 mM solution of sodium nitrite (in 0.1% HCl) (56). The concentration of GSNO was determined ($\epsilon = 908 \text{ M}^{-1} \text{ cm}^{-1}$ at 334 nm) and a reaction mixture consisting of 5 mM GSNO, 0.5 mM NADPH, 0.0167 mg/mL of

DCIP and 0.4 mg/mL of INT was prepared in order to determine the in-gel activity. All the enzymes were probed individually in separate gels.

The activities of NR and NIR was verified using a reaction mixture consisting of 5 mM sodium nitrate or 5 mM sodium nitrite, respectively, 0.5 mM NADPH, 0.0167 mg/mL of DCIP and 0.4 mg/mL of INT. Once bands reached their desired intensities, reactions were halted using destaining solution (40% methanol, 10% glacial acetic acid). Band specificity was ascertained by performing activity stains in the absence of substrate. Activity bands were quantified using SCION Image for Windows (SCION Imaging Corp.). Proper protein loading was determined by Coomassie staining for total proteins. Select activity bands were routinely cut and incubated with their respective substrates. The metabolite profiles were monitored by HPLC. Unless otherwise mentioned, all comparative experiments were performed at the late logarithmic phase of growth.

2D SDS-PAGE and protein expression

For 2D SDS-PAGE, the activity bands for CL were excised and soaked for 30 min in a solution of 1% (w/v) SDS and 1% (v/v) 2-mercaptoethanol. The bands were rinsed twice for 10 s with SDS-PAGE electrophoresis buffer (25 mM Tris-HCl, 192 mM glycine and 0.1% (w/v) SDS; pH 8.3) then placed vertically in the wells of a 10% SDS gel (8×7 cm). Electrophoresis was conducted at 80 V at room temperature until the proteins reached the separating gel. The voltage was then raised to 200 V until completion. Upon completion of the SDS-PAGE, gels were stained with the Bio-Rad Silver Staining Kit.

Recovery experiments

To ascertain that nitrosative stress was indeed triggering these metabolic changes, the SNP-treated cells grown to late logarithmic phase were transferred into control medium (without SNP). Similar experiments were performed with control cells transferred to SNP-containing medium. Following an 8 h incubation period, the cells were harvested, and CFE was assayed for protein concentration and enzymatic activity.

In-cell Western blot analyses

In-cell Western assays were modified from the Odyssey® Infrared Imaging System protocol document (Li-cor doc# 988-08599). Briefly, *P.fluorescens* was seeded in 96-well plates from a pre-culture for 8 h and treated with control, 5 mM SNP, or 10 mM SNP conditions for 24 h. Recovery experiments were performed as described previously. After treatment, the media was removed and the cells were washed thrice with phosphate buffered saline (PBS) [136.8 mM NaCl, 2.5 mM KCl, 1.83 mM Na₂HPO₄, and 0.4313 mM KH₂PO₄ at pH 7.4]. The cells were then fixed with 37% formaldehyde for 20 min at room temperature. The fixing solution was then removed and the cells were rinsed with PBS containing 0.1% tween-20. Blocking ensued using the Odyssey® blocking buffer for 2 h. Primary antibody incubations occurred over a 1 h period with gentle shaking. Mouse monoclonal anti-NO-tyrosine (Abcam), rabbit polyclonal anti-PEPC (Abcam) and rabbit polyclonal anti-glutamate dehydrogenase (GDH) were all diluted to a concentration of 1:200 in blocking buffer. GDH was utilized as an internal standard for this assay as its expression did not vary significantly with the culture conditions. Secondary antibodies consisted of donkey anti-mouse IR 680 (Li-cor; red) and goat anti-rabbit IR-780 (Li-cor; green) diluted to 1:1000. Relative levels were compared to an in-cell Bradford assay. The

infrared signal as well as the signal from the Bradford reagent was detected using an Odyssey® Infrared Imager (Li-cor).

Statistical analysis

Data were expressed as means \pm standard deviations. Statistical correlations of the data were checked for significance using the Student t test ($p \leq 0.05$). All experiments were performed at least twice and in triplicate.

Results

Bacterial growth, RNS stress and citrate consumption

P. fluorescens survived in a 10 mM SNP-stressed environment with minimal change in growth rate or cellular yield in comparison to cells grown in the control media (**Figure 3.1**). Cultures subjected to concentrations of 15 and 20 mM SNP showed severely retarded growth and no growth at all, respectively. It may be within the realm of possibilities that at these higher concentrations the physico-chemical properties of SNP in the medium utilized were conducive to the easier release of the toxicant. As SNP is known to liberate NO, it was critical to verify that this gaseous radical was being released and detoxified to the relatively innocuous nitrite/nitrate (NO₂/NO₃) (57). An increase in the concentration of NO₂ and NO₃ in 5 and 10 mM SNP-stressed cells relative to the control was observed (**Figure 3.1 - A**). In the soluble CFE isolated from the 10 mM SNP cultures, there was 6 fold more NO₂/NO₃ than the control (data not shown). Furthermore, while in the presence of SFC, no significant change in NO₂ or NO₃ was evident, in the DEANO-treated cells, these moieties were relatively higher (data not shown). Nitrosylated proteins were also more abundant in the stressed cell. Indeed, Western blot with nitrotyrosine antibody helped detect higher levels of this residue in the cells subjected to nitrosative stress (**Figure 3.1 - B**). Thus, it was evident the toxicity of SNP was being felt by the microbe.

Figure 1

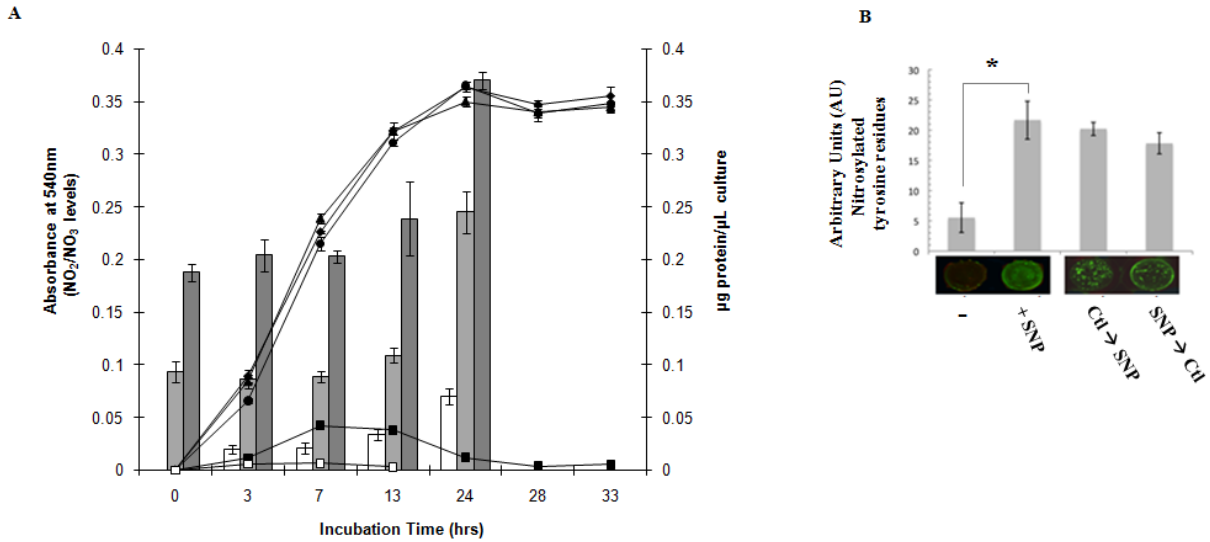


Figure 3.1 - Nitrosative stress in *P. fluorescens*. *A*, cellular yield: ▲, control cultures; ◆, 5 mM SNP-containing cultures; ●, 10 mM SNP-containing cultures; ■, 15 mM SNP-containing cultures; □, 20 mM SNP-containing cultures. Nitrite/nitrate levels in spent fluids as measured by their absorbance at 540 nm after the Griess assay: □, control cultures; ■, 5 mM SNP-containing cultures; ■, 10 mM SNP-containing cultures. *B*, In cell Western blot analysis of *P. fluorescens* under nitrosative stress. *P. fluorescens* was grown to late logarithmic phase in 96 well plates and then treated with control (-) and 10 mM SNP conditions for 24h (+ SNP). Following treatment, control cells were placed in media containing 10 mM SNP for 8 h (Ctl → SNP) and 10 mM SNP-treated cells were recovered with control media for 8 h (SNP → Ctl). Total protein concentration was assessed by the Bradford assay. The cells were then analyzed for expression of nitrosylated tyrosine residues by quantification of infrared fluorescence (n = 3. *p ≤ 0.01, mean ± standard deviation).

The RNS detoxifying enzymes

The protection against RNS has been shown to be mediated by a variety of enzyme systems involved in the direct conversion of NO into innocuous products and the denitrosylation of nitrosylated proteins (25). To ascertain if these detoxification strategies were invoked by *P. fluorescens* subjected to SNP, we probed NIR and NR. The activities of these enzymes were monitored by BN-PAGE and were found to be elevated in the SNP-stressed cells compared to the control cells (**Figure 3.2 - A**). GSNOR, an enzyme that generates reduced glutathione was identified as two isoforms in the *P. fluorescens* challenged by nitrosative stress. Their activities were markedly higher compared to the control cells (**Figure 3.2 - B**). Catalase, a detoxifying enzyme involved in the regulation of peroxide levels, was found to be 2 fold higher in activity in the SNP-treated cells (data not shown).

Figure 2

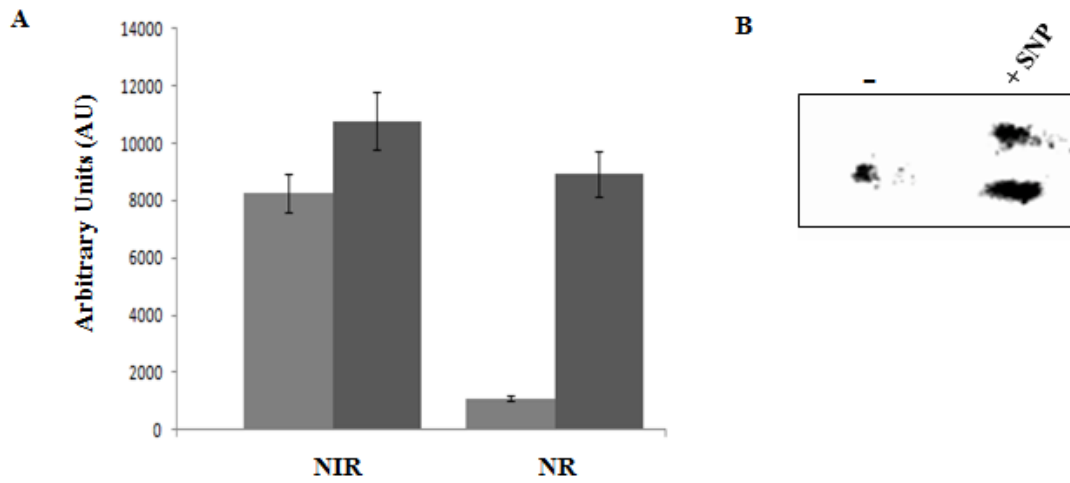


Figure 3.2 - RNS detoxifying mechanisms in *P. fluorescens*. A, BN-PAGE analysis of NIR and NR from membrane CFE: ■, control cultures; ■, 10 mM SNP-treated cultures. Bands were quantified using SCION Imaging Software (n = 3, mean \pm standard deviation). B, activity staining of GSNOR in soluble CFE (-, control cultures; + SNP, 10 mM SNP-treated cultures).

The tricarboxylic acid cycle and oxidative phosphorylation

As citrate was the sole source of carbon in this defined medium, it was important to verify how this tricarboxylic acid was metabolized in the control and SNP-stressed cells. The cells subjected to nitrosative stress had significantly more PEP, pyruvate and acetate than the control cells while levels of citrate, succinate and α -ketoglutarate were found to be lower in the stressed CFE (**Figure 3.3 - A**). The identities of these metabolites were further confirmed by spiking the samples with known standards. The heterogeneity of these metabolic profiles prompted us to examine the enzymatic adjustments that would provoke such a change.

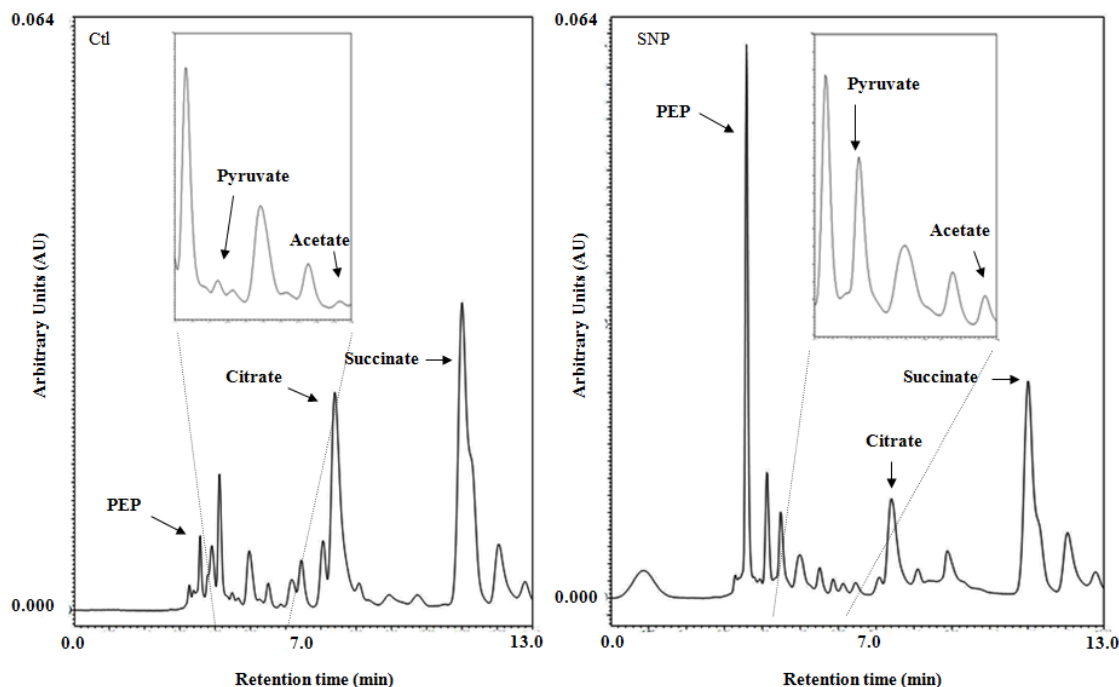
Since nitrosative stress is known to affect Fe-S clusters (58), it was important to evaluate ACN, a critical gate-keeper of the tricarboxylic acid cycle. It isomerizes citrate into isocitrate with the aid of a 4Fe-4S cluster located in its active site (58). The stressed cells did not show any activity band (**Figure 3.3 - B**) As reported before, a sharp band was evident in the control (36,52,53). This finding led us to probe enzymes further downstream in the TCA cycle that might be able to compensate for this shortcoming.

Two isocitrate metabolizing enzymes, ICDH-NAD and ICL, were shown to be markedly decreased as indicated by the lack of a formazan band in the lane containing proteins from the stressed fraction (**Figure 3.3 - C**). The activity of ICDH-NADP, a cytoplasmic enzyme which produces NADPH and α -ketoglutarate, was also found to be significantly downregulated in the SNP-stressed culture compared to the control culture (**Figure 3.3 - D**). Indeed, in the presence of NO, key cysteine and tyrosine residues in this enzyme have been shown to be modified (59). The activity of ICDH-NADP was preserved in *P. fluorescens* treated with 10 mM SFC, a chemical analog to SNP not containing the nitroso functional group (**Figure 3.3 - D**). As the TCA cycle was perturbed, it was important to evaluate the status of oxidative phosphorylation, a Fe-S

cluster rich enzyme network dedicated to the production of ATP. All the complexes (I, II, IV) that were monitored were found to be ineffective. Activity bands indicative of these proteins were barely discernable in the membrane CFE from the SNP-stressed cells (**Figure 3.3 - C**) [the activity of complex IV was preserved in *P. fluorescens* treated with 10 mM sodium ferrocyanide (**Figure 3.3 - D**)]. These bands reappeared when the RNS-stressed cells were incubated in the control media. These enzymes were similarly affected in the DEANO treated cells (data not shown).

Figure 3

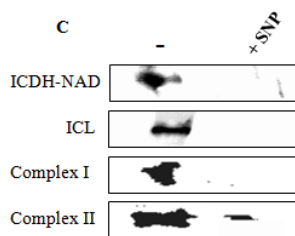
A



B



C



D

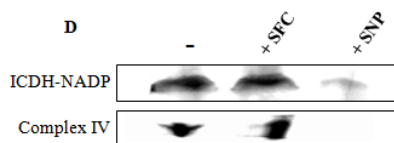


Figure 3.3 - Influence of NO on the TCA cycle. A, Representative chromatographs showing metabolite levels in soluble CFE from *P. fluorescens* grown in control and 10mM SNP-containing cultures. B, In-gel activity analysis for ACN. C, in-gel activity staining of key metabolic enzymes. D, activity stains with sodium ferrocyanide as a control (-, control cultures; + SNP, 10 mM SNP-treated cultures; + SFC, 10 mM SFC-treated cultures).

CL activity, expression and regulation

The apparent inability of SNP-stressed cultures to metabolize citrate via the TCA cycle prompted us to evaluate other alternative pathways for citrate consumption. The presence of elevated levels of acetate in the SNP-stressed cells pointed toward a possible role of CL. This enzyme can cleave citrate into oxaloacetate and acetate without the participation of ATP and coenzyme A (60,61). In this instance, CL generated oxaloacetate and acetate in the absence of ATP and coenzyme A. It increased in a time-dependent manner in the SNP-stressed cultures (**Figure 3.4 - A**). CL was also found to be modulated by the levels of SNP in the medium (**Figure 3.4 - A**). To confirm that the increased activity of this enzyme was the result of NO and not other components of SNP, the activity was monitored in cells treated with DEANO and found to be up-regulated in these cultures (**Figure 3.4 - A**). Furthermore, CL was not visible in cells subjected to 5 mM NO₂ or NO₃, indicating that this is a NO-mediated occurrence (data not shown). BN-PAGE followed by 2D SDS-PAGE revealed that the expression of this enzyme was up-regulated in the SNP-stressed cells (**Figure 3.4 - B**). In an effort to prove that nitrosative stress was indeed promoting the up-regulation of this enzyme, control cells were transferred in the stressed medium and stressed cells in the control cultures. A reverse trend in the activity of CL was observed (**Figure 3.4 - C**). When the soluble CFE from both control and stressed were incubated with citrate respectively, oxaloacetate and acetate was observed only in the latter. However, in the presence of NADP, the control CFE readily produced α -ketoglutarate and NADPH (**Figure 3.4 - D**). These observations clearly demonstrated that CL was an important component of the metabolic reconfiguration evoked by nitrosative stress in *P. fluorescens*.

Figure 4

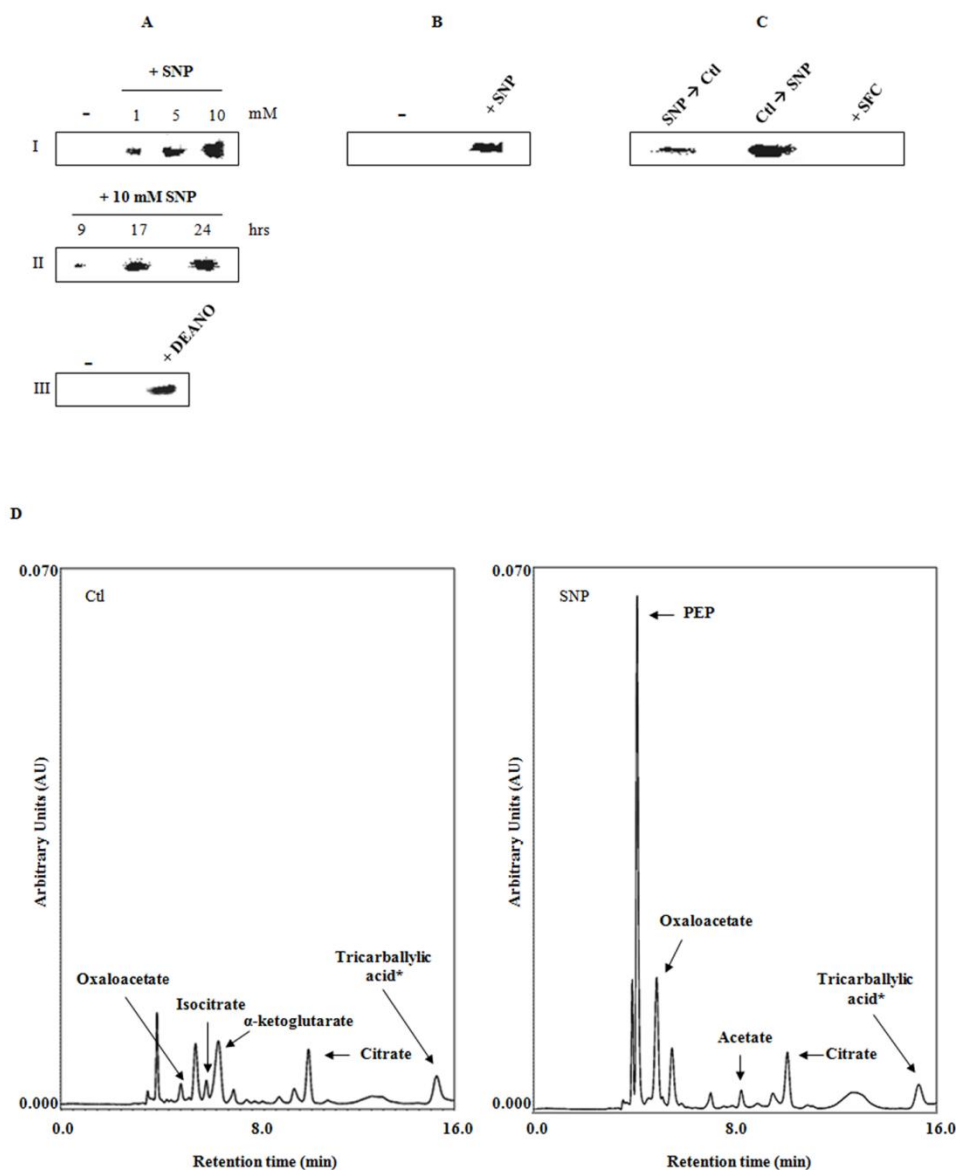


Figure 3.4 - Activity and expression analysis of CL from *P. fluorescens*. A, in-gel CL activity in soluble CFE isolated from *P. fluorescens*. **I)** The dose effect of SNP on CL activity **II)** Time dependence of CL activity in cultures treated with 10 mM SNP. **III)** CL activity in media containing 1 mM DEANO (-, control cultures; + DEANO, 1 mM DEANO-treated cultures). B, 2D SDS-PAGE (-, control cultures; + SNP, 10 mM SNP-treated cultures). C, regulation of CL activity by SNP. 10 mM SNP-treated cells were grown to late logarithmic phase then transferred to control media for 8 h and vice versa. D, HPLC analysis of CL activity. Soluble CFE from cells grown in control and 10 mM SNP-treated media were given 5 mM citrate and 0.5 mM NADP for 2 hrs (*: tricarballic acid (1 μ M) as internal standard).

Oxaloacetate and pyruvate metabolism: The role of PEPC

As oxaloacetate was readily available in the SNP-stressed cells due to the upregulation of CL, it was important to decipher how this dicarboxylic acid was being metabolized. PEPC, PEPCCK and MDH can all interact with oxaloacetate. The activity of MDH was found to be lower in the SNP-stressed system (**Figure 3.5 - A**). However, unexpectedly, the PEPC activity that was elevated in the *P. fluorescens* challenged with SNP was barely discernable in the untreated cultures (**Figure 3.5 - A**). This enzyme mediates the conversion of oxaloacetate in the presence of inorganic phosphate into the high energy PEP (62). Western blots performed in these cells demonstrated that the increase in PEPC activity in stressed bacteria was directly correlated to increased expression of this protein (**Figure 3.5 - B**). PEPCCK, the other enzyme that transforms oxaloacetate into PEP with the participation of ATP or GTP was also elevated in the cells subjected to nitrosative stress (**Figure 3.5 - A**). Hence these two enzymes were aiding the production of the high energy PEP, a metabolite that was abundant in the stressed cells. The production of PEP was found to be drastically reduced in SNP-stressed CFE treated with an antibody against PEPC. Although citrate was consumed, albeit to a lesser extent compared to the reaction without antibodies, the formation of PEP, a key metabolite essential in the production of ATP and pyruvate was severely affected (**Figure 3.5 - C**).

The presence of increased pyruvate and acetate in the soluble CFE from the stressed cells coupled with the enhanced production of PEP directed our attention towards the homeostasis of pyruvate. PK and PPDK are the two main participants in the conversion of PEP into pyruvate with the concomitant formation of ATP. The former utilizes ADP while the latter invokes the participation of AMP and PP_i as the cofactors (63). Interestingly, the activity of PK was lower in the RNS-challenged environment, while the activity of PPDK was sharply increased compared to

the control cells (**Figure 3.5 - D**). This enzymatic manipulation would indeed allow RNS-challenged *P. fluorescens* to generate ATP more efficiently. Indeed, when soluble CFE from SNP or DEANO-treated cells was incubated with oxaloacetate and AMP, ATP and pyruvate were readily formed (data not shown). As pyruvate and acetate were seemingly the end products of this metabolic reconfiguration, it was important to analyze enzymes that may be involved in their consumption. The activities of PDH, LDH and PC were all found to be lower in *P. fluorescens* exposed to nitrosative stress (**Figure 3.6 - A**). This would indeed result in the pooling of pyruvate as seen in the soluble CFE. The activity of acetate kinase was found to be up-regulated in the treated cells (**Figure 3.6 - B**), indicating a role for acetate in energy storage.

Figure 5

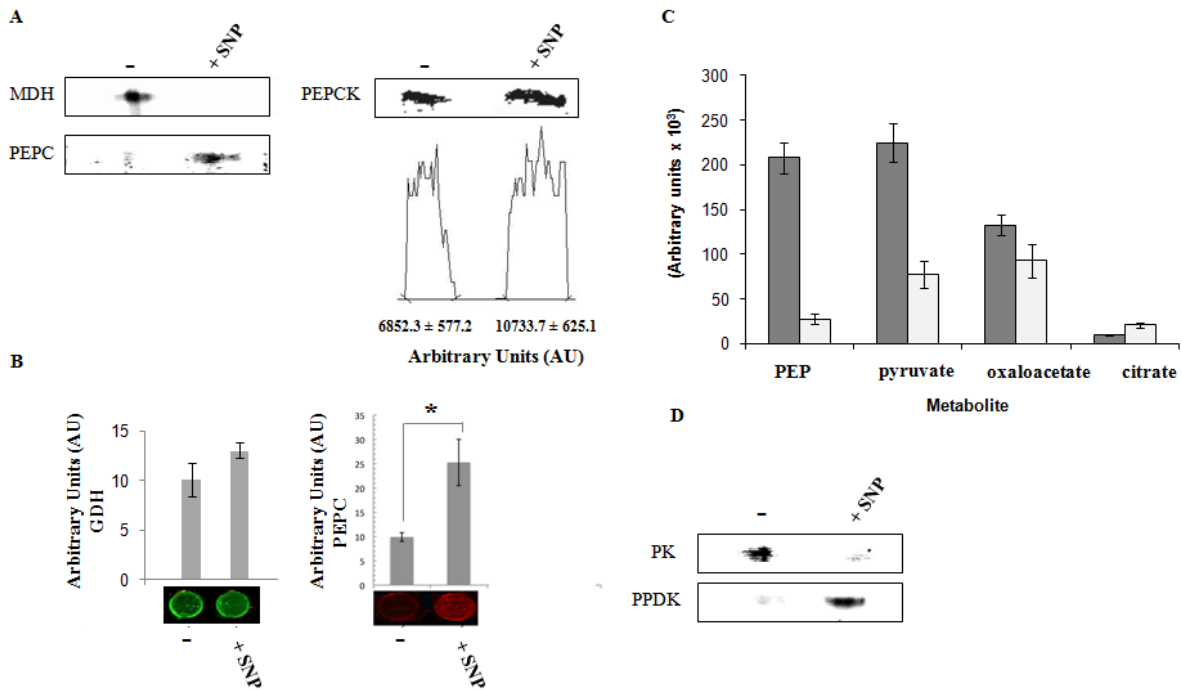


Figure 3.5 - Oxaloacetate and PEP metabolism. A, BN-PAGE analysis of oxaloacetate metabolizing enzymes. Bands were quantified using SCION Imaging Software ($n = 3 \pm$ standard deviation). B, In-cell Western blot analysis. *P. fluorescens* was grown to late logarithmic phase in 96 well plates then treated with control (-) and 10 mM SNP conditions for 24 h (+ SNP). The cells were then analyzed for (GDH) and (PEPC) and expression was quantified by infrared fluorescence ($n = 5$, mean \pm standard deviation. $*p \leq 0.01$). C, Citrate consumption in *P. fluorescens* exposed to nitrosative stress. Soluble CFE from 10 mM SNP-treated cells was incubated with 2 mM citrate, 1.0 mM Pi and 0.5 mM AMP for 30 min without (■) and with an antibody (1:500 dilution) against PEPC (□). $n = 3$, mean \pm standard deviation. D, in-gel activity stain of the pyruvate generating enzymes PK and PPDK (-, control cultures; + SNP, 10 mM SNP-treated cultures).

Figure 6

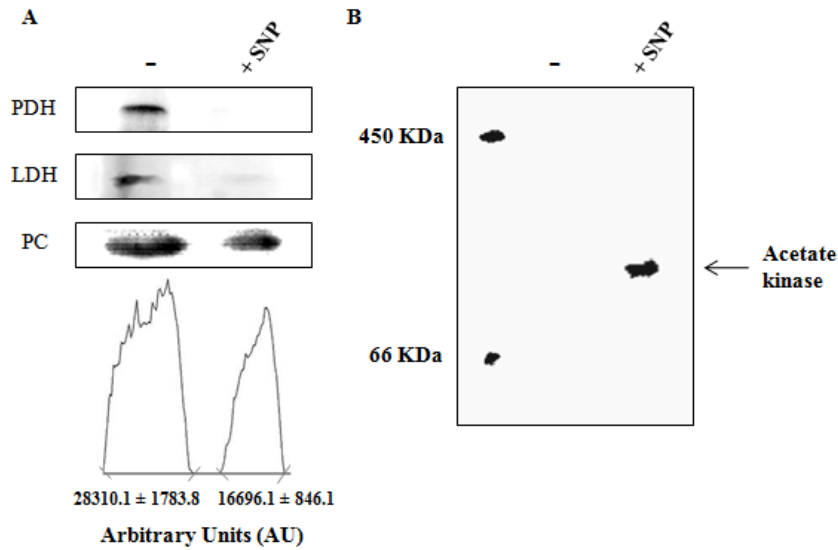


Figure 3.6 - Pyruvate and acetate utilizing enzymes. A, BN-PAGE analysis of pyruvate metabolizing enzymes. Bands were quantified using SCION Imaging Software ($n = 3 \pm$ standard deviation). B, activity staining of acetate kinase in membrane CFE (-, control cultures; + SNP, 10 mM SNP-treated cultures). BSA and ferritin were utilized as molecular mass markers to ensure proper migration.

Discussion

Although the involvement of enzymes mediating the detoxification of RNS has been widely reported, this study is the first demonstration of the pivotal role metabolism plays in combating nitrosative stress. The microbe utilizes its various metabolic networks to not only circumvent the toxic impact of RNS but also to generate energy via substrate-level phosphorylation. There is a body of literature detailing the different heme enzymes that participate in the formation of relatively non-toxic nitrate. In *E. coli*, both flavohemoglobin and a cytochrome C nitrate reductase have been implicated in the elimination of NO as NO₃ (25). In this instance, it appears that *P. fluorescens* does indeed utilize both nitrite and nitrate reductase to perform this task. Catalase, an enzyme involved in the detoxification of H₂O₂ was upregulated in the cells exposed to nitrosative stress. This is in accordance with numerous studies demonstrating the elevation of catalase activity in organisms subjected to RNS (64,65). GSNOR is an important enzyme that contributes to the survival of organisms subjected to nitrosative stress associated with the innate immune response of the human body (43). The two isoforms that showed increased activities in the SNP-challenged *P. fluorescens* may be indeed aimed at minimizing S-nitrosothiols and S-nitrosylated proteins, hallmarks of nitrosative stress.

The participation of these classical RNS-detoxifying enzymes in fending off nitrosative stress was not surprising. However, the metabolic reprogramming aimed at circumventing RNS that was observed in *P. fluorescens* is indeed a seminal finding, a phenomenon that has yet to be fully delineated. Faced with citrate, the sole source of carbon and a RNS-induced ineffective ACN and ICDH, the microbe has to find an alternative pathway to degrade citrate if it is to survive. In this instance, an ATP and coenzyme A independent CL was invoked. This enzyme mediates the formation of oxaloacetate and acetate and is common in microbial systems

subjected to anaerobiosis (66). This is not surprising as RNS severely damage the ETC and limit aerobic respiration (67). In our study, the three ETC complexes that were probed were found to be markedly ineffective. Furthermore, the inactivation of ICDH and α KGDH would impede the functioning of the TCA cycle, an adaptation critical for survival under nitrosative stress. Although ACN was found to be ineffective, it may be quite possible that this enzyme that exists in three isoforms was not detected under our experimental conditions (68).

The dicarboxylic acid, oxaloacetate was subsequently metabolized to PEP by PEPC. This enzyme primarily has an anaplerotic role in the production of oxaloacetate. However, in this study as the microbe was supplied with citrate, the sole carbon source, oxaloacetate was readily available due to upregulation of CL. Hence, it is quite conceivable that this dicarboxylic acid may be an important source of PEP. Although PEPCK with enhanced activity was evident in the RNS-stressed cells, PEPC was more prominent. The latter enzyme was not discerned in the control cultures. The inability of PEPC-inhibited CFE to generate PEP effectively suggests that this enzyme is critical in this adaptation process. The production of PEP from oxaloacetate may also have been favored due to the close proximity of this protein with PPDK, an enzyme mediating the synthesis of pyruvate and ATP with AMP and PP_i as cofactors. These enzymes migrate in association with CL, as observed by BN-PAGE. The incubation of this band did generate all the products with citrate, AMP and pyrophosphate (PP_i) as substrates (data not shown).

The presence of elevated amounts of acetate in the soluble CFE from the stressed cells directed our attention to a possible role of pyruvate in the non-enzymatic neutralization of RNS. Pyruvate has been shown *in vivo* to react with RNS to liberate acetate (69). Furthermore, there is a body of literature on the utilization of pyruvate and other ketoacids as anti-oxidants (70,71).

We have recently demonstrated the role of α KG in the scavenging of ROS with the concomitant formation of succinate (48,72). The elevated levels of acetate kinase and the accumulation of pyruvate from citrate metabolism would suggest that *P. fluorescens* may be utilizing this keto acid to quell oxidative and nitrosative stress. However, these postulations have to await further investigation.

In conclusion, our findings reveal an intriguing role of metabolism in the adaptation of *P. fluorescens* to a nitrosative environment (**Figure 3.7**). Although the classical RNS-detoxifying enzymes were invoked, the microbe also completely reprogrammed its metabolic networks to survive this toxic challenge. The noxious impact of RNS on the TCA cycle and oxidative phosphorylation was mitigated by the upregulation of CL, an enzyme that degraded citrate into oxaloacetate and acetate. The dicarboxylic acid subsequently provided the two ingredients, pyruvate and ATP, that ensured the survival of *P. fluorescens* under the insult of SNP. Thus, metabolic changes are the underlying force at the centre of most, if not all, molecular adaptation phenomena and necessary in the anti-RNS defense strategy in this microbe. Targeting the critical components of these metabolic networks may provide a potent tool against RNS-resistant bacteria.

Figure 7

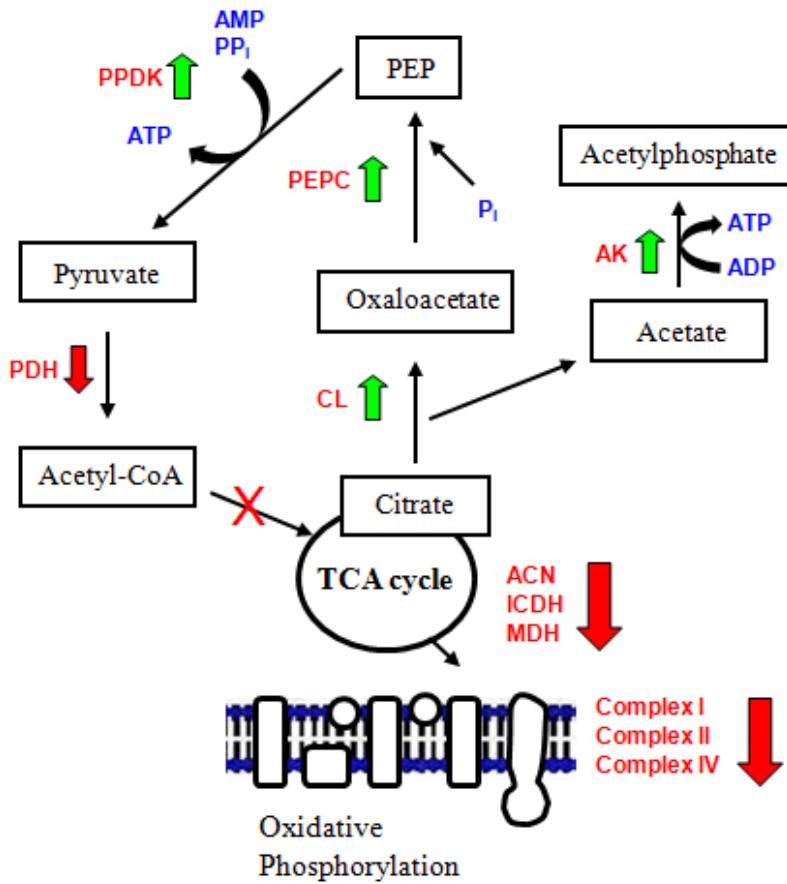


Figure 3.7 - Citrate metabolism in *Pseudomonas fluorescens* under nitrosative stress. Increased activity and expression of CL allows for the degradation of citrate and circumvention of nitrosative stress via a novel metabolic network in *P. fluorescens* subjected to SNP (\downarrow , decreased activity, \uparrow , increased activity). CL, citrate lyase; AK, acetate kinase; ICDH, isocitrate dehydrogenase; MDH, malate dehydrogenase; PEPC, phosphoenolpyruvate carboxylase; PPDK, pyruvate phosphate dikinase; PDH, pyruvate dehydrogenase.

Chapter 4: A facile electrophoretic technique to monitor phosphoenolpyruvate-dependent-kinases

The discovery of the role played by PPK in energy production under nitrosative stress prompted the validation of an in-gel technique to reliably visualize the activity of this enzyme and other phosphoenolpyruvate-dependent kinases. As opposed to SDS-PAGE, a denaturing electrophoretic method, BN-PAGE maintains proteins in their native state and allows the study of enzymatic activity. A negative charge applied to the protein sample by Coomassie Brilliant Blue allows the separation of protein mixtures as these migrate towards the positively charged anode buffer (73). The omission of detergents permits the maintenance of protein-protein interactions and thus the study of protein supercomplexes (74,75). Indeed, this technique is often applied to analyze the activity of membrane-bound complexes in the ETC (76).

It is also possible to probe the activity of proteins residing in the soluble portion of cellular fractions via BN-PAGE. Coupled to either phenazine methosulfate (PMS) or 2,6-dichloroindophenol (DCIP), the reduction of iodinitrotetrazolium (INT) creates a pink formazan precipitate at the location of the enzyme in-gel. This is particularly beneficial for the analysis of NAD^+ and NADP^+ -dependent dehydrogenases, as the reduction of these cofactors is directly coupled to INT reduction. For instance, it is feasible to simultaneously compare the activities of the NADPH-producing enzymes ICDH-NADP, malic enzyme (ME) and G6PDH, in order to gauge their contribution to oxidative defense systems (77). Other enzyme families, such as lyases, synthases and transaminases, can also be analyzed as long as the reaction forms a product that can be coupled to NAD(P)^+ -utilizing enzymes. For example, enzymes that form malate or oxaloacetate can be subjected to BN-PAGE and studied by coupling their activity to that of

exogenously-added MDH (51). Hence, in-gel activity assays following electrophoresis are adaptable and allow the analysis of various metabolic pathways.

Once the activity band is visible, it is possible to perform an array of follow-up studies. Excision of the band allows it to be processed by digestion and sequenced in order to identify the protein composition. Two-dimensional SDS-PAGE, Western blots and HPLC analyses permit the confirmation of enzymatic identity (73). While spectrophotometric studies allow the quantitative analysis of enzymatic activity and reaction kinetics, these require several controls and are not amenable to secondary studies. As such, the separation of heterogeneous protein mixtures via BN-PAGE is a rapid and cost-effective method of purifying the enzyme of interest.

In this chapter, the ability of BN-PAGE to separate the various phosphoenolpyruvate-dependent kinases is validated. The high-energy phosphate bond in PEP renders it ideal for the generation of ATP by SLP. However, spectrophotometric assays for PK, PPDK and phosphoenolpyruvate synthase (PEPS) fall short when all three kinases are present together in biological systems. A simple means of separating these enzymes prior to activity analyses may facilitate the means by which cellular bioenergetics are analyzed in living systems.

A facile electrophoretic technique to monitor phosphoenolpyruvate-dependent kinases

(Original Research)

Auger, C., Appanna, V.P., Castonguay, Z., Han, S., and Appanna, V.D.

[Published in *Electrophoresis*]

Auger, C., Appanna, V., Castonguay, Z., Han, S., Appanna, V.D. (2011) A facile electrophoretic technique to monitor phosphoenolpyruvate-dependent kinases. *Electrophoresis*. **33**:1095-101.

Abstract

Phosphoenolpyruvate (PEP)-dependent kinases are central to numerous metabolic processes and mediate the production of adenosine triphosphate (ATP) by substrate-level phosphorylation (SLP). While pyruvate kinase (PK, EC: 2.7.1.40), the final enzyme of the glycolytic pathway is critical in the anaerobic synthesis of ATP from ADP, pyruvate phosphate dikinase (PPDK, EC: 2.7.9.1), and phosphoenolpyruvate synthase (PEPS, EC: 2.7.9.2) help generate ATP from AMP coupled to PEP as a substrate. Here we demonstrate an inexpensive and effective electrophoretic technology to determine the activities of these enzymes by blue-native polyacrylamide gel electrophoresis (BN-PAGE). The generation of pyruvate is linked to exogenous lactate dehydrogenase (LDH), and the oxidation of reduced nicotinamide adenine dinucleotide (NADH) coupled to 2,6-dichloroindophenol (DCIP) and iodonitrotetrazolium chloride (INT) results in a formazan precipitate which is easily quantifiable. The selectivity of the enzymes is ensured by including either AMP or ADP and pyrophosphate (PP_i) or inorganic phosphate (P_i). Activity bands were readily obtained after incubation in the respective reaction mixtures for 20–30 min. Cell-free extract concentrations as low as 20 μ g protein equivalent yielded activity bands and substrate levels were manipulated to optimize sensitivity of this analytical technique. High-pressure liquid chromatography (HPLC), two-dimensional (2-D) SDS-PAGE (where SDS is sodium dodecyl sulfate), and immunoblot studies of the excised activity band help further characterize these PEP-dependent kinases. Furthermore, these enzymes were readily identified on the same gel by incubating it sequentially in the respective reaction mixtures. This technique provides a facile method to elucidate these kinases in biological systems.

Introduction

Adenosine triphosphate (ATP) is the universal energy currency in all organisms and biological systems have essentially evolved three disparate mechanisms to generate this high-energy phosphate derivative (78-80). Both photophosphorylation and oxidative phosphorylation invoke the participation of ATP synthase to produce ATP from an electrochemical gradient (81,82). While the former evolves O_2 , the latter reduces O_2 into H_2O (80,83). Substrate-level phosphorylation helps fix high-energy biochemicals into ATP, usually via a one-step enzymatic reaction (84). This phenomenon has been observed in *Trypanosoma brucei* and *Pseudomonas fluorescens*, which express an ADP-dependent isoform of succinyl-CoA synthase (SCS) to meet the ATP requirements of these organisms (85,86).

Additionally, organisms can also fulfill their energy quota via upregulation of the Embden-Meyerhof-Parnas pathway, which nets two ATP per molecule of glucose consumed (87). Pyruvate kinase (PK) is an important component of this metabolic network as it transfers the phosphate group of phosphoenolpyruvate (PEP) to ADP, yielding pyruvate and one ATP (88). Several bacteria and some parasitic anaerobic eukaryotes utilize pyruvate phosphate dikinase (PPDK), which catalyzes the same reaction as PK but with adenosine monophosphate (AMP) and pyrophosphate (PP_i) substituting for ADP (89-91). The rationale underlying the switch to the PP_i -dependent reaction appears to be energy efficiency, as a PP_i -driven glycolytic pathway can produce five ATP per glucose (92). Phosphoenolpyruvate synthase (PEPS) catalyzes a comparable reaction to that of PPDK, except that inorganic phosphate (P_i) is utilized instead of PP_i (93).

Traditionally, PEP-dependent kinases have been probed spectrophotometrically, with the aid of lactate dehydrogenase (LDH) as an auxiliary enzyme (93,94). The production of pyruvate

is subsequently monitored via the oxidation of nicotinamide adenine dinucleotide (NADH). Despite their simplicity, spectrophotometric analyses suffer from several shortcomings, as they require large amounts of sample and are subject to interference by endogenous LDH and other competing enzymes in the cell-free extract. The accurate measurements of enzyme activity by HPLC or by tracking radiolabeled substrates require high start up costs and a considerable investment of time (95). To mitigate these issues, we have developed a facile blue-native polyacrylamide gel electrophoresis (BN-PAGE) technique to probe these three PEP-consuming kinases. Here, we show how this simple tool can be applied to rapidly assess the activity of PEP-dependent kinases in a biological system. The generation of pyruvate is coupled to exogenous LDH, and the oxidation of NADH linked to 2,6-dichloroindophenol (DCIP) and iodonitrotetrazolium chloride (INT) helps generate a formazan precipitate at the site of the immobilized enzyme in the gel. This technique is specific, sensitive, and can identify these kinases in a single gel. The effectiveness of this electrophoretic method in monitoring PEP-dependent kinases under disparate culture conditions is also discussed.

Material and methods

Cell culture

Pseudomonas fluorescens (ATCC 13525) was grown in a defined citrate media consisting of 42 mM Na₂HPO₄, 22 mM KH₂PO₄, 15 mM NH₄Cl, 0.8 mM MgSO₄·7H₂O, and 19 mM citrate per liter of deionized distilled water. Trace elements were added as previously described and pH was adjusted to 6.8 using 2M NaOH. The media was dispensed into four aliquots of 200 mL and two aliquots of 150 mL then autoclaved for 45 min (35). Reactive nitrogen species (RNS) were introduced by addition of 10 mM sodium nitroprusside (SNP), a nitric oxide donor prior to inoculation in the medium (stressed condition). Cells from this medium were utilized to identify the three PEP-dependent enzymes in the same gel. The media was inoculated using 1 mL of *P. fluorescens* grown to the stationary phase in control defined citrate media (unstressed condition). Cultures were grown in an aerated gyratory water bath shaker, model 76 (New Brunswick Scientific) at 26°C and 140 rpm. Cells were isolated at the same growth period for analysis. Cell growth was monitored by measuring solubilized protein content by the Bradford method using the Bio-Rad Protein Assay reagent on 10 mL aliquots of culture (46).

Cellular fractionation

Bacteria were collected at the stationary stage of growth and resuspended in 500 µL of cell storage buffer (CSB; 50 mM Tris-HCl pH 7.3, 5 mM MgCl₂, 1 mM phenylmethylsulfonylfluoride, and 1 mM dithiothreitol). Following the lysis of the microbial cells via sonication and centrifugation at 180 000 × g for 3 h at 4°C, a soluble cytoplasmic fraction and a membrane pellet were isolated. The membrane pellet was resuspended in 500 µL

of CSB. The protein content in the soluble and membrane fractions was determined using the Bradford assay (46).

BN-PAGE in-gel activity

BN-PAGE was performed following a modified method described previously (35,50). Briefly, the membrane and cytosolic (soluble) fractions were prepared in a non-denaturing buffer (50 mM Bis-Tris, 500 mM ϵ -aminocaproic acid, pH 7.0, 4°C) at a concentration of 4 $\mu\text{g}/\mu\text{L}$. A final concentration of 1% maltoside was added to the membrane fractions to help solubilize membrane-bound proteins and ensure optimal protein separation. A 4–16% gradient gel was prepared with the Bio-Rad MiniProtean™ 2 system using 1 mm spacers. The final volume of the resolving gel was 5.8 mL, half of which was a 4% v/v acrylamide solution (50 mM Bis-Tris and 500 mM ϵ -aminoacproic acid [pH 7.0, 4°C]) and half of which was a 16% v/v acrylamide solution (50 mM Bis-Tris, 500 mM ϵ -aminoacproic acid, and 10% glycerol pH 7.0, 4°C). Gradient gels were formed using a gradient former (BioRad) and a peristaltic pump (Fisher). Sixty micrograms of protein was loaded into each well and electrophoresed at 4°C under native conditions at 80 V and 15 mA to ensure proper stacking. Once the protein reached the resolving gel, the voltage was raised to 150 V at 15 mA until the protein migrated half way through the gel. At the halfway mark the blue cathode buffer (50 mM Tricine, 15 mM Bis-Tris, 0.02% w/v Coomassie G-250 [pH 7.0 at 4°C]) which aids in visualizing the running front was changed to a colorless cathode buffer (50 mM Tricine, 15 mM Bis-Tris, 0.02% w/v Coomassie G-250 [pH 7 at 4°C]). After this point the gel was electrophoresed at 300 V and 25 mA for further migration through the gel.

Upon completion, the gel was equilibrated in reaction buffer (25 mM Tris-HCl, 5 mM MgCl₂ [pH 7.4]) for 15–30 min. The in-gel visualization of PEP dependent kinases was done by coupling the formation of pyruvate to LDH in an enzyme linked assay. These enzymes were located in the soluble cellular fraction. The addition of a solution containing PEP (5 mM), NADH (0.5 mM), 10 units LDH, DCIP (16.7 µg/mL), INT (0.5 mg/mL), and reaction buffer allowed for the oxidation of NADH via LDH to DCIP which in turn reduces INT at the site of the immobilized enzyme in the gel. For PK, 0.5 mM of ADP was utilized while for PPDK, 0.5 mM AMP and 0.5 mM PP_i was added. The PEPS reaction mixture was similar to the PPDK except 1.0 mM P_i was included instead of PP_i. Reactions were stopped using a destaining solution (40% methanol, 10% glacial acetic acid) and quantified using the densitometry software ImageJ for Windows. Coomassie staining ensured equal protein loading. Reactions performed without the addition of a substrate or the addition of an inhibitor (5 mM NiCl₂) ensured specificity of the reactions. Substrate and protein concentrations were varied in an effort to gauge the sensitivity of this technique. In an effort to compare this electrophoretic procedure with the established spectrophotometric assay, the soluble CFE (40 µg) was incubated in the reaction mixture with or without 1 mM of AMP. The activity of PEPS was measured by monitoring the production of pyruvate in the presence of LDH (10 units) and NADH (0.1 mM) (96). The decrease in absorbance at 340 nm was recorded. The same amount of CFE (40 µg) was loaded on the gel and following electrophoresis, activity bands were monitored upon incubation of the gel in the reaction mixture with or without AMP at various time intervals.

HPLC analysis

To aid in the further identification of the enzymes, the activity bands were precisely cut out of the gel slab and placed in reaction mixtures specific to each kinase. After 30 min of incubation, a 100 μ L of the sample reaction mixture was diluted 100-fold in milli-Q water and injected into an Alliance HPLC equipped with a C18 reverse-phase column (Synergi Hydro-RP; 4 μ m; 250 \times 4.6 mm, Phenomenex) operating at a flow rate of 0.7 mL/min at ambient temperature. A mobile phase consisting of 20 mM KH_2PO_4 (pH 2.9) was used to separate organic acids, which were detected using a Waters dual absorbance detector at 210 nm. Nucleotides were detected at 254 nm. Metabolites were identified using known standards, and peaks were quantified using the Empower software (Waters Corporation).

Silver stain and immunoblot assays

Sodium dodecyl sulfate polyacrylamide gel electrophoresis (SDS-PAGE) was performed as described in (51). For two-dimensional (2-D) assays activity bands were precisely excised from the gel, incubated in denaturing buffer (1% β -mercaptoethanol, 5% SDS) for 30 min and then loaded vertically into a 10% isocratic gel and electrophoresed at 80 V and 15 mA to allow for stacking and resolution. Following the resolution of protein bands, the gel was subjected to silver stain (97). For immunoblot assays, the proteins were electrophoretically transferred onto a nitrocellulose membrane at 25 V and 80 mA at 4°C overnight. Nonspecific binding sites were blocked using a Tris-Tween buffered saline solution (20 mM Tris-HCl, 0.8% NaCl, 1% Tween-20 [pH 7.6]) with the addition of 5% nonfat skim milk for 1 h. After this blocking step, the nitrocellulose membrane was incubated in primary antibody for 1 h, washed then incubated with secondary antibody for an hour before visualization. Polyclonal antibodies for PPDK were a

generous gift from Dr. Frédéric Bringaud (Université Bordeaux Segalen, France). Fluorescently tagged secondary antibodies (Li-Cor, Lincoln, NE, USA) allowed for visualization using an Odyssey infrared imaging system (Li-Cor). Unless otherwise mentioned, all chemicals were purchased from Sigma-Aldrich.

Results and discussion

The generation of ATP is necessary to accomplish functional work within the cell. While photophosphorylation and oxidative phosphorylation can both produce this moiety with high throughput, a portion of ATP is generated via the activity of PEP-dependent kinases. Under oxidative stress, most organisms rely on increased glycolytic output to fulfill their energy need (98,99). As there are three enzymes which may feasibly accomplish this role, we sought to develop a method which could quickly and accurately gauge their individual activities. BN-PAGE, due to its simplicity, is an ideal choice for evaluating PEP-dependent kinases. Exogenous LDH is utilized to metabolize the pyruvate produced and the oxidation of NADH is coupled to DCIP and INT to create a purple formazan precipitate in situ (**Figure 4.1**). Here, *P. fluorescens* was grown in citrate-containing medium for 24 h and the soluble fraction was isolated and probed for activity of PEP-dependent kinases.

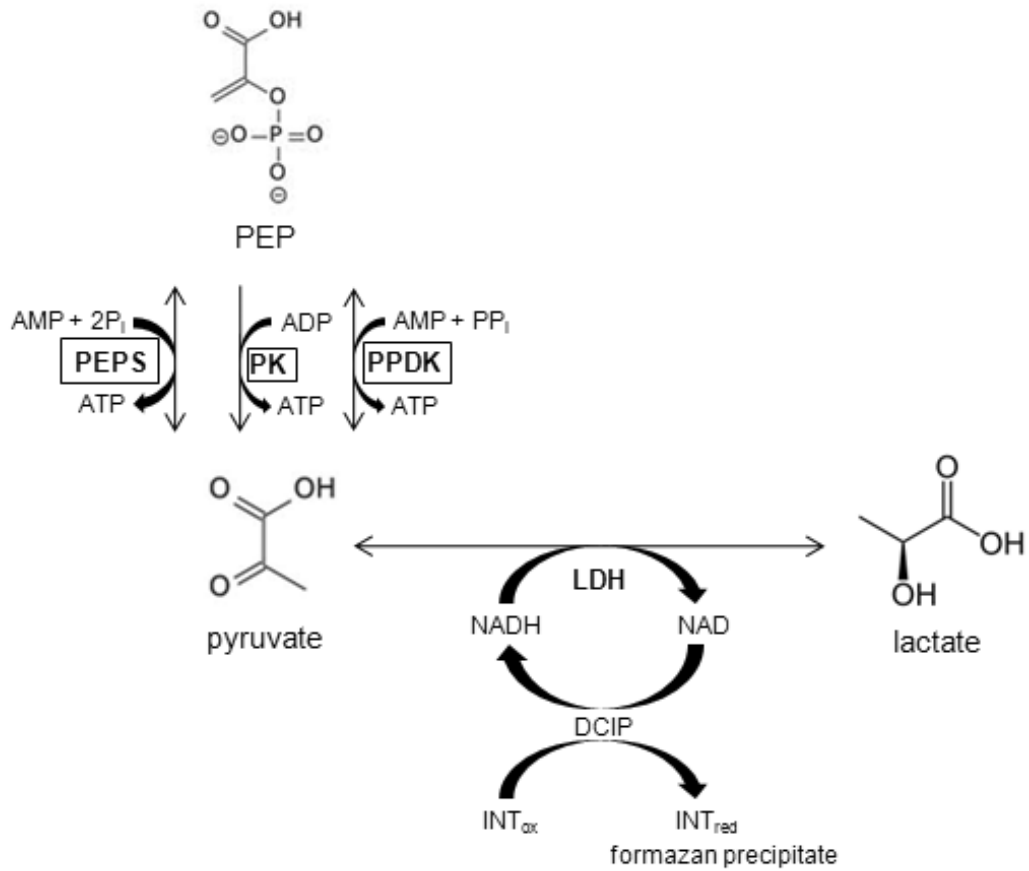


Figure 4.1 - A schematic depiction of the electrophoretic method to detect PEP-dependent kinases (note: the formazan precipitate is formed at the site where the enzyme is localized in the gel).

PK, being the most common source of glycolytic ATP production, was the first enzyme analyzed (100). In **Figure 4.2 - A**, we demonstrate the specificity of this method, as the activity band indicative of PK was not present when the substrate was removed from the reaction mixture. Furthermore, this precipitate was absent upon the addition of NiCl_2 , an inhibitor which competes for the binding site of the essential cofactor Mg^{2+} (101). In order to further verify the nature of this enzyme, the activity band attributed to PK was excised and placed in a reaction mixture containing PEP and ADP. Indeed, after a 30 min incubation, the appearance of the products pyruvate and ATP were evident by HPLC analysis (**Figure 4.2 - B**).

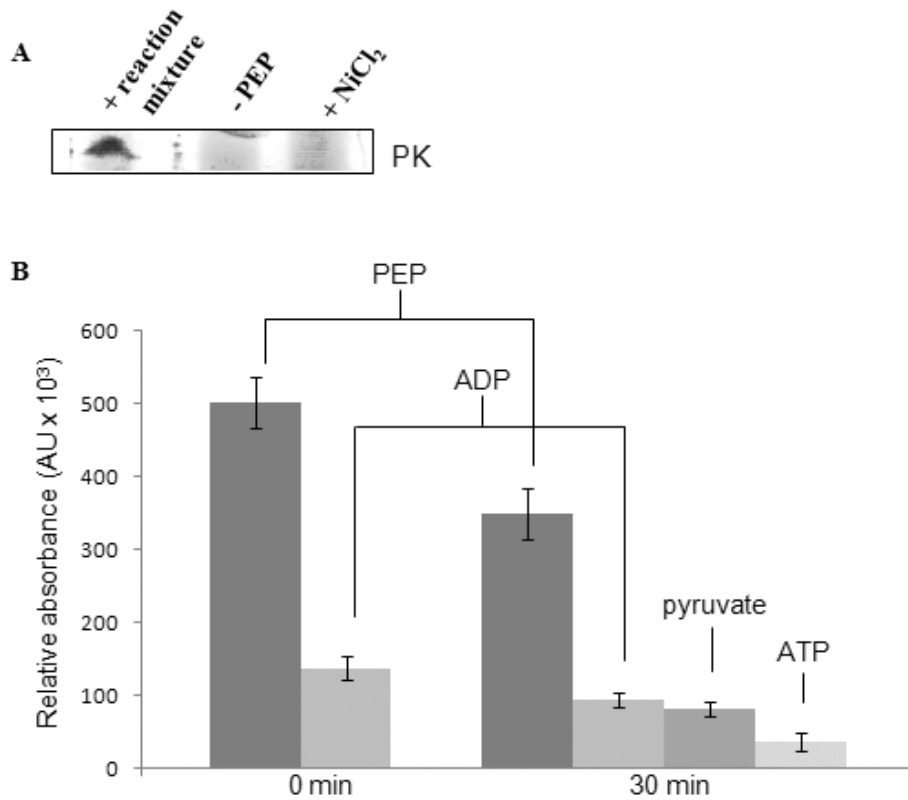


Figure 4.2 - Identification of pyruvate kinase by BN-PAGE. Panel A: A representative in-gel enzyme activity stain with a negative control (-PEP) and inhibitor (-NiCl₂); Panel B: The activity band from A was excised and incubated in the reaction mixture; substrates and products were monitored by HPLC (n = 3; mean ± standard deviation).

The effectiveness of this technique led us to explore its suitability to other PEP-dependent kinases. By replacing ADP in the reaction mixture with AMP and sodium pyrophosphate, we were able to detect the activity of PPDK in-gel. Using various protein concentrations, we examined the sensitivity of this BN-PAGE method. A formazan precipitate was visible after 30 min of incubation in the reaction mixture in a gel where as little as 40 μ g of protein was loaded (**Figure 4.3 - A**). It is important to note that as the incubation time increased, the band intensity was also magnified. However, higher protein concentrations yielded activity bands faster and time of incubation can be manipulated to obtain activity bands even with lower protein concentrations (data not shown). In order to confirm that the activity in question was indeed attributable to PPDK, bands were cut and loaded into a 2-D SDS-PAGE then subjected to Western blot analysis. A single band with a molecular mass of approximately 60 kDa was detected, thus confirming the purity of the enzyme (**Figure 4.3 - B**).

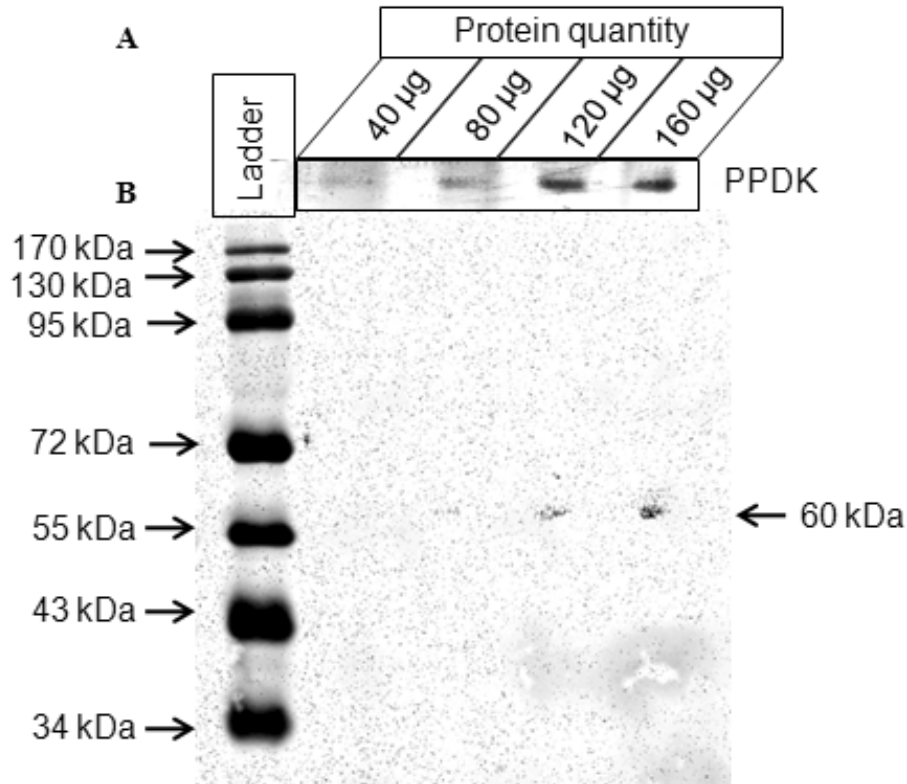


Figure 4.3 - Monitoring of pyruvate, phosphate dikinase (PPDK) by BN-PAGE. Panel A: Representative in-gel activity of PPDK at various protein concentrations. Panel B: Bands from panel A were excised and loaded into an SDS denaturing gel and analyzed by Western blot.

PEPS, an enzyme with both gluconeogenic and glycolytic roles, was probed by substituting P_i in the PPDK reaction mixture in lieu of PP_i (93). The resulting activity band could be visualized at a slightly lower molecular mass than PPDK in the native gel. The sensitivity of this method in regards to substrate concentration was verified, with concentrations ranging from 1 to 5 mM. As seen in **Figure 4.4 - A**, band intensity increased with respect to PEP concentration. Densitometry was performed using ImageJ for Windows. It appears that 3.5 mM of PEP generates a strong band. When this concentration of PEP was utilized, activity bands were observed even in gels where lower concentrations of protein were loaded (data not shown).

In living systems where all three enzymes may contribute to the ATP budget and may be intricately regulated, this method can be utilized to ascertain the activity of each PEP-dependent kinase in a single gel. SNP is an inorganic compound which donates nitric oxide in vivo (25,57). When subjected to treatment with SNP, *P. fluorescens* reprograms its metabolism to circumvent its noxious effect. Under nitrosative stress, *P. fluorescens* appeared to express all three enzymes. Soluble cell-free extract from SNP-stressed cultures was utilized to obtain all three enzymes on the same gel. In **Figure 4.4 - B**, the gel was first incubated in the reaction mixture for PK until an activity band was visible. After washing with reaction buffer, the gel was subsequently placed in the reaction mixture for PPDK until the appearance of an activity band. Following a second washing, the same gel was incubated in reaction mixture for PEPS until its activity was detectable.

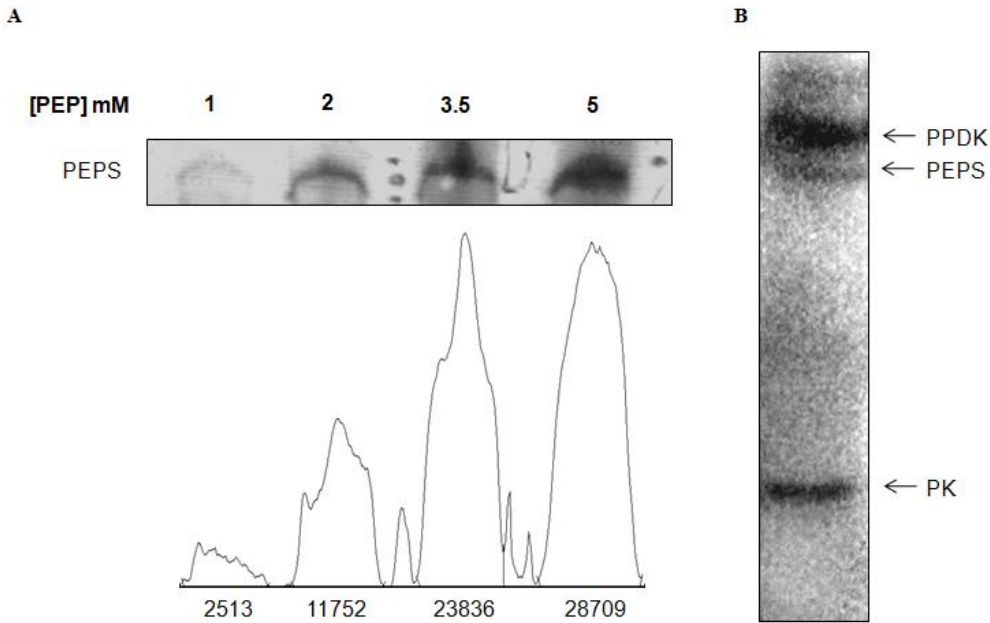


Figure 4.4 - BN-PAGE analysis of kinases generating ATP from PEP. Panel A: A representative gel demonstrating the dependence of activity band intensity on substrate concentration (note: 60 μ g of protein was loaded and the incubation time was 30 min). Panel B: A representative gel illustrating the activity of all three PEP-dependent kinases (note: following the appearance of a given activity band, the gel was washed and sequentially re-incubated in different reaction mixtures).

Additionally, this electrophoretic technique can be utilized to compare these enzymatic activities in organisms under disparate growth conditions. Under nitrosative stress, one of the adaptations utilized by this organism is the upregulation of PEPS. In **Figure 4.5 - A**, 60 μg protein equivalent from the control and SNP-treated bacteria was electrophoresed and incubated in the PEPS reaction mixture for 30 min. A sharp band was observed only in the SNP-treated cell-free extract. (Note: an activity band was barely discernable in the control after 1 h.) This is indicative of the ability of the microbe to upregulate the activity of PEPS. The validity of this finding was ascertained by comparing the activity stain to molecular mass standards and a protein loading control stained with Coomassie R-250 dye. To further prove that this enzyme was indeed PEPS, the ability of the excised gel to produce ATP from PEP, AMP, and P_i was confirmed by HPLC (data not shown). Furthermore, the activity band from A was cut and ran in a 2-D SDS-PAGE. Silver staining was utilized to determine the expression levels of this enzyme. A band with a molecular mass of approximately 75 kDa was detected (**Figure 4.5 - B**). This is consistent with previous data showing that PEPS is a dimer of 77 kDa (102). The comparative study of the BN-PAGE and spectrophotometric techniques revealed that the former is superior in terms of specificity and sensitivity. While a decrease of absorbance was observed in the enzyme coupled assay in the reaction mixture without the substrate AMP, no activity band was evident in the gel incubated in a reaction mixture devoid of AMP (**Figure 4.5 - C**). Furthermore, the densitometric readings of the activity bands had a sharp variation. The change of optical density range appeared to be more pronounced in the absence of AMP, thus, revealing the unsuitability of the spectrophotometric procedure. Similar results were obtained with PK and PPDK (data not shown).

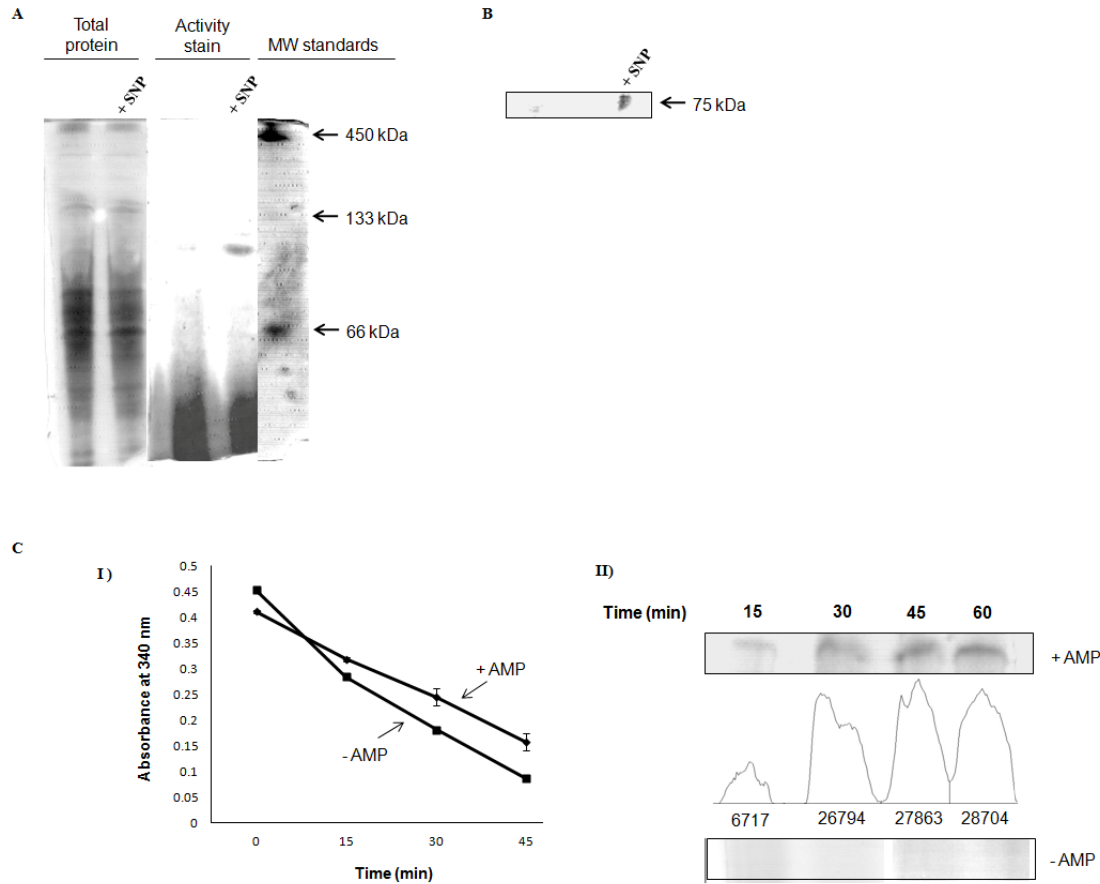


Figure 4.5 - The biochemical application of this electrophoretic method. Panel A: The detection of phosphoenolpyruvate synthase (PEPS) activity in soluble cell free extract from control and SNP-stressed *Pseudomonas fluorescens* (note: equal loading was assured by staining total protein with Coomassie blue R-250). Panel B: Activity bands from A were excised and loaded into a SDS denaturing gel and protein levels were determined by silver stain. Panel C: A comparative evaluation of the spectrophotometric and BN-PAGE techniques to monitor PEPS: I) spectrophotometric detection of PEPS in cell free extract (pyruvate formation was assessed by monitoring the decrease of NADH at 340 nm in the presence of LDH; n = 3, mean \pm standard deviation) II) BN-PAGE detection of PEPS (note: no activity was evident in the absence of AMP. Similar results were obtained with PK and PPK).

Despite the increased time required to perform the BN-PAGE analysis versus spectrophotometric assays, our method appears to be more effective, as it does not require prior purification of the enzyme and is not subjected to interference from endogenous compounds. Additionally, these in-gel activity assays differentiate between the PEP-dependent kinases, a feature where classical methods fall short. This was demonstrated by the utilization of NADH in the absence of a cofactor (**Figure 4.5 - C**). Although the spectrophotometric and BN-PAGE techniques utilize similar enzyme and substrate concentrations, the latter allows for follow-up studies of enzyme expression and characterization that are not possible using classical methods (93,103,104). Hence, this BN-PAGE method exhibits numerous advantages to the spectrophotometric analysis, an analytical technique that clearly appears to be ineffective in this instance.

In summary, PEP-dependent kinases supply numerous organisms with a portion of their ATP via substrate-level phosphorylation (SLP). This BN-PAGE technique affords a simple and inexpensive tool which can be applied to readily assess the activity of these important ATP-generating enzymes. Furthermore, once identified, the enzyme of interest can be subjected to 2-D SDS-PAGE to study its expression levels using silver stain or Western blot analyses or further purified for detailed molecular examination. Additionally, this technique can also be invoked to screen PEP-dependent kinases in organisms subjected to various environmental conditions and to evaluate if indeed SLP is an important contributor to their energy budget.

Chapter 5: A citrate-degrading metabolon and phosphotransfer network to counter nitrosative stress

The discovery that activity bands belonging to CL, PEPC and PPDK all migrate to the same location in-gel was intriguing when one considers their disparate molecular masses. As BN-PAGE allows the maintenance of protein-protein interactions, this led to the postulation that these three enzymes may be physically linked. Multi-enzymatic complexes, or metabolons, are thought to be pervasive in biological systems. However, their fragile nature renders it difficult to study these complexes *in vitro*. The idea that sequential enzymes in metabolic pathways could connect to each other dates back to the middle of the 20th century, when TCA cycle enzymes were first isolated as aggregates (105). The reasoning behind the formation of such complexes, as well as their scaffolding to cellular compartments, is sound and strongly supported by metabolic control analysis (106). Firstly, metabolites which may be acted upon by more than one enzyme are channelled to the proper product, thus minimizing their loss to other pathways. Second, metabolons prevent the metabolite from mixing with the bulk phase of the cell, allowing for high local substrate concentrations. Finally, they permit the sequestering of toxic or reactive intermediates, hence minimizing their detrimental effects (107).

Although there are some examples of stable, high-affinity enzyme associations (e.g., the bicarbonate transport metabolon), many of these supercomplexes are formed transiently, and fall apart once the cell is broken (108,109). For instance, the six enzymes that catalyze purine biosynthesis show no co-localization *in vitro*. However, fluorescent tagging demonstrates that these enzymes form a cluster *in vivo* which is regulated by purine levels (110). More recently, it has been shown that the enzymes MDH and ICDH of the TCA cycle form a complex in *Bacillus subtilis* (111). While these two enzymes do not catalyze subsequent reactions, it is hypothesized

that they may be part of a larger, globular structure that contains other TCA cycle enzymes. What is most intriguing, however, are the specific stimuli involved in linking these two enzymes. Only a combination of isocitrate, NADP and magnesium (Mg^{2+}) could stimulate the formation of the ICDH-MDH complex (111). This underscores the dynamic nature of metabolons and helps explain why their existence, while theoretically conceivable, has eluded scientists. The reductionist nature of most biochemical analyses cannot take into account the sheer number of metabolites, cofactors and other moieties that may influence metabolon formation.

In this chapter, a novel metabolon consisting of CL, PEPC and PPDK, is explored. A dysfunctional TCA cycle and ETC render it difficult to metabolize citrate and synthesize ATP aerobically when the organism is exposed to nitrosative stress. PPDK, owing to its ability to theoretically produce two ATP per molecule of PEP, is an excellent alternative to oxidative phosphorylation. The means by which this metabolon associates and dissociates is described herein. Additionally, enzymes which mediate the distribution of phosphate are studied, as these may provide the organism with nucleotides and high-energy intermediates necessary to their survival.

**A Citrate-degrading Metabolon and Phosphotransfer Network to Counter Nitric Oxide, an
Endogenous Antibacterial Agent**

(Original Research)

Auger, C., and Appanna, V.D.

[Manuscript submitted to the *Journal of Free Radical Biology & Medicine*]

Abstract

The transient assembly of protein supercomplexes known as metabolons is a phenomenon that helps render metabolic networks efficient. Indeed, the interaction of sequential enzymes in these metabolic modules contributes to an increase in metabolic flux owing to the enhanced localized substrate concentration and channelling of substrates from one enzyme to another. While it is known that reactive nitrogen species (RNS) and the state of nitrosative stress they trigger negatively affect tricarboxylic acid (TCA) cycle enzymes and oxidative phosphorylation, there is a dearth of literature describing how microorganisms adapt to and surmount this challenge. Here we identify a unique catabolic pathway acting on citrate and producing ATP when *Pseudomonas fluorescens* is subjected to RNS treatment. The assembly of citrate lyase (CL), phosphoenolpyruvate carboxylase (PEPC) and pyruvate phosphate dikinase (PPDK), as monitored by co-immunoprecipitation (Co-IP) and blue native polyacrylamide gel electrophoresis (BN-PAGE) permits the production of ATP when oxidative phosphorylation is defective. Furthermore, the up-regulation of phosphotransfer networks consisting of adenylate kinase (AK), acetate kinase (ACK) and nucleoside diphosphate kinase (NDPK) combined with the lowered activity of inorganic pyrophosphatase (PPase) allows the storage of high-energy phosphate while shifting to the use of pyrophosphate (PP_i) as a source of chemical energy. The molecular reengineering described herein provides further understanding of how metabolism plays a key role in the adaptation to nitrosative stress, and reveals novel targets that will further the development of antimicrobial agents to counter RNS-resistant pathogens.

Introduction

ATP is the universal energy currency in all living organisms and its adequate supply is central to the survival and propagation of life. This adenine moiety is commonly generated via substrate-level phosphorylation (SLP), photophosphorylation and oxidative phosphorylation. In aerobes, ATP stems predominantly from the latter (112). The NADH and FADH₂ formed via the tricarboxylic acid (TCA) cycle provide the reductive potential necessary to synthesize the high-energy phosphate. If not immediately required to accomplish cellular work, this moiety can be distributed throughout the cell in the form of high-energy compounds such as phosphocreatine, acetyl-phosphate, polyphosphates, phosphorylated nucleosides and/or stored as energy reserves in the form of carbohydrates and fatty acids (113,114).

In an effort to maximize the production of ATP during oxidative phosphorylation, an intimate interaction between complex V, the ATP-synthesizing machine and various kinases does exist (115,116). This allows for the rapid transfer of phosphate from ATP with the concomitant formation of a high-energy compound and ADP. Indeed, such a system further drives the ATP-making process. These phosphotransfer networks are crucial to the bioenergetics of an organism, ensuring an intricate balance between ATP-generating and consuming processes. In the absence of operative machinery mediated by the electron transport chain (ETC), the generation of ATP must proceed through SLP. In this instance, cellular metabolism gives rise to energy-rich phosphorylated compounds that are tapped as ATP (37). Phosphoenolpyruvate (PEP) and 1, 3- biphosphoglycerate are two key glycolytic intermediates that enable anaerobic organisms to fulfill their energy needs (117,118).

Due to their reliance on redox metals, the complexes of the ETC present themselves as ideal targets for free radicals within the cell (33,119). Nitrosative stress is known to severely

hinder oxidative phosphorylation and hence the ability of organisms to derive their ATP needs via this machinery (120). Therefore, if an organism subjected to these insults is to survive, it must devise alternative ATP-producing strategies. Although a body of literature on the detoxification of nitric oxide (NO) and reactive nitrogen species (RNS) exists, the molecular details on how organisms fulfill their ATP requirements during this challenge have yet to be unraveled (24,121,122). In this study, we have examined the ability of the model microbe *Pseudomonas fluorescens* to generate ATP in response to RNS-induced defective oxidative phosphorylation. The assembly of a citrate-catabolizing supercomplex, in addition to the increased activity of enzymes mediating the transfer of high-energy phosphate allow the microbe to survive and proliferate despite the onslaught of RNS. The significance of metabolic networks and phosphotransfer systems in maintaining ATP homeostasis is discussed. The targeting of these enzymes in RNS-resistance microbes is also commented on.

Materials and methods

Cell culturing and fractionation

Pseudomonas fluorescens 13525, obtained from the American Type Culture Collection (ATCC), was cultured on 2% agar and grown in a phosphate mineral medium containing Na_2HPO_4 (6 g), KH_2PO_4 (3 g), $\text{MgSO}_4 \cdot 7\text{H}_2\text{O}$ (0.2 g), NH_4Cl (0.8 g), and citric acid (4 g) per litre of distilled and deionized H_2O (dd H_2O). Trace elements were added to a final concentration of 1%, as described previously, and NaOH was utilized to adjust the pH to 6.8 prior to autoclaving at 121°C for 20 min (85,123). One mL of *P. fluorescens* grown to stationary phase in a control culture was introduced to 200 mL of media in an Erlenmeyer flask. Nitrosative stress was initiated via the addition of the NO donors sodium nitroprusside (SNP, 10 mM) or diethylamine NONOate (DEANO; 0.5, 1 mM) to the media (124,125). A second dose of DEANO was added during the exponential growth phase (16 h) to maintain NO levels in the medium. Cultures treated with SNP were grown alongside cultures with 10 mM sodium ferrocyanide as a control. The latter has a similar structure to SNP minus the nitroso functional group (126). As DEANO and SNP are both initiators of nitrosative stress and generated similar physiological results, they were used interchangeably. Bacteria were grown and aerated on a gyratory water bath shaker (Model 76; New Brunswick Scientific). After 24 h of growth, cells reached their stationary phase and were isolated by centrifugation (10,000 x g, 10 min, 4 °C). Pellets were washed with 0.85% NaCl and re-suspended in cell storage buffer (CSB; 50 mM Tris-HCl, 5 mM MgCl_2 , 1 mM phenylmethylsulphonyl fluoride, pH 7.3).

Cell pellets were disrupted ultrasonically and then centrifuged at 3,000 x g for 30 min at 4 °C to remove intact bacteria. Soluble and membrane cell-free extracts (CFE) were then obtained by centrifugation at 180,000 x g for 3 h. Purity of the fractions was assessed via the

analysis of glucose-6-phosphate dehydrogenase (G6PDH) and complex IV activity in the soluble and membrane portions, respectively. Protein quantities were ascertained in triplicate with bovine serum albumin as a standard, using the Bradford assay (46). CFE fractions were prepared immediately for in-gel activity assays and frozen at -20 °C for storage up to a maximum of 4 weeks.

Blue native polyacrylamide gel electrophoresis (BN-PAGE) in-gel activity assays

BN-PAGE and activity assays were performed as described (48,50). To ensure optimal protein separation, 4-16% linear gradient gels were cast with the Bio-Rad MiniProtein™ 2 system using 1 mm spacers. Soluble CFE was prepared in a native buffer (50 mM Bis-Tris, 500 mM ϵ -aminocaproic acid, pH 7.0, 4 °C) at a final concentration of 4 mg of protein per ml. Membrane CFE was prepared in a similar manner except β -dodecyl-D-maltoside was added at a concentration of 1% to the preparation to facilitate the solubilization of membrane-bound proteins. Equal protein loading was ensured by monitoring protein concentration using the Bradford assay. Each well was loaded with 60 μ g of protein prior to electrophoresis. The latter was performed at 4 °C under native conditions at 80 V and 15 mA for proper stacking, followed by 150 V and 25 mA until the migration of the proteins reached half way through the resolving gel. At the halfway point, blue cathode buffer (50 mM Tricine, 15 mM Bis-Tris, 0.02% w/v Coomassie G-250, pH 7 at 4 °C) was changed to a colorless cathode buffer (50 mM Tricine, 15 mM Bis-Tris, pH 7 at 4 °C). The electrophoresis was performed at 300 V and 25 mA beyond this point. Following electrophoresis, gel slabs were equilibrated for 15 min in a reaction buffer (25 mM Tris-HCl, 5 mM MgCl₂, at pH 7.4). Afterwards, enzyme activities were detected using select reaction mixtures.

The functionality of ETC complexes was ascertained as described (33,35). CL and PEPC reaction mixtures were prepared, containing citrate and PEP as reactions substrates respectively, as demonstrated in (120). PK and PPDK activity assays were performed as shown (127). The activity of NDPK was probed using the enzymes hexokinase and G6PDH as elaborated in (128). Acetate kinase (ACK) was analyzed in-gel with a reaction mixture consisting of 5 mM acetyl-phosphate, 1 mM ADP, 5 mM glucose, 10 units of G6PDH, 10 units of hexokinase, 1 mM NADP, 0.2 mg/mL of phenazine methosulfate (PMS) and 0.4 mg/mL of iodinitrotetrazolium (INT). ATP formation allows the synthesis of glucose-6-phosphate, which is coupled to G6PDH activity, allowing NADP reduction and formazan precipitation at the site of the enzyme *in situ*. Negative controls were performed without acetyl-phosphate or without glucose. Adenylate kinase activity was discerned with a reaction mixture containing 10 mM ADP, 5 mM glucose, 0.5 mM NADP, 10 units of hexokinase, 10 units of G6PDH, 0.2 mg/mL of PMS and 0.4 mg/mL of INT. Negative controls consisted of the same reaction mixture without ADP or without glucose. PPase activity was monitored in-gel via the formation of a phosphomolybdate complex with malachite green, as described (129). Destaining solution (40% methanol and 10% glacial acetic acid) was used to terminate the reactions. Coomassie blue staining was applied to assure equal protein loading. To identify optimal conditions for these reactions, substrate concentrations and incubation times were varied. Select activity bands were submitted to densitometry using ImageJ for Windows. All comparative experiments were performed at the late logarithmic phase of growth. BSA (66 kDa) and ferritin (450 kDa) were used as molecular weight standards in a separate lane of the BN-PAGE gel.

Enzyme confirmation and metabolite analyses via HPLC

To evaluate the influence of nitrosative stress on metabolite levels, these were analyzed by high performance liquid chromatography (HPLC). Metabolites were separated using a C₁₈ column with a polar cap (3.5 μm, amide cap, 4.6 mm × 150 mm inside diameter, Symmetry Column, Phenomenex[®], Torrance, CA, USA). The mobile phase consisted of 20 mM KH₂PO₄ (pH 2.9 with 6 N HCl) prepared in Milli-Q water and the column was eluted at a flow rate of 0.7 ml/min at 25 °C. A 2 mg protein equivalent of soluble CFE from control and 1 mM DEANO-treated cells was boiled for 5 min to precipitate protein prior to injection. Nucleotides were detected at 254 nm, while organic acids were visualized at 210 nm using a Waters UV-visible detector. Metabolites were identified by spiking biological samples with known standards, and peaks were quantified using the Empower software (Waters Corporation). The HPLC was standardized using a five-point calibration prior to each injection protocol.

The BN-PAGE activity band belonging to CL/PEPC/PPDK was rinsed twice with reaction buffer, excised from the gel and placed in reaction buffer containing 2 mM citrate, 0.5 mM AMP and 0.5 mM PP_i. After 30 min of incubation, 100 μL of the sample was collected and diluted ten-fold with Milli-Q water for HPLC analysis. While multiple time points were taken, a 30 min incubation afforded optimal results. Samples were injected immediately after the reactions in order to minimize substrate and product degradation. A similar protocol was applied to ascertain the nature of the activity band for AK. However, the reaction buffer solely contained 0.5 mM ADP, and was allowed to react with the enzyme for 45 min prior to injection.

2D SDS-PAGE and Western blots

The activity band for CL/PEPC/PPDK was precision cut from the gel and incubated at ambient temperature for 30 min in a denaturing solution of 1% (w/v) SDS and 1% (v/v) 2-mercaptoethanol. The band was rinsed twice for 10 s with SDS-PAGE electrophoresis buffer (25 mM Tris-HCl, 192 mM glycine and 0.1% (w/v) SDS; pH 8.3) then placed vertically in the well of a 10% isocratic SDS gel (8 x 7 cm). SDS-PAGE was performed according to a modified protocol (130). Electrophoresis was conducted at 80 V at room temperature until the proteins reached the separating gel. The voltage was then raised to 200 V until completion. The molecular mass of proteins was assessed using the EZ-Run Prestained Recombinant Protein Ladder (Fisher Scientific). Following electrophoresis, the proteins were transferred for 16 h at 25 V on to a nitrocellulose membrane (LI-COR) for Western blots. Non-specific binding sites on the membrane were blocked by treatment with 5% non-fat skim milk dissolved in TTBS [20 mM Tris-HCl, 0.8% NaCl, 1% Tween-20 (pH7.6)] for 1 h. Primary antibodies directed toward PEPC (Rabbit polyclonal; dilution: 1:500; Abcam), PPDK (Rabbit polyclonal; dilution: 1:1000; generous gift from Dr. Frédéric Bringaud [Université Bordeaux Segalen, France]) and phosphoserine/threonine/tyrosine (Mouse monoclonal; dilution: 1:200, Abcam) were diluted in TTBS and incubated with the membrane for 1 h. The secondary antibodies consisted of donkey anti-rabbit infrared (IR) 800-conjugated (LI-COR) and donkey anti-mouse IR 680-conjugated (LI-COR) and were applied for 1 h in the dark in TTBS. Protein expression was documented using an Odyssey Infrared Imager and accompanying software (LI-COR, Lincoln, NE, USA) which detected an infrared signal from the conjugated secondary antibody at $\lambda_{\text{excitation}}=778\text{nm}$, $\lambda_{\text{emission}}=795\text{nm}$ (IR 800) or $\lambda_{\text{excitation}}=676\text{nm}$, $\lambda_{\text{emission}}=693\text{nm}$ (IR 680).

Metabolon analyses and dissociation

BN-PAGE in-gel assays for CL, PEPC and PPDK revealed an activity band at a similar spot for all three enzymes, despite their disparate molecular masses. Incubation of this activity band in a solution of citrate, AMP and PP_i, as described above, did indeed generate pyruvate and ATP. This intriguing finding prompted us to explore whether any post-translational modifications may be involved in the formation of this metabolon. As such, bands were excised and loaded into a SDS gel for immunoblot analyses. Antibodies versus acetylated lysine residues (Rabbit polyclonal; dilution: 1:500; Abcam) and nitrosylated tyrosines (Mouse monoclonal; dilution: 1:1400; Abcam) did not generate a signal. In an attempt to dissociate these three enzymes, soluble CFE (at 4 mg protein/mL) was incubated with alkaline phosphatase (20 U) for 15 min at room temperature before BN-PAGE. Indeed, this proved effective, indicating that a phosphorylation event was involved in metabolon formation. The link between proteins was further explored via pull-down assays.

Co-immunoprecipitation

Pull-down experiments were performed according to the manufacturer's instructions (Abcam). Cell pellets were lysed in 100 µL lysis buffer (1% maltoside, 1 mg/mL BSA, pepstatin A, leupeptin) for 60 min on ice with occasional vortexing. Agarose anti-IgG conjugates were prepared by diluting them 1:1 in dilution buffer (1% maltoside, 1 mg/mL BSA). Ten µL of agarose conjugates were added to lysed samples and left to incubate for 1 h at 4°C with gentle shaking to remove proteins which spontaneously bind to the agarose anti IgG conjugates. Samples were centrifuged at 200 g for 1 min and the supernatant was saved. Ten µL of polyclonal anti-PPDK or twenty uL of polyclonal anti-PEPC was added to the diluted lysate for

1 h at 4°C with gentle shaking. Following incubation with the primary antibody, 50 µL of agarose IgG conjugate was added per tube and allowed to incubate for 1h with gentle shaking at 4°C. Following incubation, samples were centrifuged at 200 g for 5 sec. The supernatant was removed and the pellet was re-suspended in 500 µL of dilution buffer then centrifuged again at 200 g for 5 s. The supernatant was removed and the pellet was re-suspended in TBS and centrifuged. Re-suspension and centrifugation was repeated one more time using a solution of 0.5M Tris at a pH of 6.8. The pellet was re-suspended in SDS-PAGE sample buffer and heated for 5 min at 100°C. The sample was centrifuged at 200 g for 5 s and the supernatant was loaded onto a 10% SDS gel. A Western blot was performed on PEPC or PPDK, as described above.

Recovery experiments and statistical analysis

The NO-mediated modulation of PPDK activity was further confirmed with regulation experiments. Control cells grown in citrate medium for 24 h were transferred to a 10 mM SNP-containing medium. Following an 8 h exposure, the cells were collected and processed for BN PAGE as described above. Similar experiments were performed with 10 mM SNP-stressed cells transferred into a control medium. Data were expressed as means \pm standard deviations. All experiments were performed in triplicate and biological duplicate.

Results

Pseudomonas fluorescens was grown in a citrate medium with or without a NO donor until the culture reached its stationary phase, as measured by Bradford assay. At this point, bacteria were spun out of solution by centrifugation and the pellets submitted to sonication to separate the soluble and membrane fractions. The latter was prepared for BN-PAGE in order to ascertain the effect of NO on the ETC. Indeed, the addition of SNP or DEANO to the growth medium severely impeded complex I, II and IV, as visualized by in-gel activity assays (**Figure 5.1 - A**). Given the repercussions of a defective ETC, the cytoplasm was subjected to HPLC analysis with a UV-visible detector set to 254 nm to identify nucleotides. While ADP and ATP levels in the RNS-treated cells were diminished, there was a slight increase in AMP and a large increase in pyrophosphate, as seen in chromatograms (**Figure 5.1 - B**). The large decrease in ATP relative to ADP may be indicative of mechanisms responsible for the storage of the former. Indeed, phosphowires are often utilized to store high-energy phosphate in the form of phosphocreatine and acetyl-phosphate, among others (116). These data suggest that nitrosative stress triggers a shift in the bioenergetics of the organism.

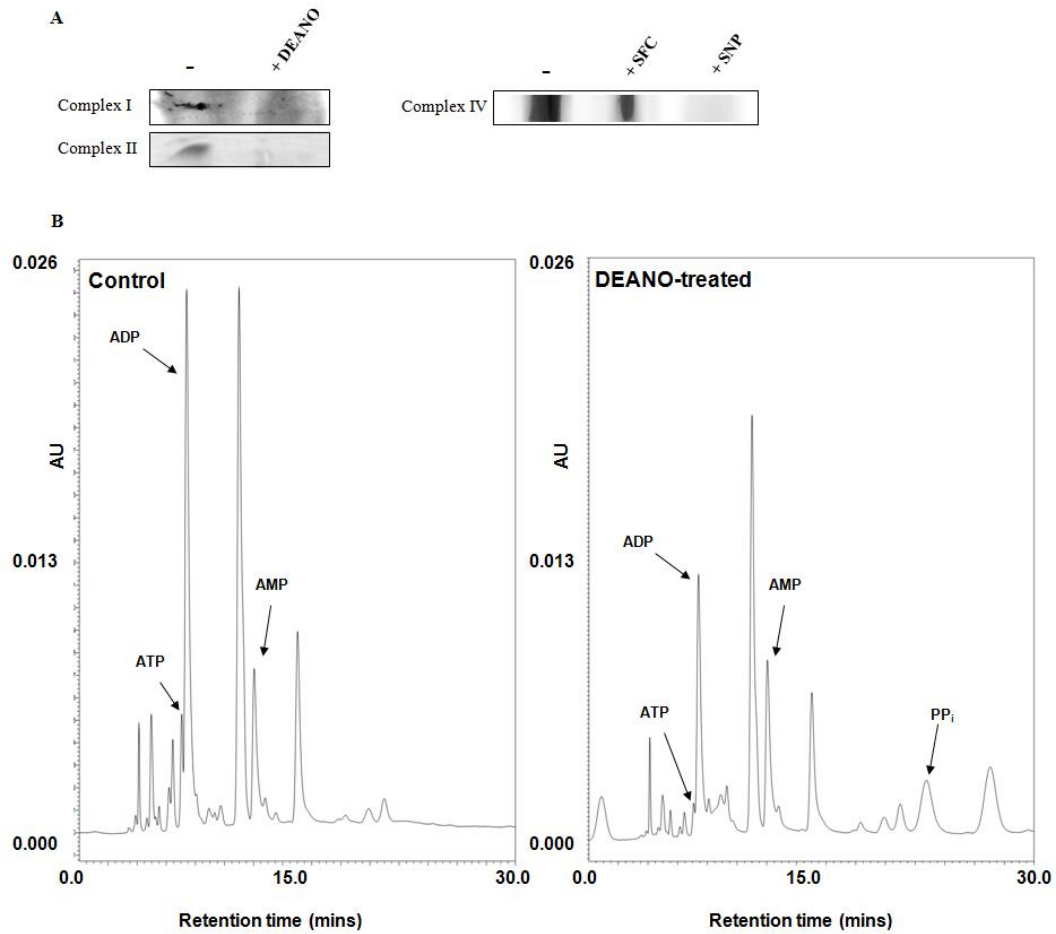


Figure 5.1 - Nucleotide and ETC analysis in *P. fluorescens* exposed to nitrosative stress. A; In-gel activity assays of protein complexes from the electron transport chain (-, untreated; +DEANO, 1 mM diethylamine NONOate, +SFC, 10 mM sodium ferrocyanide; +SNP, 10 mM sodium nitroprusside). Images shown are representative gels; n=3. **B;** Representative chromatographs displaying nucleotide levels in soluble cell free extract from *P. fluorescens* grown in control cultures and 1 mM DEANO-containing cultures; n=3.

We have previously shown that, to counteract the detrimental effects of RNS on oxidative phosphorylation, the microbe up-regulates the activity and expression of CL in order to bypass the TCA cycle and generate energy in an anaerobic manner (120). Here, it can be seen that CL and PEPC activities are sharply increased in order to generate the high-energy compound PEP when the microbe undergoes treatment with DEANO (**Figure 5.2 - A**). PK, the usual candidate for the production of pyruvate and ATP, was noticeably inactive in the stress, whereas PPDK was up-regulated in the DEANO-treated cultures (**Figure 5.2 - B, i**). This shift was apparent with the NO donor SNP as well. Reaction substrates, such as PEP, were routinely omitted from the in-gel activity assays to serve as a negative control. (**Figure 5.2 - B, ii**). To confirm that NO donors were indeed triggering the metabolic reconfiguration, regulation experiments were performed. Cells cultured to the stationary phase with SNP were transferred to control medium for 8 h and vice versa. As shown, PPDK activity was lowered as the cells returned to an untreated environment (**Figure 5.2 - B, iii**).

The primary advantage of the BN-PAGE system is that proteins remain in their native state, allowing the study of their interactions with other biomolecules as they would occur *in vivo* (131,132). The lowered activity of aconitase, a consequence of intracellular RNS, causes an up-regulation of CL, PEPC, and PPDK. Despite the disparate molecular masses of these enzymes, in-gel activity assays display a distinct formazan band in the stress at the same location for all three. This observation led us to hypothesize that these proteins were cooperating in the form of a metabolon. To confirm this, the band was excised from the native gel and incubated in a solution containing citrate, AMP and PP_i . After 30 min, the reaction mixture was subjected to HPLC analysis for the presence of reaction products. Indeed, the concentration of substrates was lowered and there was an appearance of distinct peaks characteristic of PEP, pyruvate, ATP and

oxaloacetate (**Figure 5.2 - C**). The possibility of a physical link between the three enzymes prompted us to immunoprecipitate PEPC to analyze the presence of attached proteins. Although antibodies against bacterial CL are not commercially available, PPDK was readily identified via Western blot. PEPC was also detected when PPDK was pulled down, while neither enzyme was detected in the control cells. (**Figure 5.2 - D**).

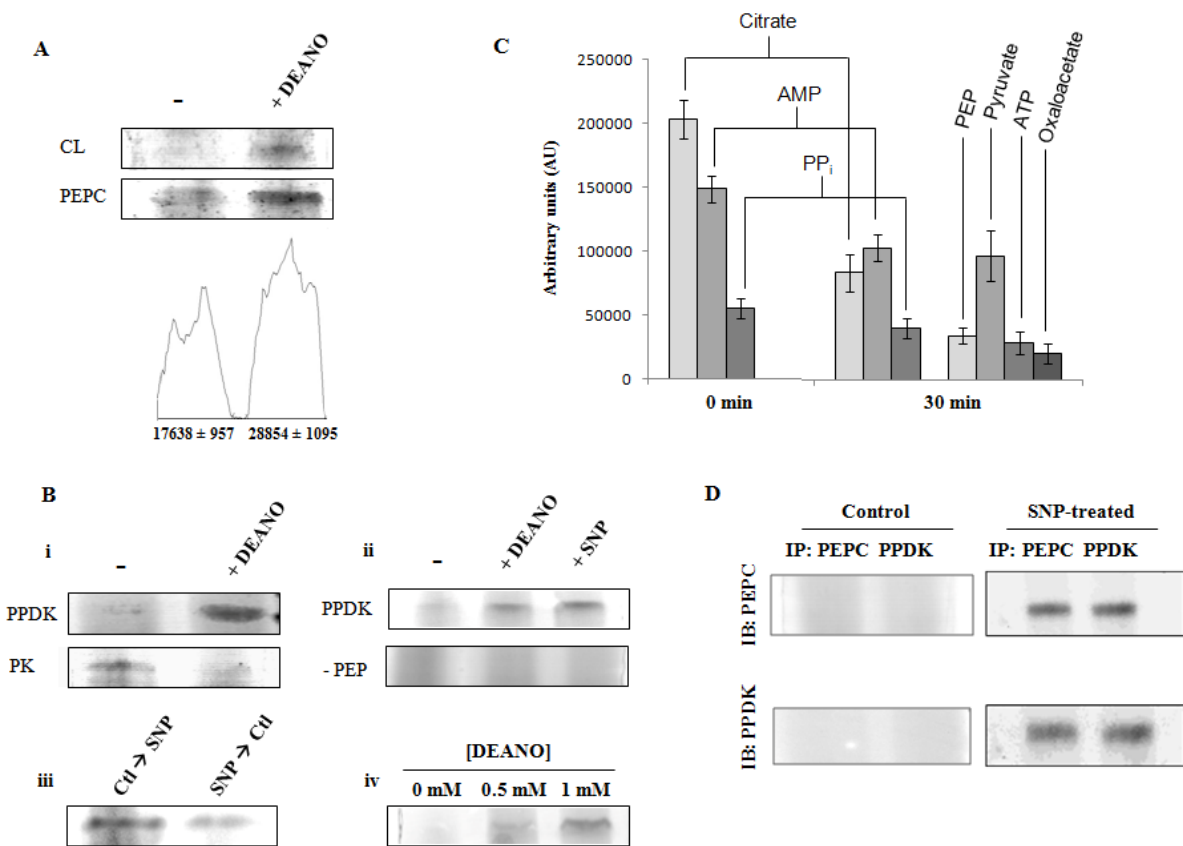


Figure 5.2 - Citrate catabolism and metabolon formation. **A**; Enzymes participating in the metabolism of citrate were probed by BN-PAGE in control (-) and 1 mM DEANO-treated cultures (CL, citrate lyase; PEPC, phosphoenolpyruvate carboxylase). **B**; **i**) The activity of phosphoenolpyruvate-dependent kinases was analyzed in-gel. **ii**) Reaction mixture without phosphoenolpyruvate served as a negative control. **iii**) PPDK activity subsequent to regulation experiments. Control cells were incubated in 10 mM SNP-containing medium for 8 h and vice versa prior to activity assays. **iv**) PPDK dose response with DEANO. **C**; The activity band for CL was excised from the gel and incubated in reaction buffer containing 2 mM citrate, 0.5 mM AMP and 0.5 mM PP_i. Consumption of the substrates and appearance of products was monitored by HPLC. n=3 ± standard deviation. **D**; Soluble CFE from control and SNP-treated cultures was utilized for immunoprecipitation (IP) using antibodies against PEPC or PPDK. The immunoprecipitates were separated on 10% SDS-PAGE, transferred and an immunoblot (IB) was performed to analyze bound proteins (PEPC, phosphoenolpyruvate carboxylase; PK, pyruvate kinase; PPDK, pyruvate phosphate dikinase) Images shown are representative gels; n=3. ImageJ for Windows was used to perform densitometry.

The assembly of metabolons is often transient, and brought about by distinct post-translational modifications (111,133). This allows them to form rapidly and come apart when the needs of the cell are met. Incubation of the soluble fraction of the organism with alkaline phosphatase for 15 min prior to BN-PAGE was applied to separate the three enzymes. Following this treatment, CL and PEPC activity bands were identified at their respective molecular mass lower in the gel in comparison to when they migrated as a metabolon (**Figure 5.3 - A**). PPDK activity was noticeably absent after dephosphorylation, thus indicating the importance of this modification to the function of the enzyme. To demonstrate this finding, the band for PPDK was excised and run through a SDS-PAGE gel. Both antibodies against PPDK and antibodies against phosphorylated amino acid residues generated a yellow signal at 60 kDA, the reported molecular mass of this enzyme (**Figure 5.3 - B**). PPDK and phosphorylated proteins could be detected separately in the green (800 nm) and red (680 nm) channels, respectively (**Figure 5.3 - C**).

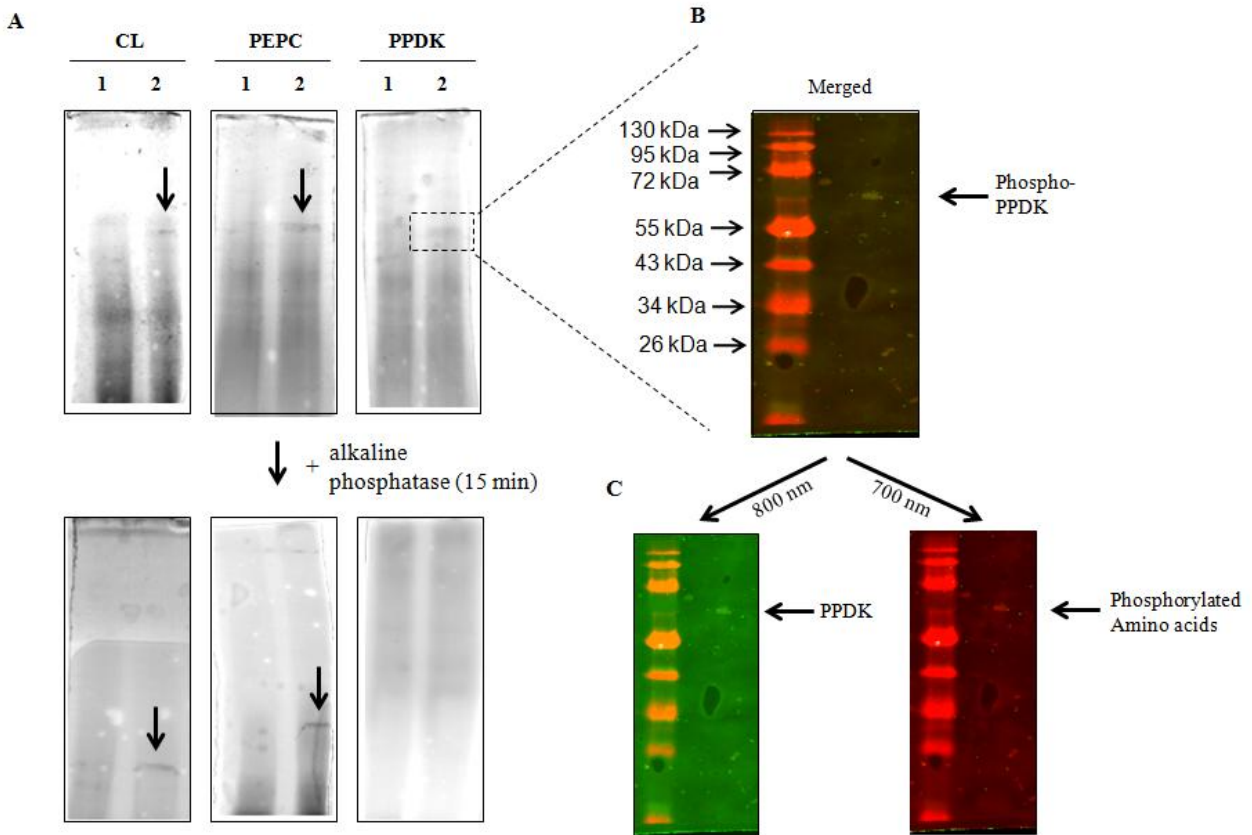


Figure 5.3 - Metabolon phosphorylation and dissociation. **A**; CL, PEPC and PPDK were probed with their respective reaction mixtures and activity bands were identified at a similar spot in the gel (top). Soluble CFE treated with 20 U of alkaline phosphatase for 15 min prior to BN-PAGE was loaded into wells and activity assays were performed after electrophoresis. CL and PEPC appeared lower in the gel after treatment, while PPDK activity was notably absent (**1**, Control; **2**, 10 mM SNP-treated). **B**; The band attributed to PPDK was excised and loaded into a 10 % SDS gel. Following electrophoresis and protein transfer, the membrane was submitted to Western blot analysis. Anti-PPDK antibodies (green-800 nm) and antibodies versus phosphoserine/threonine/tyrosine (red -680 nm) were applied and a yellow band was generated using IR-tagged secondary antibodies. **C**; A band at 60 kDa, the reported molecular weight of PPDK, was visible in both channels. Images shown are representative gels; n=4.

Activity assays were applied to measure the activity of phosphotransfer enzymes in the cell, as these allow for the storage of high-energy phosphate (116). Acetate kinase, which phosphorylates acetate and thus facilitates the production of acetyl-CoA, was found to be up-regulated in the stressed cells (**Figure 5.4 - A**). NDPK allows the transfer of high energy phosphate between nucleosides and also displayed higher activity than the control cultures (**Figure 5.4 - A**). PPase, which catalyzes the breakdown of PP_i into two phosphate ions, was analyzed in order to understand why PP_i levels were elevated in the NO-treated cultures. Indeed, this enzyme had diminished activity in the stressed cells (**Figure 5.4 - A**). Adenylate kinase, which takes two ADP molecules and generates ATP and AMP, also had higher activity in the RNS-treated cultures (**Figure 5.4 - A**). To ascertain the nature of the enzyme, activity bands are routinely excised and incubated in their respective substrates. The band indicative of AK was cut out of the gel from the control (**Figure 5.4 - B, i**) and SNP-treated (**Figure 5.4 - B, ii**) lanes and incubated in 1 mM ADP for 45 min. As seen in the chromatograms, ADP was consumed quicker in the SNP-treated cells, and the appearance of ATP and AMP was more pronounced, indicating an increased activity of the enzyme.

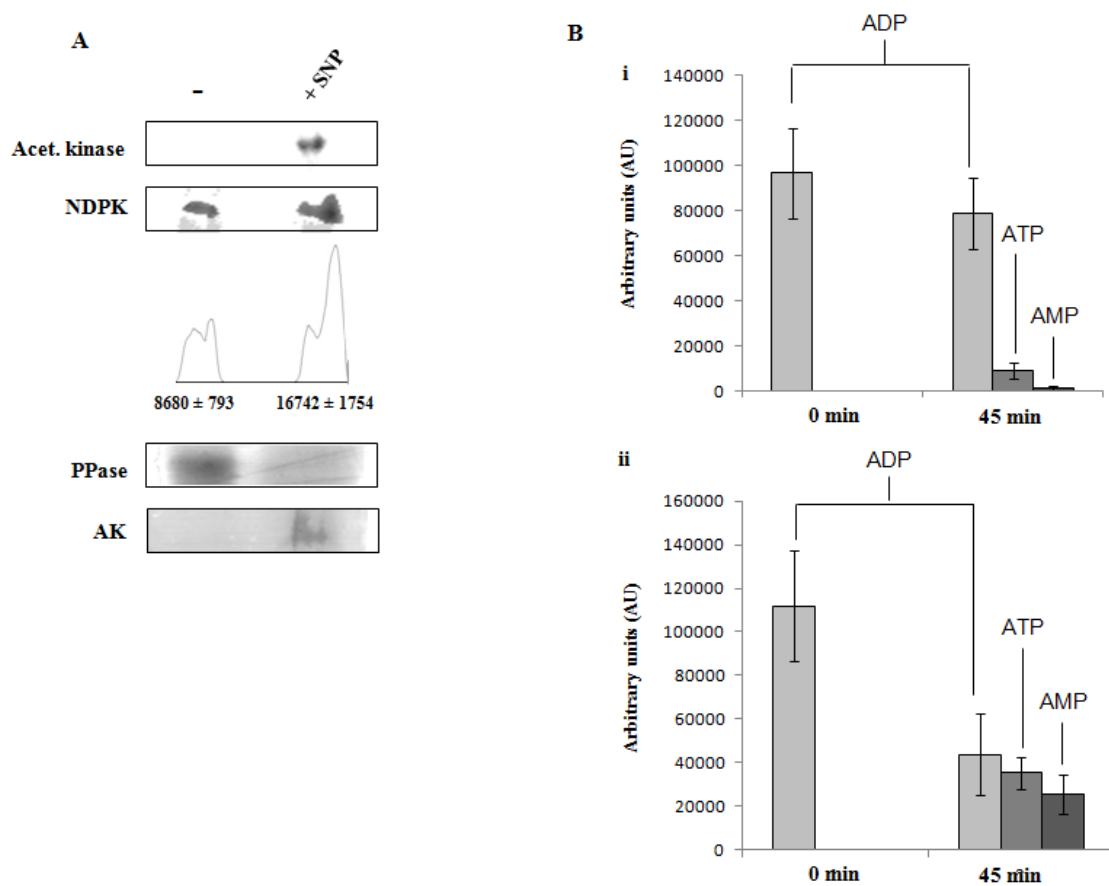


Figure 5.4 - Nucleotide production and phosphotransfer networks. **A**; The activity of various phosphotransfer enzymes was monitored in-gel. ImageJ for Windows was used to perform densitometry (AK, adenylate kinase; NDPK, nucleoside diphosphate kinase; PPase, inorganic pyrophosphatase). Gels are representative; $n = 3$. **B**; The activity band for AK from control (**i**) and 10 mM SNP-treated (**ii**) cells was excised and incubated in a solution of 0.5 mM ADP for 45 min. The appearance of products was monitored by HPLC; $n=3 \pm$ standard deviation.

Discussion

The data presented here describe a novel metabolic pathway for the anaerobic catabolism of citrate (**Figure 5.5**). Nitrosative stress brings about the assembly of CL, PEPC and PPDK, three enzymes which allow the production of ATP when the ETC of *P. fluorescens* is defective. It is a common perception that enzymes diffuse freely in biological systems, catalyzing their respective reactions when metabolites interact with them via passive diffusion. However, the formation of enzyme or protein aggregates is a more likely event as these enable metabolic networks to be more proficient. The benefits of such an arrangement are numerous. The close proximity between sequential enzymes allows the product of one reaction to be channeled to the next without equilibrating with the bulk cellular fluid. Such an event also assures a greater degree of specificity, allowing metabolites that are acted upon by a number of proteins to be funneled towards the desired end product. Indeed, these protein-protein interactions may allow certain reactions to transpire *in vivo* that would not occur if the enzyme was unaccompanied (108,134,135). Although these interactions are usually fragile and difficult to study, techniques such as BN-PAGE afford a potent tool to decipher these metabolons (109,135)

It has long been known that the presence of heme groups and iron-sulfur clusters within the electron transport chain render these complexes susceptible to oxidative and nitrosative stress. Indeed, this vulnerability underlies the success of white blood cells and their ability to subdue invading pathogens, as the formation of noxious radicals by NADPH oxidase and inducible nitric oxide synthase are key tools in combatting infectious microbes (136,137). Here, we show that the presence of SNP or DEANO in the growth medium has a detrimental effect on ATP-formation via oxidative phosphorylation, as visualized by in-gel enzyme activity assays and HPLC. Previous studies have reported that, under nitrosative stress, the microbe survives by

rerouting citrate away from the tricarboxylic acid cycle using CL in an effort to generate ATP anaerobically (120). This metabolic shift is to be expected, since the first three enzymes of the TCA cycle are sensitive to free radicals, as evidenced by their reduced activity (120,138-140). We postulated that, on the basis of their migration together in the BN-PAGE unit, CL, PEPC and PPK were acting in tandem, thus presenting a means by which ATP could be generated efficiently for the survival of the organism (120). Incubation of the band from the in-gel activity assay with the proper substrates and co-immunoprecipitation were applied to confirm this hypothesis. Initial attempts to understand how this supercomplex was assembled *in vivo* included Western blots to analyze the presence of acetylated or nitrosylated residues on the proteins, moieties that are expected given the environmental conditions of the cell. However, these modifications were not found (data not shown). Incubation of the soluble cell free extract with alkaline phosphatase prior to performing BN-PAGE was effective in separating the metabolon, indicating that a phosphorylation event is responsible for bringing these proteins in close contact. Indeed, this post-translational modification also appears to be responsible for the increase in PPK activity. Although we are the first to report on this unique multiprotein complex designed to generate ATP, others have described metabolons involving glycolytic and TCA cycle enzymes, thus lending further support to the notion that metabolic enzymes rarely function unaccompanied in biological systems (135,141,142).

It is of interest to note that, whereas CL and PEPC mediate the conversion of citrate into the high-energy intermediate PEP, it is PPK which converts this moiety into pyruvate and ATP, a role normally fulfilled by PK. While the latter utilizes ADP as a cofactor for this reaction, PPK employs AMP and PP_i. The substitution of PPK for PK is immensely beneficial to the organism, especially in conditions where oxidative phosphorylation is rendered inadequate. This

dikinase is more commonly found in plants and anaerobic parasites such as *Trypanosoma spp.* and *Entamoeba spp.*, where it presents itself as a novel therapeutic target due to the lack of PPDK analogues in mammalian systems (92,143). Energy efficiency may be an important consideration behind the preference for PPDK, as this enzyme can utilize PP_i instead of ADP. The participation of PPDK, coupled to the activity of adenylate kinase, permits the production of two ATP per molecule of PEP, while traditional glycolysis can only generate one (144). Under energy-limiting conditions, such as those invoked by the inactivation of the electron transport chain, this adaptation becomes vital.

Indeed, both PPDK and AK display increased activity in our system when exposed to NO stress. For this stratagem to remain sustainable, the maintenance of a PP_i pool is required to drive this reaction forward. Pyrophosphate is formed as a byproduct in a plethora of synthetic reactions, such as those involved in the synthesis of macromolecules like DNA and proteins (145). However, the energy stored in the anhydride bond of PP_i is not utilized as the ubiquitous inorganic pyrophosphatase (PPase) immediately hydrolyses this compound to P_i (146). Here, the down-regulation of PPase activity would certainly allow the PP_i concentration in the cell to remain elevated in an effort to propel PPDK activity. It is not unlikely that the increase in intracellular PP_i inactivates PK, as the former is known to be an allosteric inhibitor of this enzyme (145). The increased activities of phosphotransfer enzymes such as AK and NDPK, which allow the storage and distribution of high-energy phosphate, would also drive the continued activity of PPDK while fulfilling the need for nucleotides in cellular division. Indeed, the existence of phosphowires allows for the proper functioning of complex V. In this instance, ADP is converted into ATP and the energy shuttled via AK, NDPK as well as creatine kinase (116).

In conclusion, this report reveals how an intricate arrangement involving CL, PEPC and PPDK allows for the effective generation of ATP when oxidative phosphorylation is compromised by nitrosative stress. This metabolon that appears to hinge on the alkaline phosphatase-sensitive PPDK mediates the conversion of citrate into pyruvate and ATP with the participation of AMP and PP_i . A phosphotransfer system propelled by ACK, NDPK and AK generates various high-energy compounds with the concomitant formation of AMP, a key ingredient that fuels the metabolon. The pivotal role metabolism and this multi-enzyme complex play in the survival of this microbe provide important therapeutic cues against RNS-resistant bacteria.

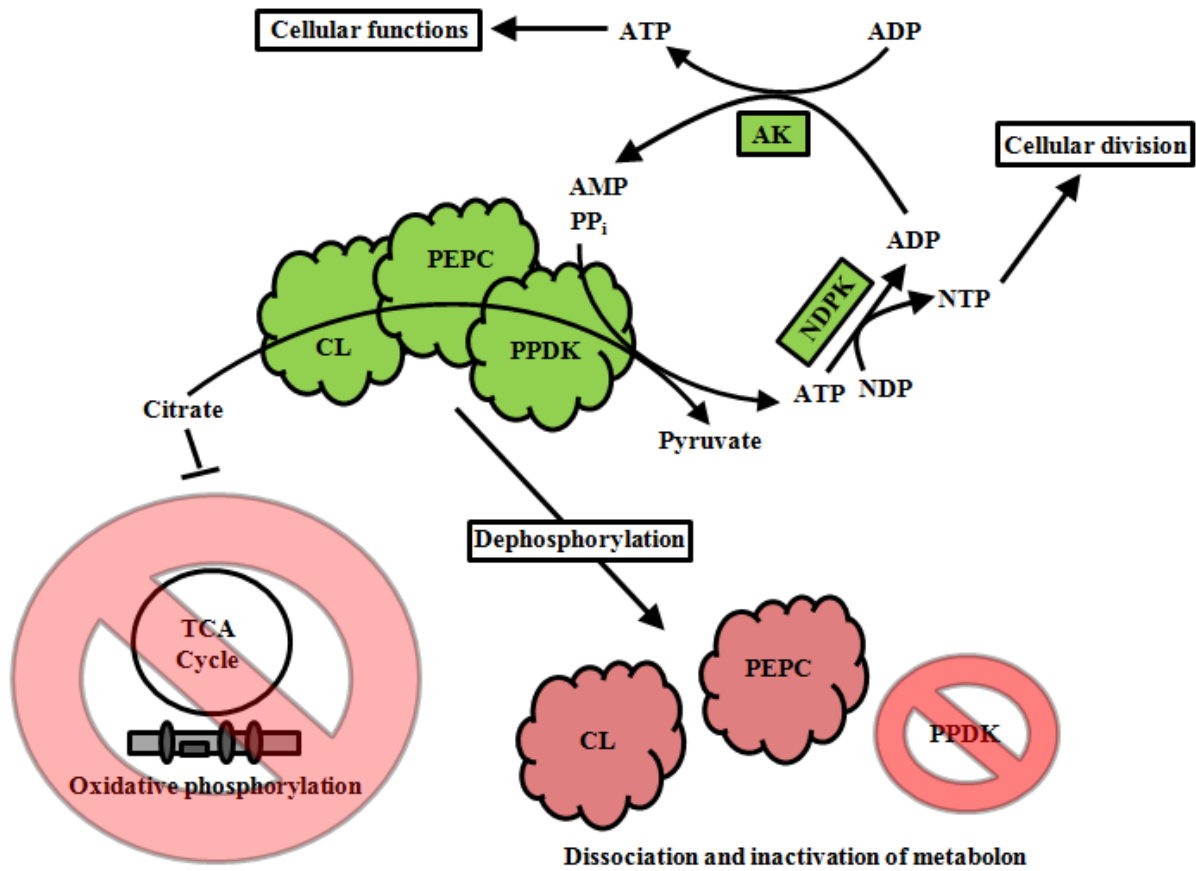


Figure 5.5 - Bioenergetics in *Pseudomonas fluorescens* exposed to nitrosative stress. A metabolon involving CL, PEPC and PPDK is assembled by the organism to effectively produce ATP, while phosphotransfer networks permit the storage of this crucial moiety

Chapter 6: Contributions to other research

The role of PPDK in ATP production by SLP when *P. fluorescens* is exposed to nitrosative stress prompted the further exploration of this enzyme and its importance to the general stress response. Indeed, the activity of this enzyme is increased upon exposure to metal pollutants as well as in different growth media (unpublished results). It would appear as though the primary factors underlying the increase in PPDK activity are a dysfunctional ETC in conjunction with a completely defective ACN. When the latter retains partial functionality, it is possible to catabolize citrate using the increased activities of ICL and ICDH-NADP, enzymes which act in tandem to pull this metabolite through a variant TCA cycle. There, ATP can be produced by SLP using the activity of succinyl-CoA synthase, as described (38). The activity of phosphotransfer networks, consisting of such enzymes as acetate kinase and adenylate kinase, has also been assessed using the work described herein (unpublished results).

The ability to gauge the activity of PEP-dependent kinases via BN-PAGE granted a better understanding of how pyruvate was being pooled under oxidative stress in *P. fluorescens*. The combined up-regulation of PEPS and down-regulation of PDH displayed by the organism has biotechnological applications in the environmentally friendly production of this keto-acid (33). The ability of the microbe to re-engineer metabolic networks without the need for genetic modification is of key importance, as it avoids the negative stigma that often comes with the introduction of new organisms in the environment (38).

BN-PAGE affords us an inexpensive means to analyze the activity of multiple enzymes simultaneously. As PEP-dependent kinases were probed using LDH as a coupling enzyme, it was postulated that transaminases and enzymes mediated nitrogen homeostasis could be visualized with GDH as a linker. Indeed, alanine, aspartate and glycine transaminases could all be studied using in-gel activity assays following electrophoresis (147). The proficiency by which metabolic perturbations are detected using BN-PAGE renders this an ideal method to analyze metal-associated diseases. As these, and other disorders, are often characterized by a dearth of ATP production due to a dysfunctional ETC, it is possible to use this technique to visualize the defective complexes of oxidative phosphorylation as well as enzymes which allow the organism to overcome these noxious effects (73,148).

Chapter 7: Conclusions and future directions

Since its discovery, the role of NO in living systems has puzzled researchers. The notion that a gaseous free radical, reactive by nature, could have such distinct and precise functions in disparate biological compartments is intriguing indeed. The ability of macrophages to engulf and isolate foreign organisms by phagocytosis renders them ideal effectors in the defense against microbial invaders. The concerted efforts of iNOS and NADPH oxidase in these specialized cells generate an oxidative burst, thus creating an environment ill-suited to the growth of fungi and bacterial pathogens. If an organism is to survive this onslaught, it must find a means to detoxify these noxious moieties and circumvent their effects on cellular processes. In this work, *P. fluorescens* is exposed to NO and RNS, a situation that hinders the TCA cycle and ATP production via the ETC, thus arresting central metabolism. To counter this, citrate is diverted away from this metabolic nodule using a metabolon consisting of CL, PEPC and PPDK. This stratagem allows the microbe to generate ATP by SLP, effectively shifting to an anaerobic lifestyle.

The premise of this work was to identify the cellular mechanisms by which bacteria adapt to RNS, as these may present themselves as novel targets for the development of antimicrobials. While *P. fluorescens* itself is rarely pathogenic, it serves as a good model for the metabolic versatility displayed by pseudomonads, and is a close relative of the highly infectious *Pseudomonas aeruginosa* (149-151). Since CL, PEPC and PPDK, as well as the metabolon they form have no known mammalian analogues, these present themselves as good therapeutic targets. However, the design of inhibitors for these proteins comes at a risk. Most drugs, including the majority of commercially-available antibiotics, function on the basis of their similarity to the actual enzymatic substrate. For instance, β -lactam antibiotics, such as penicillin

derivatives and cephalosporins, structurally mimic D-alanyl-D-alanine. These are the terminal amino acid residues on the precursor molecule N-acetylmuramic acid of peptidoglycan, the polymer forming the cell wall of bacteria. The structural similarity between the β -lactam nucleus of the antibiotic and D-alanyl-D-alanine allows the former to irreversibly bind the active site of penicillin binding proteins, enzymes which finalize the production of peptidoglycan. This, in turn, causes the degradation of the bacterial cell wall and subsequent death of the microbe (152).

Although CL, PEPC and PPDK are absent in humans, their substrates (citrate, oxaloacetate and PEP, respectively) are important to a number of metabolic hubs. As such, inhibitors based on analogues to these compounds would not be viable therapies against bacterial infections. Therefore, a comprehensive understanding of protein structures and their catalytic mechanism would be necessary to design an inhibitor that could subdue this metabolon without adversely affecting host cells. Over the course of the research project presented here, such modeling and docking studies have been performed on PPDK.

PPDK, owing to its presence in C4 plants and numerous bacterial or protozoan human pathogens, has long been recognized as a target for the development of herbicides and antibiotics (143,153). The dikinase is also present in bacterial plant pathogens of the genus *Phytophthora*, a family responsible for agricultural crop damage (154). As there is no amino acid sequence homology between bacterial PPDK and eukaryotic PK, there is potential to design a highly specific inhibitor (153). More specifically, researchers are targeting the N-terminal domain active site, which catalyzes the first two partial reactions ($\text{PPDK} + \text{ATP} + \text{P}_i \rightleftharpoons \text{PPDK-PP} + \text{AMP} + \text{P}_i \rightleftharpoons \text{PPDK-P} + \text{AMP} + \text{PP}_i$). As has been shown before, it is possible to use tight-binding space-filling ligands to block ATP binding on specific kinases (155). The results of docking studies and inhibitor screening point to alkyldihydroxyflavones as potential candidates

for the disruption of PPDK activity. As predicted, 4'-aminobutyl-flavone was a potent competitive inhibitor of this enzyme. Furthermore, it was selective for PPDK, showing no activity against hexokinase, myokinase or acetate kinase at a concentration of 129 μM . While there was inhibitory activity against PK, the K_i of 34 μM is 20-fold higher than that for PPDK (156). It would be of interest to see if these compounds have any activity against the dikinase *in vivo*. In this instance, the potential to inhibit PPDK may slow or halt the growth of *P. fluorescens*, thus killing the organism or causing the dissociation of the metabolon and forcing it to generate ATP in another manner.

As pseudomonads preferentially consume organic acids, the growth medium for these studies contained citrate as the sole source of carbon. This, however, is a reductive scenario not representative of any environment in which the microbe may be found. To ascertain the importance of PPDK in the adaptation to nitrosative stress, *P. fluorescens* was grown in media with alternative carbon sources. These include alanine, lactate, glutamine, glutamate, aspartate and malate. Indeed, in each of these scenarios, exposure to NO manifested itself by a decrease in the activity of ETC complexes and an increase in PPDK activity (**Appendix 1**). More extensive studies were performed with glucose as the sole source of carbon. In the untreated cells, this hexose is phosphorylated using an ATP-dependent hexokinase, as per the Embden-Meyerhof pathway (157). However, exposure to NO leads to a down-regulation of this enzyme, and a possible increase in the activity of an ADP-dependent glucokinase, although this requires further investigation (**Appendix 2**). The latter would not be out of the realm of possibility, as the enzyme has been discovered previously in other organisms (158,159). Such a shift would allow the bacterium to economize ATP, a necessity when faced with a defective ETC. In mammals,

ADP-dependent glucokinase is postulated to play a role in preserving ATP during clinically-relevant conditions such as ischemia and hypoxia (158).

The work published here was undertaken using a functional proteomic approach. As such, enzymatic activity was measured directly rather than surmised on the basis of genetic studies. Nonetheless, transcriptome comparisons via microarrays are beneficial for their ability to identify the complete set of genes that are up- and down-regulated in response to NO exposure (31,160). *P. fluorescens* was exposed to SNP and collected at the stationary phase of growth. At this time, RNA was isolated and a microarray was performed on the complete genome of the organism. Genes that were expressed 0.5 fold or lower and 1.5 fold and above relative to the control were analyzed with the supposition that these would correlate with the results of the activity assays and Western blots performed previously (**Appendix 3**). However, there was no evidence at this level of discourse that would explain the increased activity of CL, PEPC, PDK or the phosphotransfer enzymes. This underscores a key shortcoming of genomic studies. Put simply, many biologically important phenomena don't manifest themselves at the RNA level. Proteins are subject to a number of post-translational modifications including, but not limited to, glycosylation, acetylation, methylation and phosphorylation. These are particularly important in controlling metabolic flux. For instance, in *Salmonella enterica*, 90% of the enzymes found in central metabolism are acetylated. The latter modification is crucial to the catabolism of various carbon sources and in shuttling compounds to the proper metabolic nodules (161). As such, whole genome studies can be used to identify potential molecular targets for drug development, but should only be used as the basis for later confirmatory experiments.

Of the *P. fluorescens* genes that are highly expressed under NO treatment, a few would be excellent candidates for future studies. Guanine deaminase and xanthine dehydrogenase, two enzymes that are approximately 2 fold higher in expression, may be working in tandem to generate urate. This moiety has been shown to be a potent scavenger of ONOO⁻, and may help the bacteria mitigate the noxious effects of this compound (162). The increased activity of alanine racemase, which catalyzes the conversion between L- and D- isoforms of this amino acid, may have implications in cell wall organization as D-alanine is an essential element of peptidoglycan (163). Interestingly, the increased expression of cytochrome d ubiquinol oxidase may give the bacterium an alternative option for the generation of ATP, as complex IV is inactivated by nitrosative stress. More importantly, cytochrome d ubiquinol oxidase has been identified as a means by which pathogens protect themselves against the NO-mediated host immune response (164,165). Finally, the increased activity of ferredoxin-NADP⁺ reductase could play an important role in generating the reducing agent NADPH (166). The latter is a necessary cofactor for GSNOR and glutathione reductase, allowing these enzymes to regenerate GSH for the scavenging of ROS and RNS.

The work presented here identifies key mechanisms by which *P. fluorescens* circumvents the danger posed by NO and its derivatives, collectively known as RNS. Exposure to SNP or DEANO disables critical components of the TCA cycle and ETC, an event that has important ramifications on the bioenergetics of the organism. The activation of known RNS defense systems, consisting of such enzymes as NIR, NR and GSNOR, allows the organism to detoxify these compounds but does not explain how microbes circumvent defects in aerobic metabolism. This research project provides evidence of an alternative route for citrate metabolism consisting of the prokaryotic enzymes CL, PEPC and PPDK, of which the activities could not be predicted

on the basis of transcriptome studies alone. The convergence of these three proteins in a metabolon conformation is postulated to increase the efficiency of citrate catabolism and allows the organism to harvest the bond energy present in PP_i for the generation of the molecular unit of currency, ATP. This holistic approach to the biomolecular effects of environmental stressors affords us new insights into the adaptability of microbial systems (**Figure 7.1**). The means by which bacteria adapt to NO and RNS, key components of innate immunity, may reveal new therapeutic targets for the development of antibiotics. As we approach an era where our most potent drugs are rendered inadequate by rampant resistance, increased research on bacterial physiology and metabolism is of utmost importance.

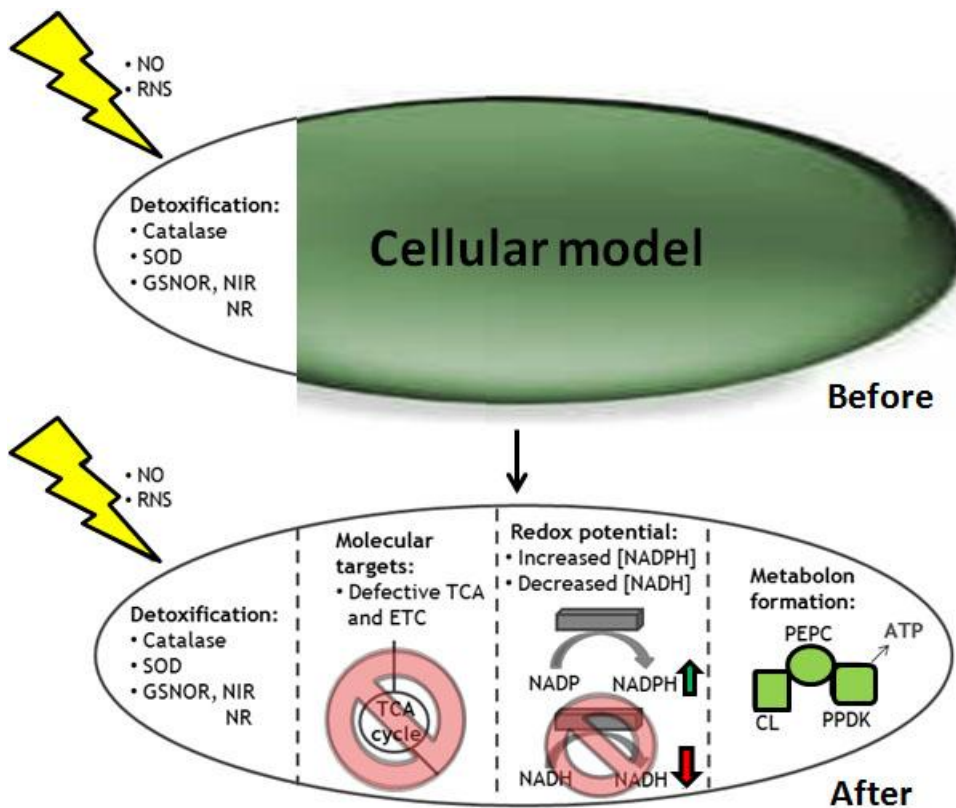


Figure 7.1 – Holistic approach to adaptation in living systems. Figure demonstrating the contributions of the work described here to our knowledge of mechanisms by which microbes adapt to and counteract the effects of NO and nitrosative stress.

Section 8: References

1. McIntyre, N. (2007) Sir Alexander Fleming. *J Med Biogr* 15, 234
2. Fischbach, M. A., and Walsh, C. T. (2009) Antibiotics for emerging pathogens. *Science* 325, 1089-1093
3. Silver, L. L. (2011) Challenges of antibacterial discovery. *Clin Microbiol Rev* 24, 71-109
4. Gould, I. M., and Bal, A. M. (2013) New antibiotic agents in the pipeline and how they can help overcome microbial resistance. *Virulence* 4, 185-191
5. Bassetti, M., Merelli, M., Temperoni, C., and Astilean, A. (2013) New antibiotics for bad bugs: where are we? *Ann Clin Microbiol Antimicrob* 12, 22
6. Palmer, A. C., and Kishony, R. (2013) Understanding, predicting and manipulating the genotypic evolution of antibiotic resistance. *Nat Rev Genet* 14, 243-248
7. Tavares, L. S., Silva, C. S., de Souza, V. C., da Silva, V. L., Diniz, C. G., and Santos, M. O. (2013) Strategies and molecular tools to fight antimicrobial resistance: resistome, transcriptome, and antimicrobial peptides. *Front Microbiol* 4, 412
8. Rasko, D. A., and Sperandio, V. (2010) Anti-virulence strategies to combat bacteria-mediated disease. *Nat Rev Drug Discov* 9, 117-128
9. Hamad, B. (2010) The antibiotics market. *Nat Rev Drug Discov* 9, 675-676
10. Bergstrom, R. (2011) The role of the pharmaceutical industry in meeting the public health threat of antibacterial resistance. *Drug Resist Updat* 14, 77-78
11. Coates, A. R., Halls, G., and Hu, Y. (2011) Novel classes of antibiotics or more of the same? *Br J Pharmacol* 163, 184-194
12. Clatworthy, A. E., Pierson, E., and Hung, D. T. (2007) Targeting virulence: a new paradigm for antimicrobial therapy. *Nat Chem Biol* 3, 541-548
13. Tillotson, G. S., and Theriault, N. (2013) New and alternative approaches to tackling antibiotic resistance. *F1000Prime Rep* 5, 51
14. Liu, C. I., Liu, G. Y., Song, Y., Yin, F., Hensler, M. E., Jeng, W. Y., Nizet, V., Wang, A. H., and Oldfield, E. (2008) A cholesterol biosynthesis inhibitor blocks *Staphylococcus aureus* virulence. *Science* 319, 1391-1394
15. McConell, G. K., Rattigan, S., Lee-Young, R. S., Wadley, G. D., and Merry, T. L. (2012) Skeletal muscle nitric oxide signaling and exercise: a focus on glucose metabolism. *Am J Physiol Endocrinol Metab* 303, E301-307
16. Delker, S. L., Xue, F., Li, H., Jamal, J., Silverman, R. B., and Poulos, T. L. (2010) Role of zinc in isoform-selective inhibitor binding to neuronal nitric oxide synthase. *Biochemistry* 49, 10803-10810
17. Qian, J., and Fulton, D. (2013) Post-translational regulation of endothelial nitric oxide synthase in vascular endothelium. *Front Physiol* 4, 347
18. Forstermann, U., and Sessa, W. C. (2012) Nitric oxide synthases: regulation and function. *Eur Heart J* 33, 829-837, 837a-837d
19. Shesely, E. G., Maeda, N., Kim, H. S., Desai, K. M., Krege, J. H., Laubach, V. E., Sherman, P. A., Sessa, W. C., and Smithies, O. (1996) Elevated blood pressures in mice lacking endothelial nitric oxide synthase. *Proc Natl Acad Sci U S A* 93, 13176-13181
20. Forstermann, U., Closs, E. I., Pollock, J. S., Nakane, M., Schwarz, P., Gath, I., and Kleinert, H. (1994) Nitric oxide synthase isozymes. Characterization, purification, molecular cloning, and functions. *Hypertension* 23, 1121-1131

21. Zhou, L., and Zhu, D. Y. (2009) Neuronal nitric oxide synthase: structure, subcellular localization, regulation, and clinical implications. *Nitric Oxide* 20, 223-230
22. Melikian, N., Seddon, M. D., Casadei, B., Chowienczyk, P. J., and Shah, A. M. (2009) Neuronal nitric oxide synthase and human vascular regulation. *Trends Cardiovasc Med* 19, 256-262
23. Berg, D. T., Gupta, A., Richardson, M. A., O'Brien, L. A., Calnek, D., and Grinnell, B. W. (2007) Negative regulation of inducible nitric-oxide synthase expression mediated through transforming growth factor-beta-dependent modulation of transcription factor TCF11. *J Biol Chem* 282, 36837-36844
24. Laver, J. R., Stevanin, T. M., Messenger, S. L., Lunn, A. D., Lee, M. E., Moir, J. W., Poole, R. K., and Read, R. C. (2010) Bacterial nitric oxide detoxification prevents host cell S-nitrosothiol formation: a novel mechanism of bacterial pathogenesis. *FASEB J* 24, 286-295
25. Poole, R. K. (2005) Nitric oxide and nitrosative stress tolerance in bacteria. *Biochem Soc Trans* 33, 176-180
26. Pacher, P., Beckman, J. S., and Liaudet, L. (2007) Nitric oxide and peroxynitrite in health and disease. *Physiol Rev* 87, 315-424
27. Hutchings, M. I., Mandhana, N., and Spiro, S. (2002) The NorR protein of *Escherichia coli* activates expression of the flavorubredoxin gene *norV* in response to reactive nitrogen species. *J Bacteriol* 184, 4640-4643
28. Gross, F., Durner, J., and Gaupels, F. (2013) Nitric oxide, antioxidants and prooxidants in plant defence responses. *Front Plant Sci* 4, 419
29. Tinajero-Trejo, M., Vreugdenhil, A., Sedelnikova, S. E., Davidge, K. S., and Poole, R. K. (2013) Nitric oxide reactivities of the two globins of the foodborne pathogen *Campylobacter jejuni*: roles in protection from nitrosative stress and analysis of potential reductants. *Nitric Oxide* 34, 65-75
30. Stern, A. M., Hay, A. J., Liu, Z., Desland, F. A., Zhang, J., Zhong, Z., and Zhu, J. (2012) The NorR regulon is critical for *Vibrio cholerae* resistance to nitric oxide and sustained colonization of the intestines. *MBio* 3, e00013-00012
31. Nobre, L. S., and Saraiva, L. M. (2013) Effect of combined oxidative and nitrosative stresses on *Staphylococcus aureus* transcriptome. *Appl Microbiol Biotechnol* 97, 2563-2573
32. Stoimenova, E., Vasileva-Tonkova, E., Sotirova, A., Galabova, D., and Lalchev, Z. (2009) Evaluation of different carbon sources for growth and biosurfactant production by *Pseudomonas fluorescens* isolated from wastewaters. *Z Naturforsch C* 64, 96-102
33. Bignucolo, A., Appanna, V. P., Thomas, S. C., Auger, C., Han, S., Omri, A., and Appanna, V. D. (2013) Hydrogen peroxide stress provokes a metabolic reprogramming in *Pseudomonas fluorescens*: enhanced production of pyruvate. *J Biotechnol* 167, 309-315
34. Lemire, J., Auger, C., Mailloux, R., and Appanna, V. D. (2014) Mitochondrial lactate metabolism is involved in antioxidative defense in human astrocytoma cells. *J Neurosci Res* 92, 464-475
35. Lemire, J., Milandu, Y., Auger, C., Bignucolo, A., Appanna, V. P., and Appanna, V. D. (2010) Histidine is a source of the antioxidant, alpha-ketoglutarate, in *Pseudomonas fluorescens* challenged by oxidative stress. *FEMS Microbiol Lett* 309, 170-177
36. Chenier, D., Bériault, R., Mailloux, R., Baquie, M., Abramia, G., Lemire, J., and Appanna, V. (2008) Involvement of fumarase C and NADH oxidase in metabolic

- adaptation of *Pseudomonas fluorescens* cells evoked by aluminum and gallium toxicity. *Appl Environ Microbiol* 74, 3977-3984
37. Lemire, J., Mailloux, R., Auger, C., Whalen, D., and Appanna, V. D. (2010) *Pseudomonas fluorescens* orchestrates a fine metabolic-balancing act to counter aluminium toxicity. *Environ Microbiol* 12, 1384-1390
 38. Auger, C., Han, S., Appanna, V. P., Thomas, S. C., Ulibarri, G., and Appanna, V. D. (2013) Metabolic reengineering invoked by microbial systems to decontaminate aluminum: implications for bioremediation technologies. *Biotechnol Adv* 31, 266-273
 39. Rojo, F. (2010) Carbon catabolite repression in *Pseudomonas* : optimizing metabolic versatility and interactions with the environment. *FEMS Microbiol Rev* 34, 658-684
 40. Pun, P. B., Lu, J., Kan, E. M., and Mochhala, S. (2010) Gases in the mitochondria. *Mitochondrion* 10, 83-93
 41. Durzan, D. J., and Pedroso, M. C. (2002) Nitric oxide and reactive nitrogen oxide species in plants. *Biotechnol Genet Eng Rev* 19, 293-337
 42. Emre, Y., and Nubel, T. (2010) Uncoupling protein UCP2: when mitochondrial activity meets immunity. *FEBS Lett* 584, 1437-1442
 43. Benhar, M., Forrester, M. T., and Stamler, J. S. (2009) Protein denitrosylation: enzymatic mechanisms and cellular functions. *Nat Rev Mol Cell Biol* 10, 721-732
 44. van Wonderen, J. H., Burlat, B., Richardson, D. J., Cheesman, M. R., and Butt, J. N. (2008) The nitric oxide reductase activity of cytochrome c nitrite reductase from *Escherichia coli*. *J Biol Chem* 283, 9587-9594
 45. McLean, S., Bowman, L. A., Sanguinetti, G., Read, R. C., and Poole, R. K. (2010) Peroxynitrite toxicity in *Escherichia coli* K12 elicits expression of oxidative stress responses and protein nitration and nitrosylation. *J Biol Chem* 285, 20724-20731
 46. Bradford, M. M. (1976) A rapid and sensitive method for the quantitation of microgram quantities of protein utilizing the principle of protein-dye binding. *Anal Biochem* 72, 248-254
 47. Singh, R., Lemire, J., Mailloux, R. J., and Appanna, V. D. (2008) A novel strategy involved in [corrected] anti-oxidative defense: the conversion of NADH into NADPH by a metabolic network. *PLoS One* 3, e2682
 48. Mailloux, R. J., Singh, R., Brewer, G., Auger, C., Lemire, J., and Appanna, V. D. (2009) Alpha-ketoglutarate dehydrogenase and glutamate dehydrogenase work in tandem to modulate the antioxidant alpha-ketoglutarate during oxidative stress in *Pseudomonas fluorescens*. *J Bacteriol* 191, 3804-3810
 49. Miranda, K. M., Espey, M. G., and Wink, D. A. (2001) A rapid, simple spectrophotometric method for simultaneous detection of nitrate and nitrite. *Nitric Oxide* 5, 62-71
 50. Schagger, H., and von Jagow, G. (1991) Blue native electrophoresis for isolation of membrane protein complexes in enzymatically active form. *Anal Biochem* 199, 223-231
 51. Singh, R., Chenier, D., Beriault, R., Mailloux, R., Hamel, R. D., and Appanna, V. D. (2005) Blue native polyacrylamide gel electrophoresis and the monitoring of malate- and oxaloacetate-producing enzymes. *J Biochem Biophys Methods* 64, 189-199
 52. Middaugh, J., Hamel, R., Jean-Baptiste, G., Beriault, R., Chenier, D., and Appanna, V. D. (2005) Aluminum triggers decreased aconitase activity via Fe-S cluster disruption and the overexpression of isocitrate dehydrogenase and isocitrate lyase: a metabolic network mediating cellular survival. *J Biol Chem* 280, 3159-3165

53. Mailloux, R. J., Hamel, R., and Appanna, V. D. (2006) Aluminum toxicity elicits a dysfunctional TCA cycle and succinate accumulation in hepatocytes. *J Biochem Mol Toxicol* 20, 198-208
54. Lemire, J., Mailloux, R., and Appanna, V. D. (2008) Zinc toxicity alters mitochondrial metabolism and leads to decreased ATP production in hepatocytes. *J Appl Toxicol* 28, 175-182
55. Mailloux, R. J., and Appanna, V. D. (2007) Aluminum toxicity triggers the nuclear translocation of HIF-1alpha and promotes anaerobiosis in hepatocytes. *Toxicol In Vitro* 21, 16-24
56. Gibson, A., Babbedge, R., Brave, S. R., Hart, S. L., Hobbs, A. J., Tucker, J. F., Wallace, P., and Moore, P. K. (1992) An investigation of some S-nitrosothiols, and of hydroxy-arginine, on the mouse anococcygeus. *Br J Pharmacol* 107, 715-721
57. Pelletier, A. M., Venkataramana, S., Miller, K. G., Bennett, B. M., Nair, D. G., Lourenssen, S., and Blennerhassett, M. G. (2010) Neuronal nitric oxide inhibits intestinal smooth muscle growth. *Am J Physiol Gastrointest Liver Physiol* 298, G896-907
58. Tortora, V., Quijano, C., Freeman, B., Radi, R., and Castro, L. (2007) Mitochondrial aconitase reaction with nitric oxide, S-nitrosoglutathione, and peroxynitrite: mechanisms and relative contributions to aconitase inactivation. *Free Radic Biol Med* 42, 1075-1088
59. Lee, J. H., Yang, E. S., and Park, J. W. (2003) Inactivation of NADP⁺-dependent isocitrate dehydrogenase by peroxynitrite. Implications for cytotoxicity and alcohol-induced liver injury. *J Biol Chem* 278, 51360-51371
60. Schneider, K., Kastner, C. N., Meyer, M., Wessel, M., Dimroth, P., and Bott, M. (2002) Identification of a gene cluster in *Klebsiella pneumoniae* which includes citX, a gene required for biosynthesis of the citrate lyase prosthetic group. *J Bacteriol* 184, 2439-2446
61. Kanao, T., Fukui, T., Atomi, H., and Imanaka, T. (2001) ATP-citrate lyase from the green sulfur bacterium *Chlorobium limicola* is a heteromeric enzyme composed of two distinct gene products. *Eur J Biochem* 268, 1670-1678
62. Buch, A., Archana, G., and Naresh Kumar, G. (2010) Heterologous expression of phosphoenolpyruvate carboxylase enhances the phosphate solubilizing ability of fluorescent pseudomonads by altering the glucose catabolism to improve biomass yield. *Bioresour Technol* 101, 679-687
63. Varela-Gomez, M., Moreno-Sanchez, R., Pardo, J. P., and Perez-Montfort, R. (2004) Kinetic mechanism and metabolic role of pyruvate phosphate dikinase from *Entamoeba histolytica*. *J Biol Chem* 279, 54124-54130
64. Heinzelmann, S., and Bauer, G. (2010) Multiple protective functions of catalase against intercellular apoptosis-inducing ROS signaling of human tumor cells. *Biol Chem* 391, 675-693
65. Gebicka, L., and Didik, J. (2009) Catalytic scavenging of peroxynitrite by catalase. *J Inorg Biochem* 103, 1375-1379
66. Blancato, V. S., Repizo, G. D., Suarez, C. A., and Magni, C. (2008) Transcriptional regulation of the citrate gene cluster of *Enterococcus faecalis* Involves the GntR family transcriptional activator CitO. *J Bacteriol* 190, 7419-7430
67. Borisov, V. B., Forte, E., Giuffre, A., Konstantinov, A., and Sarti, P. (2009) Reaction of nitric oxide with the oxidized di-heme and heme-copper oxygen-reducing centers of terminal oxidases: Different reaction pathways and end-products. *J Inorg Biochem* 103, 1185-1187

68. Denayer, S., Matthijs, S., and Cornelis, P. (2006) Resistance to vanadium in *Pseudomonas fluorescens* ATCC 17400 caused by mutations in TCA cycle enzymes. *FEMS Microbiol Lett* 264, 59-64
69. Varma, S. D., and Hegde, K. R. (2007) Lens thiol depletion by peroxynitrite. Protective effect of pyruvate. *Mol Cell Biochem* 298, 199-204
70. Frenzel, J., Richter, J., and Eschrich, K. (2005) Pyruvate protects glucose-deprived Muller cells from nitric oxide-induced oxidative stress by radical scavenging. *Glia* 52, 276-288
71. Das, U. N. (2006) Is pyruvate an endogenous anti-inflammatory molecule? *Nutrition* 22, 965-972
72. Mailloux, R. J., Puiseux-Dao, S., and Appanna, V. D. (2009) Alpha-ketoglutarate abrogates the nuclear localization of HIF-1alpha in aluminum-exposed hepatocytes. *Biochimie* 91, 408-415
73. Han, S., Auger, C., Castonguay, Z., Appanna, V. P., Thomas, S. C., and Appanna, V. D. (2013) The unravelling of metabolic dysfunctions linked to metal-associated diseases by blue native polyacrylamide gel electrophoresis. *Anal Bioanal Chem* 405, 1821-1831
74. Wittig, I., Braun, H. P., and Schagger, H. (2006) Blue native PAGE. *Nat Protoc* 1, 418-428
75. Ramzan, R., Weber, P., Linne, U., and Vogt, S. (2013) GAPDH: the missing link between glycolysis and mitochondrial oxidative phosphorylation? *Biochem Soc Trans* 41, 1294-1297
76. Genova, M. L., and Lenaz, G. (2013) Functional role of mitochondrial respiratory supercomplexes. *Biochim Biophys Acta* 1837, 427-443
77. Beriault, R., Chenier, D., Singh, R., Middaugh, J., Mailloux, R., and Appanna, V. (2005) Detection and purification of glucose 6-phosphate dehydrogenase, malic enzyme, and NADP-dependent isocitrate dehydrogenase by blue native polyacrylamide gel electrophoresis. *Electrophoresis* 26, 2892-2897
78. Traba, J., Satrustegui, J., and del Arco, A. (2011) Adenine nucleotide transporters in organelles: novel genes and functions. *Cell Mol Life Sci* 68, 1183-1206
79. Bolanos, J. P., Almeida, A., and Moncada, S. (2010) Glycolysis: a bioenergetic or a survival pathway? *Trends Biochem Sci* 35, 145-149
80. Saraste, M. (1999) Oxidative phosphorylation at the fin de siecle. *Science* 283, 1488-1493
81. Huttemann, M., Lee, I., Pecinova, A., Pecina, P., Przyklenk, K., and Doan, J. W. (2008) Regulation of oxidative phosphorylation, the mitochondrial membrane potential, and their role in human disease. *J Bioenerg Biomembr* 40, 445-456
82. Joliot, P., and Joliot, A. (2008) Quantification of the electrochemical proton gradient and activation of ATP synthase in leaves. *Biochim Biophys Acta* 1777, 676-683
83. Nelson, N., and Ben-Shem, A. (2004) The complex architecture of oxygenic photosynthesis. *Nat Rev Mol Cell Biol* 5, 971-982
84. Wu, K., Aoki, C., Elste, A., Rogalski-Wilk, A. A., and Siekevitz, P. (1997) The synthesis of ATP by glycolytic enzymes in the postsynaptic density and the effect of endogenously generated nitric oxide. *Proc Natl Acad Sci U S A* 94, 13273-13278
85. Singh, R., Lemire, J., Mailloux, R. J., Chenier, D., Hamel, R., and Appanna, V. D. (2009) An ATP and oxalate generating variant tricarboxylic acid cycle counters aluminum toxicity in *Pseudomonas fluorescens*. *PLoS One* 4, e7344

86. van Weelden, S. W., van Hellemond, J. J., Opperdoes, F. R., and Tielens, A. G. (2005) New functions for parts of the Krebs cycle in procyclic *Trypanosoma brucei*, a cycle not operating as a cycle. *J Biol Chem* 280, 12451-12460
87. Berg, I. A., Kockelkorn, D., Ramos-Vera, W. H., Say, R. F., Zarzycki, J., Hugler, M., Alber, B. E., and Fuchs, G. (2010) Autotrophic carbon fixation in archaea. *Nat Rev Microbiol* 8, 447-460
88. Kumar, S., and Barth, A. (2010) Phosphoenolpyruvate and Mg²⁺ binding to pyruvate kinase monitored by infrared spectroscopy. *Biophys J* 98, 1931-1940
89. Feng, X. M., Cao, L. J., Adam, R. D., Zhang, X. C., and Lu, S. Q. (2008) The catalyzing role of PPDK in *Giardia lamblia*. *Biochem Biophys Res Commun* 367, 394-398
90. Moreno-Sanchez, R., Encalada, R., Marin-Hernandez, A., and Saavedra, E. (2008) Experimental validation of metabolic pathway modeling. *FEBS J* 275, 3454-3469
91. Opperdoes, F. R., De Jonckheere, J. F., and Tielens, A. G. (2011) *Naegleria gruberi* metabolism. *Int J Parasitol* 41, 915-924
92. Slamovits, C. H., and Keeling, P. J. (2006) Pyruvate-phosphate dikinase of oxymonads and parabasalia and the evolution of pyrophosphate-dependent glycolysis in anaerobic eukaryotes. *Eukaryot Cell* 5, 148-154
93. Tjaden, B., Plagens, A., Dorr, C., Siebers, B., and Hensel, R. (2006) Phosphoenolpyruvate synthetase and pyruvate, phosphate dikinase of *Thermoproteus tenax*: key pieces in the puzzle of archaeal carbohydrate metabolism. *Mol Microbiol* 60, 287-298
94. Imanaka, H., Yamatsu, A., Fukui, T., Atomi, H., and Imanaka, T. (2006) Phosphoenolpyruvate synthase plays an essential role for glycolysis in the modified Embden-Meyerhof pathway in *Thermococcus kodakarensis*. *Mol Microbiol* 61, 898-909
95. Wu, Z. L. (2011) Phosphatase-coupled universal kinase assay and kinetics for first-order-rate coupling reaction. *PLoS One* 6, e23172
96. Hutchins, A. M., Holden, J. F., and Adams, M. W. (2001) Phosphoenolpyruvate synthetase from the hyperthermophilic archaeon *Pyrococcus furiosus*. *J Bacteriol* 183, 709-715
97. Kerenyi, L., and Gallyas, F. (1973) [Errors in quantitative estimations on agar electrophoresis using silver stain]. *Clin Chim Acta* 47, 425-436
98. Bolanos, J. P., Herrero-Mendez, A., Fernandez-Fernandez, S., and Almeida, A. (2007) Linking glycolysis with oxidative stress in neural cells: a regulatory role for nitric oxide. *Biochem Soc Trans* 35, 1224-1227
99. Shi, D. Y., Xie, F. Z., Zhai, C., Stern, J. S., Liu, Y., and Liu, S. L. (2009) The role of cellular oxidative stress in regulating glycolysis energy metabolism in hepatoma cells. *Mol Cancer* 8, 32
100. Scatena, R., Bottoni, P., Pontoglio, A., Mastrototaro, L., and Giardina, B. (2008) Glycolytic enzyme inhibitors in cancer treatment. *Expert Opin Investig Drugs* 17, 1533-1545
101. Crow, V. L., and Pritchard, G. G. (1977) The effect of monovalent and divalent cations on the activity of *Streptococcus lactis* C10 pyruvate kinase. *Biochim Biophys Acta* 481, 105-114
102. Narindrasorasak, S., and Bridger, W. A. (1977) Phosphoenolpyruvate synthetase of *Escherichia coli*: molecular weight, subunit composition, and identification of phosphohistidine in phosphoenzyme intermediate. *J Biol Chem* 252, 3121-3127

103. Zoraghi, R., See, R. H., Gong, H., Lian, T., Swayze, R., Finlay, B. B., Brunham, R. C., McMaster, W. R., and Reiner, N. E. (2010) Functional analysis, overexpression, and kinetic characterization of pyruvate kinase from methicillin-resistant *Staphylococcus aureus*. *Biochemistry* 49, 7733-7747
104. Varghese, B., Swaminathan, G., Plotnikov, A., Tzimas, C., Yang, N., Rui, H., and Fuchs, S. Y. (2010) Prolactin inhibits activity of pyruvate kinase M2 to stimulate cell proliferation. *Mol Endocrinol* 24, 2356-2365
105. Green, D. E. (1956) Studies in organized enzyme systems. *Harvey Lect*, 177-227
106. Kholodenko, B. N., Westerhoff, H. V., Schwaber, J., and Cascante, M. (2000) Engineering a living cell to desired metabolite concentrations and fluxes: pathways with multifunctional enzymes. *Metab Eng* 2, 1-13
107. Mathews, C. K. (1993) The cell-bag of enzymes or network of channels? *J Bacteriol* 175, 6377-6381
108. McMurtrie, H. L., Cleary, H. J., Alvarez, B. V., Loiselle, F. B., Sterling, D., Morgan, P. E., Johnson, D. E., and Casey, J. R. (2004) The bicarbonate transport metabolon. *J Enzyme Inhib Med Chem* 19, 231-236
109. Williamson, M. P., and Sutcliffe, M. J. (2010) Protein-protein interactions. *Biochem Soc Trans* 38, 875-878
110. An, S., Kumar, R., Sheets, E. D., and Benkovic, S. J. (2008) Reversible compartmentalization of de novo purine biosynthetic complexes in living cells. *Science* 320, 103-106
111. Bartholomae, M., Meyer, F. M., Commichau, F. M., Burkovski, A., Hillen, W., and Seidel, G. (2013) Complex formation between malate dehydrogenase and isocitrate dehydrogenase from *Bacillus subtilis* is regulated by tricarboxylic acid cycle metabolites. *FEBS J*, 12679
112. von Ballmoos, C., Wiedenmann, A., and Dimroth, P. (2009) Essentials for ATP synthesis by F1F0 ATP synthases. *Annu Rev Biochem* 78, 649-672
113. Dzeja, P. P., Bast, P., Pucar, D., Wieringa, B., and Terzic, A. (2007) Defective metabolic signaling in adenylate kinase AK1 gene knock-out hearts compromises post-ischemic coronary reflow. *J Biol Chem* 282, 31366-31372
114. Bonora, M., Patergnani, S., Rimessi, A., De Marchi, E., Suski, J. M., Bononi, A., Giorgi, C., Marchi, S., Missiroli, S., Poletti, F., Wieckowski, M. R., and Pinton, P. (2012) ATP synthesis and storage. *Purinergic Signal* 8, 343-357
115. Carrasco, A. J., Dzeja, P. P., Alekseev, A. E., Pucar, D., Zingman, L. V., Abraham, M. R., Hodgson, D., Bienengraeber, M., Puceat, M., Janssen, E., Wieringa, B., and Terzic, A. (2001) Adenylate kinase phosphotransfer communicates cellular energetic signals to ATP-sensitive potassium channels. *Proc Natl Acad Sci U S A* 98, 7623-7628
116. Dzeja, P. P., and Terzic, A. (2003) Phosphotransfer networks and cellular energetics. *J Exp Biol* 206, 2039-2047
117. Coustou, V., Besteiro, S., Biran, M., Diolez, P., Bouchaud, V., Voisin, P., Michels, P. A., Canioni, P., Baltz, T., and Bringaud, F. (2003) ATP generation in the *Trypanosoma brucei* procyclic form: cytosolic substrate level is essential, but not oxidative phosphorylation. *J Biol Chem* 278, 49625-49635
118. Bringaud, F., Baltz, D., and Baltz, T. (1998) Functional and molecular characterization of a glycosomal PPI-dependent enzyme in trypanosomatids: pyruvate, phosphate dikinase. *Proc Natl Acad Sci U S A* 95, 7963-7968

119. Wang, S. B., Murray, C. I., Chung, H. S., and Van Eyk, J. E. (2013) Redox regulation of mitochondrial ATP synthase. *Trends Cardiovasc Med* 23, 14-18
120. Auger, C., Lemire, J., Cecchini, D., Bignucolo, A., and Appanna, V. D. (2011) The metabolic reprogramming evoked by nitrosative stress triggers the anaerobic utilization of citrate in *Pseudomonas fluorescens*. *PLoS One* 6, e28469
121. Poole, K. (2012) Stress responses as determinants of antimicrobial resistance in Gram-negative bacteria. *Trends Microbiol* 20, 227-234
122. Shepherd, M., Barynin, V., Lu, C., Bernhardt, P. V., Wu, G., Yeh, S. R., Egawa, T., Sedelnikova, S. E., Rice, D. W., Wilson, J. L., and Poole, R. K. (2010) The single-domain globin from the pathogenic bacterium *Campylobacter jejuni*: novel D-helix conformation, proximal hydrogen bonding that influences ligand binding, and peroxidase-like redox properties. *J Biol Chem* 285, 12747-12754
123. Anderson, S., Appanna, V. D., Huang, J., and Viswanatha, T. (1992) A novel role for calcite in calcium homeostasis. *FEBS Lett* 308, 94-96
124. Bourret, T. J., Boylan, J. A., Lawrence, K. A., and Gherardini, F. C. (2011) Nitrosative damage to free and zinc-bound cysteine thiols underlies nitric oxide toxicity in wild-type *Borrelia burgdorferi*. *Mol Microbiol* 81, 259-273
125. Rogstam, A., Larsson, J. T., Kjelgaard, P., and von Wachenfeldt, C. (2007) Mechanisms of adaptation to nitrosative stress in *Bacillus subtilis*. *J Bacteriol* 189, 3063-3071
126. Kumar, P., Tewari, R. K., and Sharma, P. N. (2010) Sodium nitroprusside-mediated alleviation of iron deficiency and modulation of antioxidant responses in maize plants. *AoB Plants* 2010, plq002
127. Auger, C., Appanna, V., Castonguay, Z., Han, S., and Appanna, V. D. (2012) A facile electrophoretic technique to monitor phosphoenolpyruvate-dependent kinases. *Electrophoresis* 33, 1095-1101
128. Mailloux, R. J., Darwich, R., Lemire, J., and Appanna, V. (2008) The monitoring of nucleotide diphosphate kinase activity by blue native polyacrylamide gel electrophoresis. *Electrophoresis* 29, 1484-1489
129. Hernandez-Domiguez, E. E., Valencia-Turcotte, L. G., and Rodriguez-Sotres, R. (2012) Changes in expression of soluble inorganic pyrophosphatases of *Phaseolus vulgaris* under phosphate starvation. *Plant Sci* 187, 39-48
130. Laemmli, U. K. (1970) Cleavage of structural proteins during the assembly of the head of bacteriophage T4. *Nature* 227, 680-685
131. Van Coster, R., Smet, J., George, E., De Meirleir, L., Seneca, S., Van Hove, J., Sebire, G., Verhelst, H., De Bleecker, J., Van Vlem, B., Verloo, P., and Leroy, J. (2001) Blue native polyacrylamide gel electrophoresis: a powerful tool in diagnosis of oxidative phosphorylation defects. *Pediatr Res* 50, 658-665
132. Fiala, G. J., Schamel, W. W., and Blumenthal, B. (2011) Blue native polyacrylamide gel electrophoresis (BN-PAGE) for analysis of multiprotein complexes from cellular lysates. *J Vis Exp*
133. Araiza-Olivera, D., Chiquete-Felix, N., Rosas-Lemus, M., Sampedro, J. G., Pena, A., Mujica, A., and Uribe-Carvajal, S. (2013) A glycolytic metabolon in *Saccharomyces cerevisiae* is stabilized by F-actin. *FEBS J* 280, 3887-3905
134. Sowah, D., and Casey, J. R. (2011) An intramolecular transport metabolon: fusion of carbonic anhydrase II to the COOH terminus of the Cl(-)/HCO(3)(-)-exchanger, AE1. *Am J Physiol Cell Physiol* 301, C336-346

135. Winkel, B. S. (2004) Metabolic channeling in plants. *Annu Rev Plant Biol* 55, 85-107
136. Kroller-Schon, S., Steven, S., Kossmann, S., Scholz, A., Daub, S., Oelze, M., Xia, N., Hausding, M., Mikhed, Y., Zinssius, E., Mader, M., Stamm, P., Treiber, N., Scharffetter-Kochanek, K., Li, H., Schulz, E., Wenzel, P., Munzel, T., and Daiber, A. (2014) Molecular mechanisms of the crosstalk between mitochondria and NADPH oxidase through reactive oxygen species-studies in white blood cells and in animal models. *Antioxid Redox Signal* 20, 247-266
137. Alvarez, M. N., Peluffo, G., Piacenza, L., and Radi, R. (2011) Intraphagosomal peroxynitrite as a macrophage-derived cytotoxin against internalized *Trypanosoma cruzi*: consequences for oxidative killing and role of microbial peroxiredoxins in infectivity. *J Biol Chem* 286, 6627-6640
138. Yang, E. S., Richter, C., Chun, J. S., Huh, T. L., Kang, S. S., and Park, J. W. (2002) Inactivation of NADP(+)-dependent isocitrate dehydrogenase by nitric oxide. *Free Radic Biol Med* 33, 927-937
139. Gupta, K. J., Shah, J. K., Brotman, Y., Jahnke, K., Willmitzer, L., Kaiser, W. M., Bauwe, H., and Igamberdiev, A. U. (2012) Inhibition of aconitase by nitric oxide leads to induction of the alternative oxidase and to a shift of metabolism towards biosynthesis of amino acids. *J Exp Bot* 63, 1773-1784
140. Richardson, A. R., Payne, E. C., Younger, N., Karlinsey, J. E., Thomas, V. C., Becker, L. A., Navarre, W. W., Castor, M. E., Libby, S. J., and Fang, F. C. (2011) Multiple targets of nitric oxide in the tricarboxylic acid cycle of *Salmonella enterica serovar typhimurium*. *Cell Host Microbe* 10, 33-43
141. Reithmeier, R. A. (2001) A membrane metabolon linking carbonic anhydrase with chloride/bicarbonate anion exchangers. *Blood Cells Mol Dis* 27, 85-89
142. Dhar-Chowdhury, P., Harrell, M. D., Han, S. Y., Jankowska, D., Parachuru, L., Morrissey, A., Srivastava, S., Liu, W., Malester, B., Yoshida, H., and Coetzee, W. A. (2005) The glycolytic enzymes, glyceraldehyde-3-phosphate dehydrogenase, triose-phosphate isomerase, and pyruvate kinase are components of the K(ATP) channel macromolecular complex and regulate its function. *J Biol Chem* 280, 38464-38470
143. Saavedra, E., Encalada, R., Pineda, E., Jasso-Chavez, R., and Moreno-Sanchez, R. (2005) Glycolysis in *Entamoeba histolytica*. Biochemical characterization of recombinant glycolytic enzymes and flux control analysis. *FEBS J* 272, 1767-1783
144. Chastain, C. J., Failing, C. J., Manandhar, L., Zimmerman, M. A., Lakner, M. M., and Nguyen, T. H. (2011) Functional evolution of C(4) pyruvate, orthophosphate dikinase. *J Exp Bot* 62, 3083-3091
145. Bielen, A. A., Willquist, K., Engman, J., van der Oost, J., van Niel, E. W., and Kengen, S. W. (2010) Pyrophosphate as a central energy carrier in the hydrogen-producing extremely thermophilic *Caldicellulosiruptor saccharolyticus*. *FEMS Microbiol Lett* 307, 48-54
146. Deamer, D., and Weber, A. L. (2010) Bioenergetics and life's origins. *Cold Spring Harb Perspect Biol* 2, a004929
147. Han, S., Auger, C., Appanna, V. P., Lemire, J., Castonguay, Z., Akbarov, E., and Appanna, V. D. (2012) A blue native polyacrylamide gel electrophoretic technology to probe the functional proteomics mediating nitrogen homeostasis in *Pseudomonas fluorescens*. *J Microbiol Methods* 90, 206-210

148. Reinoso, C. A., Auger, C., Appanna, V. D., and Vasquez, C. C. (2012) Tellurite-exposed *Escherichia coli* exhibits increased intracellular alpha-ketoglutarate. *Biochem Biophys Res Commun* 421, 721-726
149. Lindholm, D. A., Murray, C. K., Akers, K. S., O'Brien, S. D., Alderete, J. F., and Vento, T. J. (2013) Novel *Pseudomonas fluorescens* septic sacroiliitis in a healthy soldier. *Mil Med* 178, e963-966
150. Madi, A., Alnabhani, Z., Leneveu, C., Mijouin, L., Feuilloley, M., and Connil, N. (2013) *Pseudomonas fluorescens* can induce and divert the human beta-defensin-2 secretion in intestinal epithelial cells to enhance its virulence. *Arch Microbiol* 195, 189-195
151. Wong, V., Levi, K., Baddal, B., Turton, J., and Boswell, T. C. (2011) Spread of *Pseudomonas fluorescens* due to contaminated drinking water in a bone marrow transplant unit. *J Clin Microbiol* 49, 2093-2096
152. Fisher, J. F., Meroueh, S. O., and Mobashery, S. (2005) Bacterial resistance to beta-lactam antibiotics: compelling opportunism, compelling opportunity. *Chem Rev* 105, 395-424
153. Palayam, M., Lakshminarayanan, K., Radhakrishnan, M., and Krishnaswamy, G. (2012) Preliminary analysis to target pyruvate phosphate dikinase from wolbachia endosymbiont of *Brugia malayi* for designing anti-filarial agents. *Interdiscip Sci* 4, 74-82
154. Marshall, J. S., Ashton, A. R., Govers, F., and Hardham, A. R. (2001) Isolation and characterization of four genes encoding pyruvate, phosphate dikinase in the oomycete plant pathogen *Phytophthora cinnamomi*. *Curr Genet* 40, 73-81
155. Norman, R. A., Toader, D., and Ferguson, A. D. (2012) Structural approaches to obtain kinase selectivity. *Trends Pharmacol Sci* 33, 273-278
156. Wu, C., Dunaway-Mariano, D., and Mariano, P. S. (2013) Design, synthesis, and evaluation of inhibitors of pyruvate phosphate dikinase. *J Org Chem* 78, 1910-1922
157. Frese, M., Schatschneider, S., Voss, J., Vorholter, F. J., and Niehaus, K. (2014) Characterization of the pyrophosphate-dependent 6-phosphofruktokinase from *Xanthomonas campestris* pv. *campestris*. *Arch Biochem Biophys* 546, 53-63
158. Ronimus, R. S., and Morgan, H. W. (2004) Cloning and biochemical characterization of a novel mouse ADP-dependent glucokinase. *Biochem Biophys Res Commun* 315, 652-658
159. Dorr, C., Zaparty, M., Tjaden, B., Brinkmann, H., and Siebers, B. (2003) The hexokinase of the hyperthermophile *Thermoproteus tenax*. ATP-dependent hexokinases and ADP-dependent glucokinases, two alternatives for glucose phosphorylation in Archaea. *J Biol Chem* 278, 18744-18753
160. Arai, H., Roh, J. H., Eraso, J. M., and Kaplan, S. (2013) Transcriptome response to nitrosative stress in *Rhodobacter sphaeroides* 2.4.1. *Biosci Biotechnol Biochem* 77, 111-118
161. Wang, Q., Zhang, Y., Yang, C., Xiong, H., Lin, Y., Yao, J., Li, H., Xie, L., Zhao, W., Yao, Y., Ning, Z. B., Zeng, R., Xiong, Y., Guan, K. L., Zhao, S., and Zhao, G. P. (2010) Acetylation of metabolic enzymes coordinates carbon source utilization and metabolic flux. *Science* 327, 1004-1007
162. Hooper, D. C., Spitsin, S., Kean, R. B., Champion, J. M., Dickson, G. M., Chaudhry, I., and Koprowski, H. (1998) Uric acid, a natural scavenger of peroxynitrite, in experimental allergic encephalomyelitis and multiple sclerosis. *Proc Natl Acad Sci U S A* 95, 675-680

163. Panizzutti, R., de Souza Leite, M., Pinheiro, C. M., and Meyer-Fernandes, J. R. (2006) The occurrence of free D-alanine and an alanine racemase activity in *Leishmania amazonensis*. *FEMS Microbiol Lett* 256, 16-21
164. Giuffre, A., Borisov, V. B., Arese, M., Sarti, P., and Forte, E. (2014) Cytochrome bd oxidase and bacterial tolerance to oxidative and nitrosative stress. *Biochim Biophys Acta* s0007-2728
165. Forte, E., Borisov, V. B., Konstantinov, A. A., Brunori, M., Giuffre, A., and Sarti, P. (2007) Cytochrome bd, a key oxidase in bacterial survival and tolerance to nitrosative stress. *Ital J Biochem* 56, 265-269
166. Moolna, A., and Bowsher, C. G. (2010) The physiological importance of photosynthetic ferredoxin NADP⁺ oxidoreductase (FNR) isoforms in wheat. *J Exp Bot* 61, 2669-2681

Appendix I: Nitrosative stress and alternate carbon sources

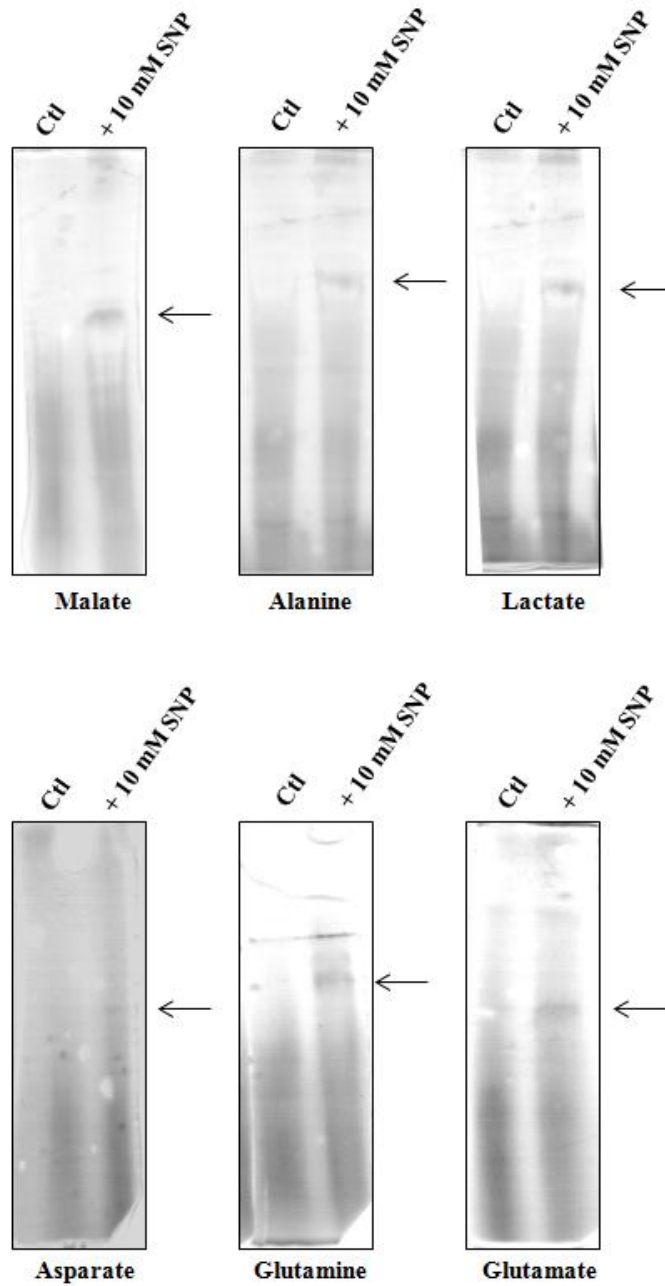


Figure 9.1 – PPDK in-gel activity assays. *P. fluorescens* was grown in media minus citrate containing the labeled substrate as the sole source of carbon (19 mM). Following the isolation of CFE and BN-PAGE, PPDK was probed in-gel using the aforementioned reaction mixture. Representative gels; n = 3.

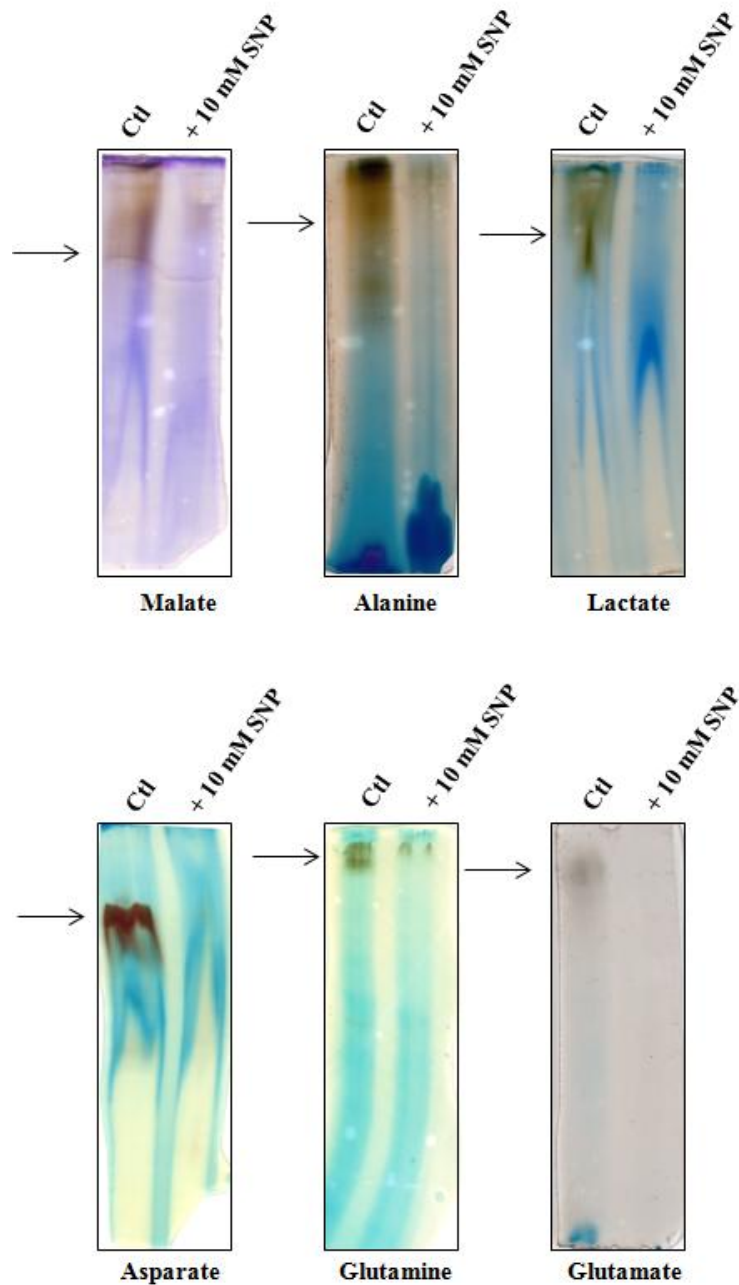


Figure 9.2 – Complex IV in-gel activity assays. *P. fluorescens* was grown in media minus citrate containing the labeled substrate as the sole source of carbon (19 mM). Following the isolation of CFE and BN-PAGE, Complex IV was probed in-gel using the aforementioned reaction mixture. Representative gels; n = 3 (Note: oxidized diaminobenzidine appears as a brown color).

Appendix II: Nitrosative stress and glucose consumption

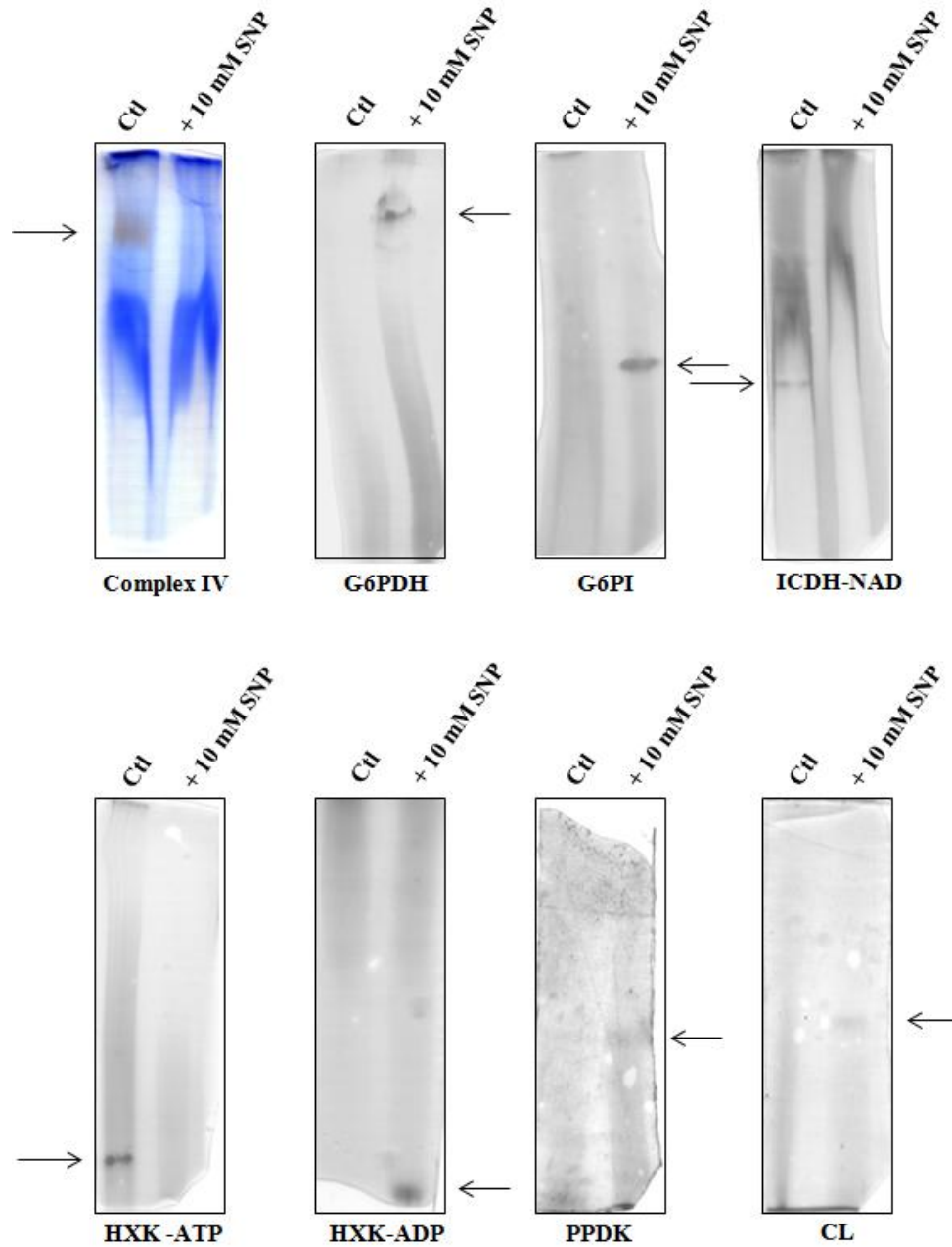


Figure 9.3 – In-gel activity assays from *P. fluorescens* grown on glucose. *P. fluorescens* was grown in media minus citrate containing glucose as the sole source of carbon (19 mM). Following the isolation of CFE and BN-PAGE, various enzymes were probed. Representative gels; n = 3

Appendix III: Effects of nitrosative stress on the transcriptome

Table 9.1 – Microarray analysis of *P. fluorescens* exposed to 10 mM SNP.

<u>Gene ID</u>	<u>Product</u>	<u>Expression VS control</u>	<u>Fold change</u>
PFL_1239	cobalamin biosynthesis protein CobD	↓	0.37
PFL_5261	diacylglycerol kinase	↓	0.39
PFL_2104	TfoX C-terminal domain superfamily	↓	0.4
PFL_1661	ribose operon repressor	↓	0.41
PFL_4428	probable permease of ABC transporter PA0204	↓	0.37
PFL_4776	2-dehydropantoate 2-reductase	↑	1.59
PFL_1819	electron transfer flavoprotein, beta subunit	↑	1.59
PFL_4308	ribosomal protein S1	↑	1.59
PFL_3043	flaA2 protein (flaA2)	↑	1.59
PFL_2805	oxidoreductase, short chain	↑	1.59
PFL_5631	ribulose-phosphate 3-epimerase	↑	1.60
PFL_3731	cytochrome d ubiquinol oxidase, subunit I	↑	1.60
PFL_4426	cobyric acid synthase CobQ	↑	1.60
PFL_5663	RNA polymerase sigma factor RpoD	↑	1.61

PFL_1791	maf protein	↑	1.61
PFL_2529	RNA polymerase sigma-70 factor, ECF subfamily	↑	1.62
PFL_4773	porin D	↑	1.62
PFL_4896	ribosomal protein L31	↑	1.64
PFL_3897	isocitrate lyase	↑	1.66
PFL_4203	chemotaxis protein CheV	↑	1.66
PFL_4268	transcriptional regulator CysB	↑	1.67
PFL_6003	DNA-binding response regulator AlgR	↑	1.67
PFL_1094	ribosomal protein S16	↑	1.68
PFL_6049	ribosomal protein L28	↑	1.68
PFL_3886	ATP-dependent Clp protease adaptor protein ClpS	↑	1.68
PFL_3885	ATP-dependent clp protease, ATP-binding subunit	↑	1.68
PFL_6036	alanine racemase	↑	1.69
PFL_2360	amino acid ABC transporter, periplasmic	↑	1.70
PFL_5597	translation elongation factor Tu	↑	1.71
PFL_6142	transcriptional regulator, AraC family	↑	1.72
PFL_4644	temperature acclimation protein b	↑	1.73

PFL_2112	translation initiation factor IF-3	↑	1.76
PFL_2101	ribose ABC transporter, periplasmic	↑	1.80
PFL_3064	enoyl-CoA hydratase/isomerase FadB1x	↑	1.82
PFL_1886	guanine deaminase	↑	1.82
PFL_1888	xanthine dehydrogenase, XdhB subunit	↑	1.84
PFL_2531	2-oxoisovalerate dehydrogenase E3 component	↑	1.90
PFL_5560	ribosomal protein S11	↑	1.92
PFL_2355	transcriptional regulator, MerR family	↑	1.93
PFL_4387	ABC transporter, periplasmic substrate-binding	↑	1.93
PFL_5042	chemotaxis protein CheV	↑	1.94
PFL_1241	ferredoxin--NADP reductase	↑	1.95
PFL_3065	acyl-CoA dehydrogenase family protein	↑	1.97
PFL_1399	alcohol dehydrogenase II	↑	1.97
PFL_5558	DNA-directed RNA polymerase, alpha subunit	↑	2.00
PFL_4625	RNA polymerase sigma-70 factor, ECF subfamily	↑	2.01
PFL_0968	fumarylacetoacetase	↑	2.05

PFL_1889	xanthine dehydrogenase, XdhA subunit	↑	2.10
PFL_4868	glycerol kinase	↑	2.15
PFL_1300	branched-chain amino acid ABC transporter	↑	2.32
PFL_5364	cytochrome d ubiquinol oxidase, subunit I	↑	3.10